Comparing land motion in Chiang Mai and Bangkok, Thailand, using Sentinel-1 InSAR Time Series

KUNLACHA INPAI

A THESIS SUBMITTED IN PARTIAL FULFILLMENT OF

THE REQUIREMENTS FOR MASTER DEGREE OF SCIENCE

IN GEOINFORMATICS

FACULTY OF GEOINFORMATICS

BURAPHA UNIVERSITY

2023

เปรียบเทียบการเคลื่อนที่ของแผ่นดินด้วยวิธี InSAR Time Series บริเวณเชียงใหม่และกรุงเทพฯ ประเทศไทย โดยใช้ดาวเทียม Sentinel-1

กุลชา อินไผ่

วิทยานิพนธ์นี้เป็นส่วนหนึ่งของการศึกษาตามหลักสูตรวิทยาศาสตรมหาบัณฑิต
สาขาวิชาภูมิสารสนเทศศาสตร์
คณะภูมิสารสนเทศศาสตร์ มหาวิทยาลัยบูรพา
2566

Comparing land motion in Chiang Mai and Bangkok, Thailand, using Sentinel-1 InSAR Time Series

KUNLACHA INPAI

A THESIS SUBMITTED IN PARTIAL FULFILLMENT OF
THE REQUIREMENTS FOR MASTER DEGREE OF SCIENCE
IN GEOINFORMATICS
FACULTY OF GEOINFORMATICS
BURAPHA UNIVERSITY
2023

The Thesis of Kunlacha Inpai has been approved by the examining committee to be partial fulfillment of the requirements for the Master Degree of Science in Geoinformatics of Burapha University

Advisory Committee	Examining Committee
Principal advisor	
....	.... Principal examiner
(Professor Dr.-ing. Timo Balz)	(Professor Dr. Fan Hong)
	.... Member
Co-advisor	(Assistant Professor Dr. Jianzhong Lu)
....	.... Member
(Dr. Kitsanai Charoenjit)	(Professor Dr.-ing. Timo Balz)
....	.... Member
(Assistant Professor Dr. Sukonmeth Jitmahantakul)	(Dr. Kitsanai Charoenjit)

.... Acting Dean of the Faculty of Geoinformatics
(Assistant Professor Dr. Arnon Wongkaew)
....

This Thesis has been approved by Graduate School Burapha University to be partial fulfillment of the requirements for the Master Degree of Science in Geoinformatics of Burapha University

.... Dean of Graduate School
(Associate Professor Dr. Witawat Jangiam)
....

64910084: MAJOR: GEOINFORMATICS; M.Sc. (GEOINFORMATICS)
KEYWORDS: Chiang Mai and Bangkok, land motion, monitoring, PS-InSAR, Sentinel-1

KUNLACHA INPAI : COMPARING LAND MOTION IN CHIANG MAI AND BANGKOK, THAILAND, USING SENTINEL-1 INSAR TIME SERIES. ADVISORY COMMITTEE: TIMO BALZ, KITSANAI CHAROENJIT SUKONMETH JITMAHANTAKUL 2023.

Bangkok, Thailand's capital city, and Chiang Mai, located in northern Thailand, are both susceptible to land motion influenced by natural and anthropogenic factors. These two cities differ significantly in their geological settings and depositional environments. Bangkok's upper formation primarily consists of Neogene clay deposits, which are highly sensitive to water and prone to compaction, leading to land subsidence. Conversely, Chiang Mai's land motion is influenced by factors such as geological structure, lithology, and morphology, contributing to slope instability and subsidence. As a result, the sustainable development and preservation of these cities rely on the precise identification, monitoring, and measurement of areas prone to geological hazards.

Radar interferometry, specifically the persistent scatterer interferometry (PS-InSAR) technique, has emerged as a powerful tool for monitoring land motion due to its high resolution, accuracy, extensive coverage, and cost-effectiveness. This research employs Sentinel-1 data to effectively monitor land deformation in both Chiang Mai and Bangkok, despite their differing geological environments and depositional settings. The study combines geological, morphological, and ground measurement data to create comprehensive deformation maps.

In the analysis of land motion, 61 images from descending and ascending orbits were utilized for Bangkok, and 62 images for Chiang Mai, spanning from January 2020 to May 2023. Bangkok's land motion is primarily driven by the geological evolution of the Thon Buri Basin during the early Miocene, resulting in a deltaic plain environment dominated by Bangkok clay. Excessive construction and groundwater extraction have exacerbated land subsidence in residential areas, with an extreme subsidence rate of 24 mm/year. In contrast, Chiang Mai experiences a combination of vertical subsidence and horizontal movement influenced by factors such as depositional environment, morphology, and lithology, resulting in potential vertical motion with an extreme subsidence rate of 14 mm/year. Additionally, natural factors like precipitation and slope angles contribute to horizontal motion in the mountainous areas.

The findings highlight morphological and geological hazards affecting urban areas in Chiang Mai and Bangkok, primarily driven by natural factors including geology, morphology, and depositional environment. The PS-InSAR technique, with its high-density point measurements, effectively identifies deformation zones in both cities. Despite their distinct geological and morphological environments, both Chiang Mai and Bangkok face land subsidence issues exacerbated by rapid urbanization, leading to significant structural damage and increased flood risk in low-lying and riverfront areas. This research underscores the potential of advanced PS-InSAR techniques for geological hazard and land deformation monitoring, while also addressing the associated challenges and advantages specific to Chiang Mai and Bangkok.

ACKNOWLEDGEMENTS

Many people accompanied and supported me. It gives me great joy to now have the opportunity to thank every one of them. First and foremost, I would like to express my gratitude to Prof.Dr. Ing.Timo Balz, my supervisor, and thank you to my co-advisors, Asst.Prof.Dr.Sukonmeth Jitmahantakul and Dr.Kitsanai Charoenjit, with special thanks to Dr. Pattama Phodee and Dr.Weerachat Wiwegwin, for their suggestions. I would also like to express my gratitude to the other SCGI Master Program students at my college, as well as the other members of my Master's, Ph.D., and SAR teams at Burapha University's Faculty of Geoinformatics and Wuhan University's State Key Laboratory of Information Engineering in Surveying, Mapping, and Remote Sensing. The second special thanks go to SARPROZ Software for the land deformation processing support software and the SARPROZ team for allowing me to utilize their program.

Finally, I will be eternally grateful to my family and Miss Supaluk Mungdee for their unwavering support, encouragement, and advice. Thank you so much to GISTDA for providing such a wonderful opportunity and experience in China and Thailand. Above all, I owe it to myself to be patient, concentrate, chill, work hard, and rest to complete my dissertation.

Kunlacha Inpai

TABLE OF CONTENTS

Page

ABSTRACT .... D

ACKNOWLEDGEMENTS .... F

TABLE OF CONTENTS .... G

LIST OF TABLES I

LIST OF FIGURES .... J

CHAPTER 1 INTRODUCTION 1

1.1 Background 1

1.2 Problem Statement 2

1.3 Research Questions 3

1.4 Research Objectives 3

1.5 Contribution of knowledge 3

CHAPTER 2 LITERATURE REVIEW 5

2.1 Tectonic Setting and Basin in Thailand 5

2.2 Depositional Environment and Sediment Deposit in the Chiang Mai Basin and Bangkok Deltaic Plain 7

2.3 Synthetic Aperture Radar (SAR) 16

2.4 Synthetic Aperture Radar Interferometry (InSAR) 20

2.5 Persistent Scatterer (PS)-InSAR for land displacement estimation 21

CHAPTER 3 MATERIAL AND METHODOLOGY 24

3.1 Study area 24

3.1.1 Bangkok 24

3.1.2 Chiang Mai 25

3.2 Data set 26

3.3 Methodology 30

CHAPTER 4 LITERATURE REVIEW 33

4.1 Bangkok Result from the PS-InSAR time series 33

4.2 Chiang Mai Result from the PS-InSAR time series 40
CHAPTER 5 DISCUSSION AND CONCLUSION 49
5.1 Discussion 49
5.1.1 Land Motion Pattern from PS-InSAR Detection 49
5.1.2 The Geological characteristics and Land Motion....................................51
5.1.3 Local factors and Land Motion 57
5.2 Conclusion 62
REFERENCES 64
BIOGRAPHY 69

LIST OF TABLES

Page

Table 1 Summary of sediment accumulation in different depositional environments (Panchuk, 2019). 9

Table 2 Summary of InSAR research performed in the past on land subsidence in Bangkok and the surrounding region. 14

Table 3 Property of the SAR images in the Bangkok area and the Chiang Mai area. 26

Table 4 An association between the velocity of RSQ, which is equal to or higher than 0.8, and significant statistics of descending (DES) and ascending (AS) orbits in the Bangkok study area. 47

Table 5 An association between the velocity of RSQ, which is equal to or higher than 0.8, and significant statistics of descending (DES) and ascending (AS) orbits in the Chiang Mai study area. 48

Table 6 Groundwater Level Fluctuations in the Sand-Gravel Sediment Aquifer from 2017 to 2021. 60

LIST OF FIGURES

Page

Figure 1 Southeast Asian continent's main tectonic features (modified from Metcalfe, 2011). 5

Figure 2 Cenozoic basins and structural map in Thailand (created by Morley, 2015). 7

Figure 3 Depositional Environments Type is related to Typography (modified from Panchuk, 2019). 8

Figure 4 Topography of Chiang Mai Basin (modified from Mitrearth, 2023). 10

Figure 5 Chiang Mai Basin and sediment deposition (modified from Morley, 2009; Mankhemthong et al., 2019). 11

Figure 6 Topography of Lower Central Plain (modified from Yamanaka et. al, 2011). 12

Figure 7 Thon Buri Basin and sediment deposition (modified from Phien-wej et. al, 2006; JICA, 1995). 13

Figure 8 An antenna sends out a radar pulse to the ground, which is then returned to the antenna by ground reflection. 16

Figure 9 The synthetic aperture radar geometry. 17

Figure 10 A SAR Image shows residence areas appear bright, the lake appears dark, and vegetated areas appear medium tone. 18

Figure 11 The spectrum of electromagnetic radiation and the bands of radar (created by ESA, 2023). 19

Figure 12 History of SAR missions, including its primary characteristics from 1980 to 2025 (created by Detektia, 2023). 19

Figure 13 The Interferometric Synthetic Aperture Radar basic concept (modified from Sousa & Bastos, 2013). 20

Figure 14 Bangkok study area (blue box) with Sentinel-1A footprint of descending track (red box) and ascending track (yellow box). 24

Figure 15 Chiang Mai study area (blue box) with Sentinel-1A footprint of descending track (red box) and ascending track (yellow box). 25

Figure 16 The detail of the dataset in the PS-InSAR method (a) Descending orbit of Bangkok (b) Ascending orbit of Bangkok, (c) Descending orbit of Chiang Mai, and (d) Ascending orbit of Chiang Mai. 27

Figure 17 The detail of the dataset in the PS-InSAR method (a) The total number of Sentinel-1A descending from Bangkok with 30 images, (b) The total number of Sentinel-1A ascending from Bangkok with 31 images, (c) The total number of Sentinel-1A descending from Chiang Mai with 32 images, and (d) The total number of Sentinel-1A ascending from Chiang Mai with 30 images. 29

Figure 18 Research method workflow. 32

Figure 19 The deformation map of the area of interest from the descending orbit (a) and ascending orbit (b) in Bangkok. 34

Figure 20 The time series of land displacement at two points in the western zone of Bangkok (Khet Phasi Charoen) from the descending track (left) and ascending track (right) shows the motion exhibits great linearity; the most significant deformations are in the residence areas, with maximum values of -24.4 mm/year from the descending track and -22.2 mm/year from the ascending track. The two stacks' results show the same subsidence trend, but the descending track has a 2.2 mm higher subsidence rate than the ascending track. 36

Figure 21 The time series of land displacement at two points in the northern zone of Bangkok (Khet Lak Si) from the descending track (left) and ascending track (right) shows the motion exhibits great linearity; the most significant deformations are in the office buildings and residence areas, with maximum values of -13.4 mm/year from the descending track and -12.1 mm/year from the ascending track. The two stacks' results show the same subsidence trend, but the descending track has a 1.3 mm higher subsidence rate than the ascending track. 37

Figure 22 The time series of land displacement at two points in the center of Bangkok (Khet Huai Khang) from the descending track (left) and ascending track (right) shows the motion exhibits great linearity; the most significant deformations are in the office buildings and residence areas, with maximum values of -13.7 mm/year from the descending track and -14.9 mm/year from the ascending track. The two stacks' results show the same subsidence trend, but the ascending track has a 1.2 mm higher subsidence rate than the descending track. 38

Figure 23 The time series of land displacement at two points in the southern zone of Bangkok (Khet Phra Khanong) from the descending track (left) and ascending track (right) shows the motion exhibits great linearity; the most significant deformations are in the residence areas, with maximum values of -12.1 mm/year from the descending track and -11.3 mm/year from the ascending track. The two stacks' results show the same subsidence trend, but the descending track has a 0.8 mm higher subsidence rate than the ascending track. 39

Figure 24 The time series of land displacement at two points in the eastern zone of Bangkok (Khet Lat Krabang) from the descending track (left) and ascending track (right) shows the motion exhibits great linearity; the most significant deformations are in the industrial zone and residence areas, with maximum values of -14.9 mm/year from the descending track and -13.5 mm/year from the ascending track. The two stacks' results show the same subsidence trend, but the descending track has a 1.4 mm higher subsidence rate than the ascending track. 40

Figure 25 The deformation map of the area of interest from the descending orbit (a) and ascending orbit (b) in Chiang Mai. 42

Figure 26 The time series of land displacement at two points in the west of Chiang Mai (Amphoe San Patong) from the descending track (left) and ascending track (right) shows the motion exhibits great linearity; the most significant deformations are in the industrial areas, with maximum values of -12.4 mm/year from the descending track and -14.7 mm/year from the ascending track. The two stacks' results show the same subsidence trend, but the ascending track has a 2.3 mm higher subsidence rate than the descending track. 43

Figure 27 The time series of land displacement at two points in the east of Chiang Mai (Amphoe San Kamphang) from the descending track (left) and ascending track (right) shows the motion exhibits great linearity; the most significant deformations are in the residence areas, with maximum values of -11.8 mm/year from the descending track and -7.8 mm/year from the ascending track. The two stacks' results show the same subsidence trend, but the descending track has a 4 mm higher subsidence rate than the ascending track. 44

Figure 28 The time series of land displacement at two points in the east of Chiang Mai (Amphoe Muang Lamphun) from the descending track (left) and ascending track (right) shows the motion exhibits great linearity; the most significant deformations are in the residence areas, with maximum values of -13 mm/year from the descending track and -10 mm/year from the ascending track. The two stacks' results show the same subsidence trend, but the descending track has a 3 mm higher subsidence rate than the ascending track. 45

Figure 29 The time series of land displacement at two points in the western zone of Chiang Mai (Amphoe Hang Dong) from the descending track (left) and ascending track (right) shows the motion exhibits great linearity; the most significant deformations are in the mountain areas, with maximum values of 4.7 mm/year from the descending track and -28.3 mm/year from the ascending track. The two stacks' results show a different trend with a deficit value of 33 mm; the descending track shows positive motion, or motion toward the sensor, while the ascending track shows negative motion, or motion away from the sensor, both of which indicate horizontal motion primarily toward the east. 46

Figure 30 The vertical motion can be seen most clearly in the western part of Bangkok by the intersection of stable points between descending and ascending tracks in 2020–2023. 50

Figure 31 The intersection of stable points between descending and ascending tracks in 2020–2023 shows the horizontal motion can be seen clearly in the mountain areas of the western parts (red box), while the vertical motion can be seen in both the low plain areas, which is the edge of Chiang Mai Basin (blue box). 51

Figure 32 The vertical motion of Bangkok relates to a geological and depositional environment where the red area shows the high rate of subsidence and is flood plain clay and recent tidal flat clay on marine clay deposits; the yellow area shows the moderate rate of subsidence and is flood plain clay on old tidal flat clay and marine clay deposits; the green area shows the low to stable rate; and the blue area shows the uplift area where there is higher terrain and near the mountain on the east of Bangkok. 55

Figure 33 The land motion of Chiang Mai relates to a geological map and deposition environment where the small yellow area shows the subsidence is near the edge of the Chiang Mai basin and it's a floodplain-alluvial deposition, while a mountain area on the west of Chiang Mai is represented by the red (indicating subsidence from an ascending track) and blue (indicating uplift from a descending track), and the different directions of motion indicate horizontal motion. 56

Figure 34 The damage from land subsidence in Khet Nong Khaem, the western region of Bangkok City by the news report in May 2023 (CH7HD News, 2023). 58

Figure 35 Bangkok Metropolitan Administrator's draft land-use zoning plan for the Bangkok Comprehensive Plan from 2020 by The Department of City Planning........59

Figure 36 The damage from flooding and landslides in Amphoe Hang Dong, Chiang Mai by the news report in May 2022 (Khaosod, 2023; Bangkokbiznews, 2023). 60

Figure 37 Chiang Mai landslide susceptibility map (update 2020) by the Department of Mineral Resources. 61

CHAPTER 1
INTRODUCTION

1.1 Background

Chiang Mai is in northern Thailand, while Bangkok is the capital city of Thailand. Both are prominent cities and attractive to visit because they have a rich of landmarks with a long history, cultural heritage, and contemporary vibrancy. Chiang Mai City is located in a basin plain environment between the mountains and is a captivating city known for its ancient temples, traditional festivals, and lush natural landscapes, which led to its fame for traveling. The city showcases a harmonious blend of traditional northern Thai culture and modern development. The variety of beautiful nature is controlled by the geological setting, leading to the topography being attractive for tourists to visit; however, the geological setting also makes the land move and puts some areas in Chiang Mai at risk for disaster, especially in lower plain areas that experience flooding, and the high terrain causes landslides in the rainy season. On the other hand, Bangkok City is located in a deltaic plain environment and has the Chao Phraya River, which links to the Gulf of Thailand. Bangkok is renowned for its royal history until now, iconic landmarks, and rapid modernization. Moreover, Bangkok has emerged as a global metropolis, embracing modernity while preserving its cultural heritage. The city's innovation and technology, represented by the futuristic structures of the central business area, reflect Thailand's economic rise. This makes Bangkok one of the best destinations to visit. Nowadays, Bangkok City experiences widespread land subsidence because of urban development and the long-term overexploitation of groundwater resources. From 1960 to 1970, the first detection of land subsidence was in Bangkok and nearby (Haley & Aldrich 1970; Brand and Paveenchana 1971; Edward 1976; Nutalaya 1981; Nutalaya, Chandra, & Balasubramaniam 1984). In 1970, the Royal Thai Survey Department (RTSD) installed the leveling benchmarks, and the maximum subsidence rate was detected at over 120 mm/year between 1978 and 1981 (Aobpaet et al. 2012). Moreover, the subsidence rate decreased by 35 mm/year between 1985 and 1988 and by 30 mm/year between 1988 and 1991 (Ramnarong 1983; Yong, Maathuis, and Turcott 1995; Ramnarong et al. 1998; Bontebal 2001; Phien-wej et al. 2006). The RTSD (2010) reported leveling results with maximum subsidence rates of 20 mm/year.

The Sentinel-1 satellite mission can be used to monitor land motion in various regions. Sentinel-1 is a European Space Agency (ESA) satellite mission equipped with Synthetic Aperture Radar (SAR) sensors that can capture radar images of the Earth's surface. The satellite is in a sun-synchronous orbit and collects data in various transmission modes (HH, HV, VH, and VV) with ascending and descending paths. The SAR images can be processed to detect land deformation, including subsidence or uplift. Since many years ago, the Interferometry Synthetic Aperture Radar (InSAR) time series approach has been utilized to monitor land deformation accurately and precisely. The electromagnetic wave is sent to the land surface and reflects from the object on the surface back to the satellite’s antenna. Interferometric phase measurement using the wrap and unwrap phases used to analyze the SAR images in a time series method. To determine the displacement on the Earth's surface in the Line of Sight (LOS) with high precision on a millimeter scale. Therefore, this research uses the InSAR time series technique for detecting land motion in Chiang Mai and Bangkok, Thailand, to compare the results between the different geology and depositional environments from this technique and to analyze the direction of land motion for allocating the surveillance area.

1.2 Problem Statement

Land motion is one of the factors contributing to the hazards in the city because it damages human life and human construction. Land surface movements are usually caused by natural and human-induced factors. Chiang Mai and Bangkok, Thailand, are captivating cities for traveling, but they are different in their geological environments and affected by land motion. While Chiang Mai City showcases the basin plain environment in northern Thailand, Bangkok City is in a deltaic plain environment and is experiencing land subsidence.

Many capital cities throughout the world are affected by land subsidence, which causes damage to infrastructure and the possibility of harm. Bangkok, Thailand, is experiencing subsidence in the land, and previous research has demonstrated that groundwater overuse, urban constructions, and the geological environment are the causes of land subsidence (Haley & Aldrich 1970; Brand and Paveenchana 1971; Nutalaya 1981; Ramnarong 1983; Nutalaya, Chandra, & Balasubramaniam 1984; Yong, Maathuis, and Turcott 1995; Ramnarong et al. 1998; Bontebal 2001; Phien-wej et al. 2006; Aobpaet et al. 2012). Bangkok has been a metropolis that has relied on groundwater as its primary source of water supply for a long time. In addition, Bangkok had an

urban rail transport system and an industrial zone, leading to the creation of several areas of land subsidence (Pumpuang and Aobpaet 2020). City administrators solved this problem by controlling groundwater extraction, which led to Bangkok's water consumption routine changing and influencing the overall trend of land subsidence. Therefore, monitoring and evaluation of changes in land subsidence should be continued. In contrast, Chiang Mai is facing land motion due to the geological setting and recent seismic activity, which is limited the low to moderate levels with a correlation to the active fault (Charusiri et al. 2022). Investigations in northern Thailand identified several normal faults in the Cenozoic basin that have the potential to create motion. The Chiang Mai Basin has been controlled by low-angle normal faults (Moley 2009; Mankhemthong et al. 2019), which can potentially cause land motion and put some areas at risk for disaster. Thus, this study focuses on Chiang Mai City and Bangkok City to find the habitat and analyze the direction of the land motion because both cities are important for Thailand's economy. They should obtain the disaster assessment, and the factor of land motion will be reported to people in those areas that had a high or low incidence of damage.

Presently, the application of satellite technology is interesting and helpful in extensive field surveys because it can monitor wide areas and collect data in every weather condition, both day and night. The Persistent Scatterer Interferometry Synthetic Aperture Radar (PS-InSAR) technique is useful and fast to detect surface deformation. Furthermore, Chiang Mai and Bangkok have different factors in land motion, such as geological settings and rock formation, groundwater extraction, urbanization and industry development, and human activities. The human-induced factor can be controlled and changed all the time for disaster protection, but the natural factor cannot. Thus, comparing the measurement of land motion in different geology and depositional environments is very important because the evaluation of land motion will help us understand the behavior of natural factors and figure out how to deal with problems that might arise later.

1.3 Research Questions

The justification for this study's consideration of the scientific question and providing a solution to the research question is: How PS-InSAR techniques with Sentinel-1 images can identify the land motion in Chiang Mai and Bangkok? The PS-InSAR techniques demonstrate land motion by relative velocity (mm/year) in Chiang Mai and Bangkok. How different geological environments influence the motion between Chiang Mai and Bangkok? This question can analyze the spatial pattern of the PS-InSAR time series result and correlate it to the geology and depositional environment.

1.4 Research Objectives

This research focuses on land motion to compare the results of the displacement rate in LOS using the InSAR time series technique in different geology and depositional environments. The Sentinel-1 is the radar satellite image that will be provided for the InSAR technique, which can measure land motion with high accuracy and precision. This research will study the motion in Chiang Mai City, which represents the basin environment, and Bangkok City, which represents the deltaic plain environment.

- To measure the motion in Chiang Mai and Bangkok using the Sentinel-1 InSAR time series technique.
- To analyze the motion’s direction from descending and ascending orbits in Chiang Mai and Bangkok.
- To compare the motion in Chiang Mai and Bangkok related to geology and depositional environments.

1.5 Contribution of knowledge

Land motion has influenced Chiang Mai and Bangkok, Thailand. Chiang Mai City represents the basin environment that experiences land motion because of the geological structure in this region. On the other hand, Bangkok City represents the deltaic plain environment that has suffered from land subsidence because of human activities such as groundwater overuse, urban construction, and natural factors. However, both land motions in different geology and depositional environments do not suddenly occur. The PS-InSAR technique (Ferretti et al., 2001) can detect land deformation in the city with high precision in millimeters (Perissin, 2008). This technique was used with Sentinel-1 terrain observations by progressive scan (TOPS) and Single Look Complex (SLC) mode to measure and investigate the motion in Chiang Mai and Bangkok, Thailand. The PS-InSAR time series techniques comprise pre-processing, SAR processing, and multi-image PS-InSAR. Sentinel-1 data has 12 days of revisit time and operates all day and all night.

The motion occurs on the Earth’s surface. The result of this research will give information to compare with other research and provide the users with the knowledge to be concerned about the future of land use in Chiang Mai and Bangkok, Thailand. The up-to-date outcome has been demonstrated to be advantageous for the people in the study area, as it will help them consider their protection from disaster in the future. Moreover, this finding will assist the public sector in comprehending the direction of land motion and being aware of land motion factors in Chiang Mai and Bangkok.

CHAPTER 2
LITERATURE REVIEW

2.1 Tectonic Setting and Basin in Thailand

Thailand is one of the countries in Southeast Asia that is spread across four plates of the Earth's crust. The Indian Plate, Australian Plate, Eurasia Plate, and Philippine Plate are the four plates that make up the Earth's crust (Figure 1). Thailand was discovered to be the southernmost section of the Eurasia Plate during the Late Cenozoic period. The Eurasia Plate is nearly motionless. The Indian tectonic plate, on the other hand, is moving north and colliding with the Eurasia Plate. As a result, the boundary of the plates forms a trench and many faults in Southeast Asia, such as the Sagaing Fault, the Red River Fault, and the active fault in Northern Thailand.

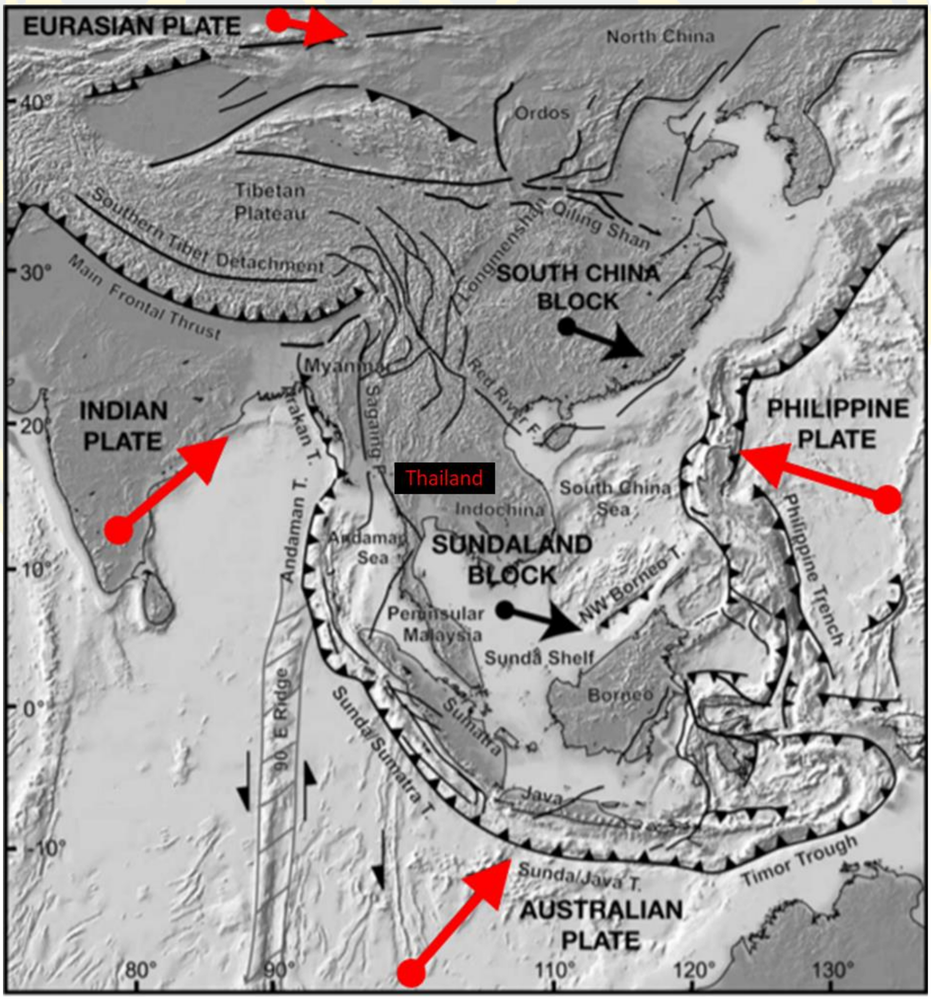

Figure 1 Southeast Asian continent's main tectonic features (modified from Metcalfe, 2011).

A convergence rate due to Australia's movement toward Southeast Asia of 65–70 mm/year (Metcalfe, 1996). Additionally, at an average rate of 10 mm/year, Southeast Asia may be moving toward Eurasia. These plate margins show extensive deformation. Along the Andaman and Sumatra-Java coasts, partitioning of oblique convergence creates extensive subduction and transform faulting, both of which are present in complicated zones of deformation (Malod & Kemal, 1996). Thailand has been experiencing deformation due to right-lateral and left-lateral slip on the northwest- and northeast-striking faults, respectively, with basins expanding north-south (Packham, 1993; Polachan et al., 1991). The strike-slip faults that strike northwest and the structural grain in pre-Triassic rocks determine the position and geometry of the basins (O'Leary, 1989). The major N-S trending basins in Thailand are considered to have evolved from the Late Eocene to the Early Oligocene. They are often bordered by normal faults, and it is commonly believed that the interaction of India, Australia, Burma, and Southeast Asia plates has played a role in determining the occurrence of all Cenozoic basins in Thailand (Packham, 1990, 1993; Charusiri and Pum-Im, 2009).

Cenozoic basins in Thailand are classified based on their geological structure, tectonic evolution, morphology, geophysics, stratigraphy, palynology, and micropaleontology, as shown in Figure 2. The basin is almost entirely located in the N-S trend, including the Northern, Central, Gulf of Thailand, and Andaman segments. Chiang Mai Basin (CM) is the largest basin in the northern segment, along with other basins such as Lampang Basin (LP), Chiang Rai Basin (CR), and Nan Basin (N). The central basin is divided into three sub-segments, including Upper Chao Praya, Lower Chao Praya, and Phetchabun. Basins in this segment include Phitsanulok Basin (PH), Ayutthaya Basin (AY), Suphan Buri Basin (SB), and Thonburi Basin (TB). The Gulf of Thailand segment consists of the Eastern Gulf and Western Gulf subsegments, for instance, Chumphon Basin (CHP), Hua Hin Basin (HH), and Songkhla Basin (SO). The Andaman Segment is only the Mergui Basin (MER).

The beginning of the deposition system of Thailand basins, or the stratigraphic history, is in the early Tertiary period, when there were first isolated lacustrine and alluvial deposits in the Oligocene (Charusiri and Pum-Im, 2009). Sediment accumulation time in each basin is different; some basins accumulate thick sediment in post-rift basins, while other basins accumulate sediment in active half-grabens during the same time (Morley, 2015). Subsequent stratigraphy starts with an alluvial and fluvial depositional environment in the lower section. Some basins are characterized by sedimentation with significant carbon-prone units. The middle section is switched to marginal marine and transgressive fluvial deposition, covered by the upper section, which is alluvial and regressive fluvial deposition.

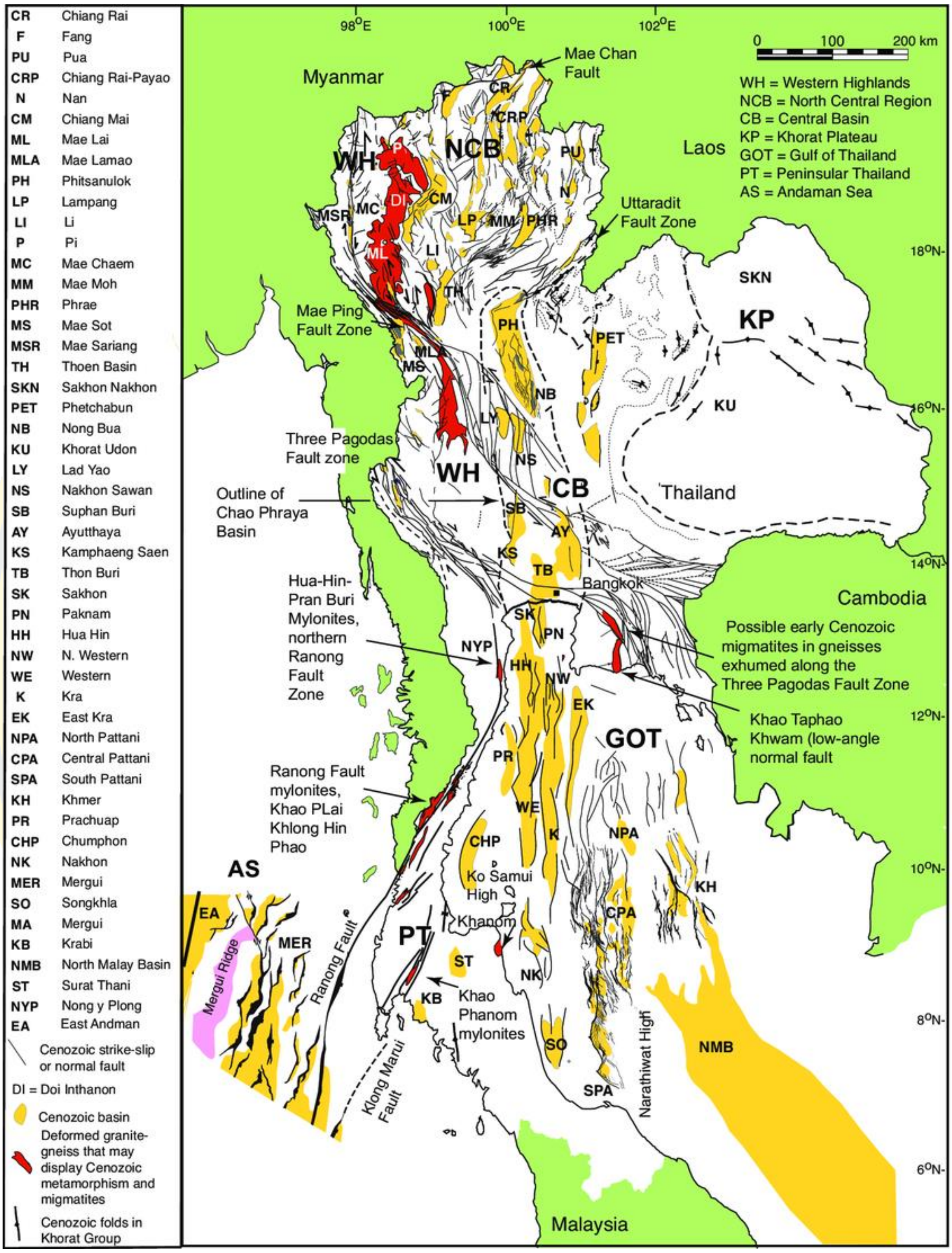

Figure 2 Cenozoic basins and structural map in Thailand (created by Morley, 2015).

2.2 Depositional Environment and Sediment Deposit in the Chiang Mai Basin and Bangkok Deltaic Plain

A depositional environment is a setting in which sediments accumulate. The differences in geological structure and morphology are different in the sediment deposition. Some important types of depositional environments are illustrated in Figure 3. Each depositional type needs a specific condition for accumulating and forming the environment due to certain biological processes, physical processes, and chemical reactions. Depositional environments can be broadly categorized as terrestrial, marine, and a zone of transition. Terrestrial describes the conditions under which deposits form on land. These might be depositional areas like rivers or freshwater lakes. The Chiang Mai Basin represents terrestrial deposition. Environments connected to seas and oceans are referred to as marine. An example of a transitional depositional environment is a delta, which is a place where freshwater rivers flow into seas or oceans. The Bangkok Deltaic Plain represents the transitional deposition.

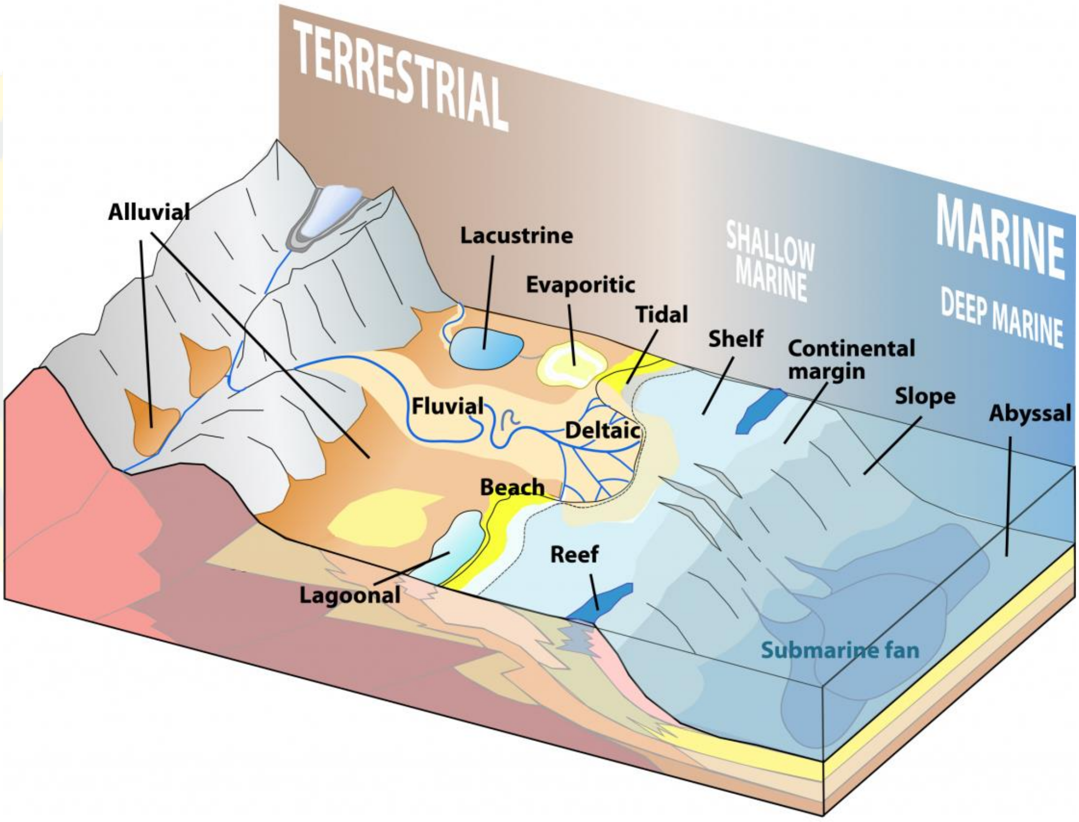

Figure 3 Depositional Environments Type is related to Typography (modified from Panchuk, 2019).

Additionally, certain depositional environments are where various clastic sedimentary rock types are formed. The primary environmental factors that affect the formation of clastic rocks have to do with the energy available to move sediments and the distance the sediments migrate before being deposited. The relationship between the environment and sediment accumulation is shown in Table 1.

Table 1 Summary of sediment accumulation in different depositional environments (Panchuk, 2019).

Environment	Depositional Settings	Sediments	Transport Processes
Alluvial	Steep valleys meet plains	Coarse angular fragments	Gravity, moving water
Fluvial	Streams	Conglomerate, sand, silt, organic matter	Moving water
Lacustrine	Lakes	Sand, silt, clay, organic matter	Moving water
Evaporite	Lakes (arid zone)	Salts, clay	Still water
Deltaic	Deltas	Sand, silt, clay, organic matter	Moving water
Beach	Beaches, spits, sandbars	Sand	Waves, long-shore currents
Tidal	Tidal flats	Fine-grained sand, silt, clay	Tidal currents
Lagoonal	Lagoon	Carbonates, silt, clay	Little transportation
Reef	Reefs	Carbonates	Waves, tidal currents
Submarine fan	Continental slopes	Conglomerate, sand, silt, clay	Underwater gravity

Most of the sediments in depositional settings such as sandbars, gravel in streams, and steep slopes do not become sedimentary rock because this is the initial lithification process. Sediments must have been deposited in a basin where they can be stored for a long enough period to transform into rock. This process takes millions or tens of millions of years, and most of these basins are the result of plate tectonic activity.

The Chiang Mai Basin is the biggest Cenozoic basin in northern Thailand (Morley and Racey, 2011). It is an intermontane basin with an east-west extension. The eastern mountain range is Doi Khun Tan, and the western mountain range is the Doi Suthep-Pui range. The shape of the Chiang Mai Basin is similar to a stomach, with a length from north to south of 140 km and a maximum from east to west of 35 km. Chiang Mai Basin covers approximately 3000 km2, and the elevation is around 335 meters above sea level in the north and 280 meters above sea level in the south (Wattananikorn, 1995). The Ping River, which is one of the basin's major rivers, typically flows from north to south.

Figure 4 Topography of Chiang Mai Basin (modified from Mitrearth, 2023).

Chiang Mai Basin is an evaluation of low-angle normal faults (LANF) in late Oligocene–Miocene rift basins (Morley, 2009). A significant LANF system borders it on the western side (Dunning et al., 1995; Rhodes et al., 2000). Metamorphic rock, including orthogneiss and paragneiss, is discernible in the footwall of the LANF fault (Dunning et al., 1995; Macdonald et al., 2010). On the other hand, the hanging wall is the Chiang Mai Basin. According to seismic reflection data, the Chiang Mai basin is filled with an estimated 5,000 km3 of material that has been eroded or translated eastward over a period of 15-20 million years. (Morley, 2015). The maximum thickness of the basin is between 2 and 2.5 kilometers (Chinbunchorn et al., 1989; Wattananikorn et al., 1995). Most of these basins are filled with fluvial and lacustrine sediments, ranging in thickness from a few hundred meters to 2 to 3 kilometers (Fenton et al., 2003; Charusiri and Pum Im, 2009). Sedimentary Deposition in Chiang Mai Basin divides into 4 main units: the top unit (up to 150 m) is the Pleistocene-Recent sediments (Qa; fluvial environment; and Qt; alluvial environment), such as gravel, sand, and clay, as represented in light yellow color in Figure 5. The second unit (up to 150 m) is semi-consolidated, such as sandstones, siltstones, mudstones, conglomerates, and gravels, as represented in yellow. These sediments, which are characteristic of Miocene sediments, were formed in lacustrine, fluvial, and alluvial environments. The Western Highlands' Doi Suthep-Pui and Doi Inthanon regions produced the majority of the deposits, which were then carried eastward by debris flows, floods, and braided streams during the Early-Middle Miocene uplift of the Western Highlands (Rhodes et al., 2005). The third unit is claystone with sandstone thinly bedded that was deposited in the Late Oligocene to Miocene (Morley et al., 2011), as represented by the dark yellow color. The western basin edges find sheared

Paleozoic metasediment rock like a clastic alluvial fan environment, as represented by the light brown color. Most of the metamorphic rocks in these deposits' clasts are of low grade, but there are an increasing number of gneissic clasts (Rhodes et al., 2005). The fourth unit is the Palaeozoic sediment rock, as represented in light orange, which is comprised of a little metamorphosed limestone, sandstone, shale, and chert (Adisaipattanakul, 2014). The basement of Chiang Mai Basin is Triassic metamorphic rock, as represented by the pink color.

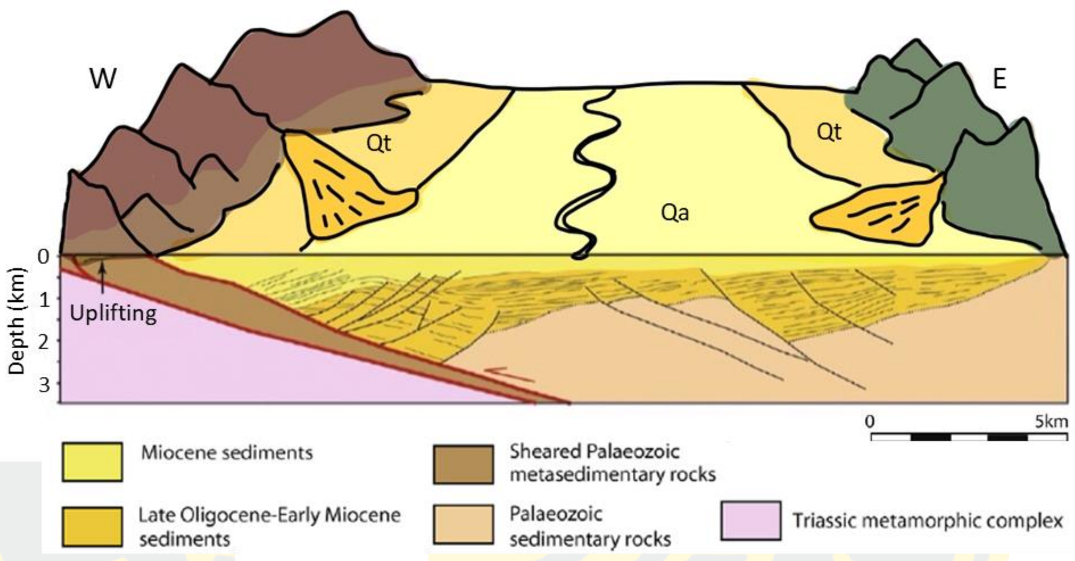

Figure 5 Chiang Mai Basin and sediment deposition (modified from Morley, 2009; Mankhemthong et al., 2019).

The structural evolution of the Chiang Mai Basin begins with an early stage of high-angle normal faulting in the Late Oligocene–Early Miocene. A LANF after that severed the early normal fault system that developed in the Early Miocene, presumably with a ramp-flat shape that induced bedding rotation of the earlier high-angle faults. This result shows the difference in sediments between the pre-LANF and the syn-LANF sections in the basin that had expanded in the east-west direction (following the LANF direction) (Morley, 2009). Furthermore, main normal or normal-oblique faults with displacements ranging from a few hundred meters to several kilometers control the basin rifting (Morley et al., 2011). Some of the characteristics of these basin-bounding faults may have been developed by previous strike-slip faults that were reactivated (Uttamo et al., 2000; Morley, 2007). According to Replumaz and Tapponnier (2003), the two main strike-slip faults in Thailand, the Mae Ping and Three Pagodas faults, were active as sinistral faults up to the early Oligocene. Subsequently, Central Thailand experienced the formation of extensional basins during the Oligocene, with activity moving northward (Morley, 2011).

The Bangkok deltaic plain is in the Lower Central Plain of Thailand, or the southern part of the Thon Buri Basin (Morley 2015). The NW-SE active fault known as the Three Pagoda Fault is the geological structure that controls the topography of the Basin (Morley, 2015), which comprises a hill, high terrace, middle terrace, alluvial fans, floodplain, tidal flat, and delta. The lower central plain has four rivers: the Mae Klong River, the Tha Chin River, the Cho Phaya River, and the Bang Pakong River. These rivers run into the Gulf of Thailand in the southern part, which is the deltaic depositional environment. The western high terrace is represented in yellow-brown color in Figure 6, close to Uthaitani, Ratchaburi, and Kanjanaburi provinces. On the other hand, the eastern high terrace is close to Saraburi, Lopburi, Nakhon Nayok, Sachengsao, and Pachinburi provinces.

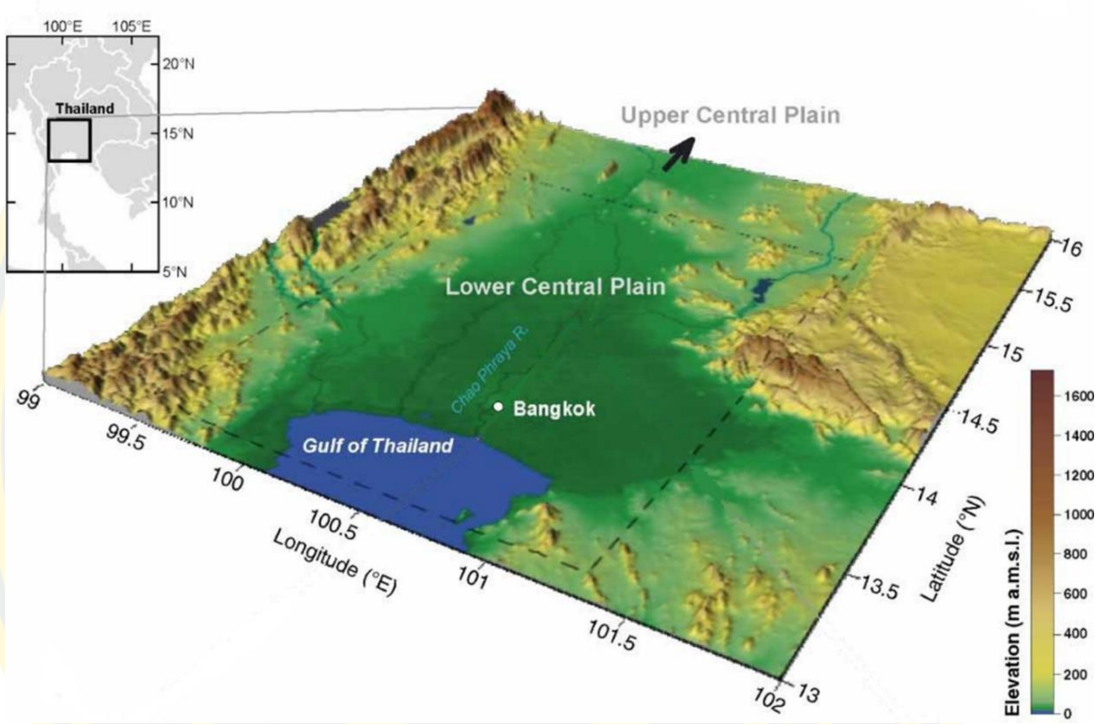

Figure 6 Topography of Lower Central Plain (modified from Yamanaka et. al, 2011).

Sedimentary deposition in the Bangkok Deltaic Plain is mainly soft clay, or Bangkok clay, of the upper unit, which is deposited in the fluvial depositional environment and interbedded with the tidal-shallow marine environment in the Quaternary period (Holocene epoch). Bangkok clay unit is the first layer and covers a wide area such as Bangkok, Nonthaburi, Pathum Thani, Phra Nakhon Si Ayutthaya, Nakhon Nayok, Suphanburi, Samut Prakarn, Samut Sakhon, and Nakhon Pathom, which are represented in yellow in Figure 7. The second unit is the late Pleistocene sediment (dark grey-black clay) that was deposited in the marine and fluvial depositional environments and is represented in a light brown color. The third unit is middle Pleistocene sediment that was deposited in the alluvial depositional environment and is represented in gray. The middle and high terraces are represented in light green and dark green, respectively, which is the lower unit of sediment deposition (clay, silt, sand, gravels, and laterite), and the bedrock is pre-tertiary basement rock (granite complex and metamorphic rock) and is represented in dark orange.

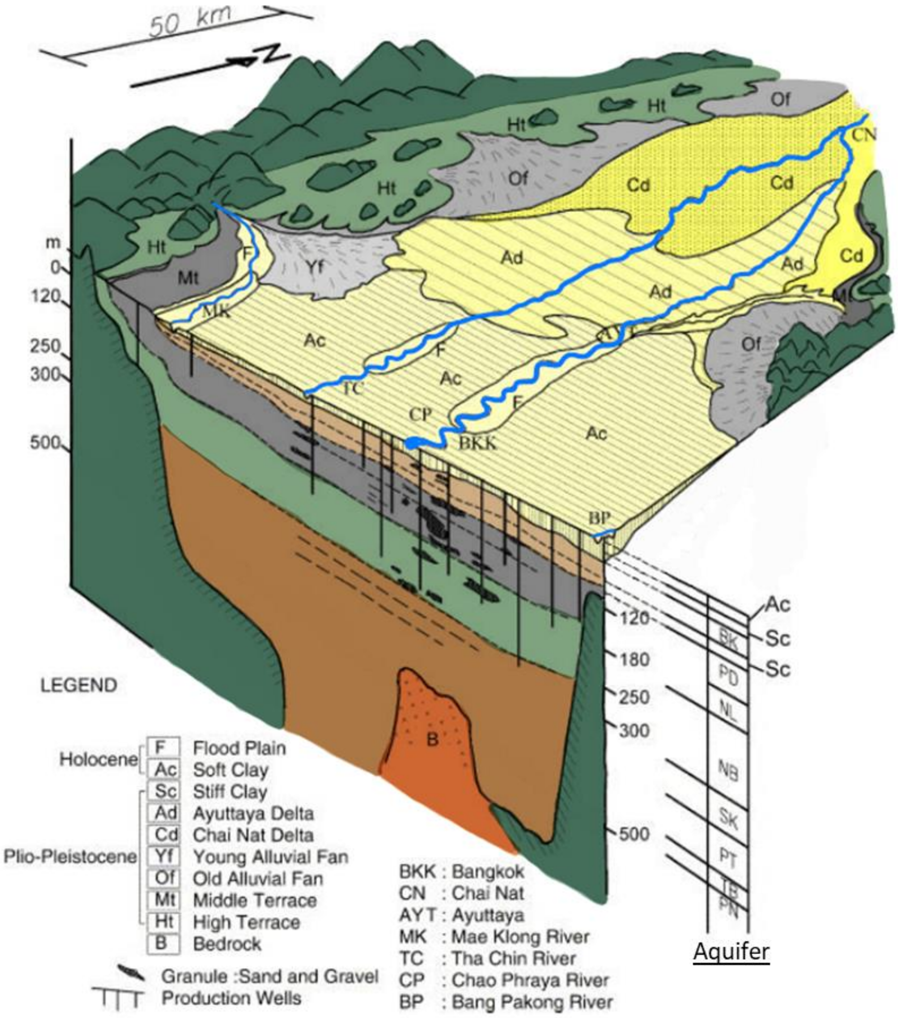

Figure 7 Thon Buri Basin and sediment deposition (modified from Phien-wej et. al, 2006; JICA, 1995).

Bangkok's main aquifers are composed of sand, gravel, and clay, with soft clay sitting on top of rigid clay, as shown in Figure 7. The first layer is the Bangkok Aquifer (BA) about 50 m depth zone, the second layer is Phra Pradaeng Aquifer (PD) about 100 m depth zone, the third layer is Nakorn Luang Aquifer (NL) about 150 m depth zone, the fourth layer is Nonthaburi Aquifer (NB) about 200 m depth zone, the fifth layer is Sam Khok Aquifer (SK) about 300 m depth zone, the sixth layer is Phraya Thai Aquifer (PT) about 350 m depth zone, the seventh layer is Thon Buri Aquifer (TB) about 450 m depth zone, and the last layer is Pak Nam Aquifer (PN) about 550 m depth zone. All aquifers are mainly sand and gravel interbedded with clay, according to log data from groundwater wells. The Bangkok clay stratigraphic sequence in the Thon Buri Basin is the most significant unit in terms of land subsidence (Sinsakul, 2000) because the Bangkok clay of the Quaternary Basin, which is composed of soft marine clay and ranges in thickness from 15 to 30 meters, is generally capable of producing any sort of land subsidence occurrence.

Bangkok City and the surrounding area likely experienced three separate types of land subsidence: local subsidence brought on by groundwater extraction; compaction subsidence brought on by a heavy construction load; and regional subsidence brought on by the thermal subsidence of the Thon Buri Basin. Land subsidence is especially prone to occur in Bangkok City's unconsolidated sediments, such as clay, silt, sand, and peat. Bangkok’s subsidence problem occurred in 1970 because of high population density and overuse of groundwater (Haley & Aldrich 1970; Brand and Paveenchana 1971; Edward 1976; Nutalaya 1981; Nutalaya, Chandra, & Balasubramaniam 1984), which led to the aquifer's water not instantly returning to its previous state. In 1970, the Royal Thai Survey Department (RTSD) installed the leveling benchmarks, and the maximum subsidence rate was detected at over 120 mm/year between 1978 and 1981 (Aobpaet et al. 2012). Moreover, the subsidence rate decreased by 35 mm/year between 1985 and 1988 and by 30 mm/year between 1988 and 1991 (Ramnarong 1983; Yong, Maathuis, and Turcott 1995; Ramnarong et al. 1998; Bontebal 2001; Phien-wej et al. 2006). The RTSD (2010) reported leveling results with maximum subsidence rates of 20 mm/year. Nowadays, new satellite technology can be used to monitor land motion in various regions. Since many years ago, the Interferometry Synthetic Aperture Radar (InSAR) time series approach has been utilized to monitor land deformation accurately and precisely. Therefore, the long-term investigation of ground surface deformation requires new technology to detect land subsidence in Bangkok, such as Aobpaet (2012), Piromthong (2015), Chaithavee (2015), Luachapichatikul (2019), and Pumpuang and Aobpate (2020), as shown in Table 2.

Table 2 Summary of InSAR research performed in the past on land subsidence in Bangkok and the surrounding region.

Researcher	Data	Period	Techniques	Analysis
A. Aobpate, 2012	19 images Radarsat-1	Oct 2005 - Mar 2010	PS and SBAS Time series	Groundwater and differential settling
S. Chaithavee, 2015	26 images TerraSAR-X	Sep 2009 - Aug 2012	PS and SBAS Time series	Groundwater
P. Piromthong, 2015	18 images ERS1 & ERS2	Feb 1996 - Jan 2000	PS and SBAS Time series	Groundwater
S. Luachapichatikul, 2019	80 images ASC 93 images DES Sentinel-1	Jan 2016 - 2019	PS-InSAR Time series	Geological subsidence
A. Pumpuang and A. Aobpate, 2020	9 images Radarsat-1	N/A	PS-InSAR Time series	Groundwater
This research	31 images AS 30 images DES Sentinel-1	Jan 2020 – May 2023	PS-InSAR Time series	Geology and Depositional Environment

Aobpaet (2012) studied land subsidence in Bangkok and the surrounding area using the InSAR time series techniques for measuring land subsidence and evaluating the combination of PS and SBAS methods. The study area covers Bangkok, Pathumthani, Nonthaburi, and Samutprakarn. The result of Radarsat-1 images from October 2005 to March 2010 shows a maximum relative subsidence rate of around 30 mm/year, and compared with the leveling benchmarks, it was found that the InSAR result has a slower rate due to the phase unwrapping issue. Despite its limitations, InSAR can be used as a geodetic.

Piromthong (2015) used InSAR time series techniques to study Greater Bangkok. This study aims to monitor the land subsidence of a 10,000 sq. km. area in Bangkok from February 1996 to January 2000. Using ERS1 and ERS2 images with PS and SBAS time series and validation with GNSS leveling to analyze the subsidence rate and combine it with others (Aobpaet, 2012; Chaithavee, 2015), The result of the vertical velocity rate during 1996–2012 varied from 0 to -30 mm/year depending on the area, which is a high subsidence rate in the density of the residence area. However, the results do not agree with some point results from GNSS leveling because of phase unwrapping inaccuracy and atmospheric correlation.

Chaithavee (2015) used TerraSAR-X images from September 2009 to August 2012 to study the eastern part of Bangkok using InSAR time series techniques. The objective is to investigate the subsidence trend in eastern Bangkok and combine this result with the results of Radarsat-1 images from 2005–2010 (Aobpaet, 2012) to find the relationship between velocity rate and groundwater factor. This study had the same limitations as Piromthong (2015), but the scatterer point had a high density due to the X-band satellite’s high resolution.

Luachapichatikul (2019) studied land subsidence in the western part of Bangkok using Sentinel-1 images from 2016 to 2019 using PS-InSAR time series techniques and validation with benchmark points. The goals are to analyze the subsidence rate in western Bangkok and to assess Sentinel-1 time-series performance from descending and ascending orbits. The result shows a maximum relative subsidence rate of around 20 mm/year in western Bangkok. The limitation is high decorrelation in agricultural areas such as Chachoengsao and Nakhon Nayok.

Pumpuang and Aobpaet (2020) monitored land subsidence in eastern and western Bangkok using Radarsat-2 images. The result displayed the highest subsidence in the east more than in the west because large industrial estates in eastern Bangkok are to blame for the excessive groundwater extraction. The limitation is low PS points in agricultural areas, and the number of SAR images is too small and does not have the details of the collection period.

In previous research using the InSAR time series techniques to study land subsidence in Bangkok and surrounding areas, three researchers combined the persistent scatterer (PS) and small baseline (SBAS) methods (Aobpaet, 2012; Piromthong, 2015; Chaithavee, 2015), but this research and two other researchers (Luachapichatikul, 2019; Pumpuang and Aobpaet, 2020) used only the persistent scatterer method. Every previous study, including this one, used a different acquisition time and number of satellite images. However, all previous InSAR research found that the limits of the InSAR techniques did not agree with the geodetic station at some point because of the atmospheric decorrelation and the unwrapped phase inaccuracy. The PS-InSAR time series technique can be used to measure and track ground surface movement on Earth (Aobpaet, 2012; Piromthong, 2015; Chaithavee, 2015; Luachapichatikul, 2019; Pumpuang and Aobpate, 2020). Furthermore, the objective of this research is to compare land motion in Bangkok City with different depositional environments, such as Chiang Mai City, which is experienced in land motion because of the geological setting but does not have the previous InSAR research using the InSAR time series techniques to study the motion in Chiang Mai City. Thus, this research will measure the motion in Chiang Mai and Bangkok using the Sentinel-1 InSAR time series technique and compare the motion in Chiang Mai and Bangkok related to depositional environments.

2.3 Synthetic Aperture Radar (SAR)

Radio detection and ranging (Radar) is a term used to describe both a process and a piece of technology. Active remote sensing devices, like radar, measure the backscattered signal by sending a pulse of electromagnetic radiation toward the surface of the Earth. Backscatter is the portion of the dispersed radiation that is focused on the radar receiver. An object scatters an incident pulse with different intensities and scattering patterns in all directions, depending on the incident direction. The electrical and physical characteristics of the target determine the measured backscattered signal's phase and amplitude. The radar approach uses the two-way travel time of the generated pulse, which includes the journey to the target and the journey back to the receiver, to determine the detected objects' backscatter intensity and range (the spacing between the target and radar).

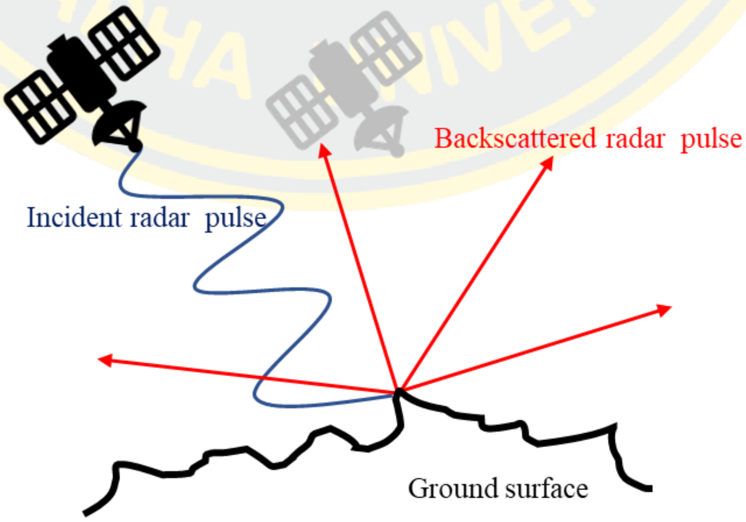

Figure 8 An antenna sends out a radar pulse to the ground, which is then returned to the antenna by ground reflection.

The microwave imaging technology known as Synthetic Aperture Radar (SAR) employs a side-looking scanning geometry, which causes the pulses it releases to obliquely impact the ground surface. Also, it can penetrate clouds and operate both during the day and at night. SAR creates a longer antenna out of the forward motion of the satellite, increasing the spatial resolution of the images. The SAR image, which looks like a mosaic of pixels, is made up of successive pulses of waves. Each pixel outputs a complex integer that contains the incoming signal's amplitude and phase information from that resolution cell (pixel).

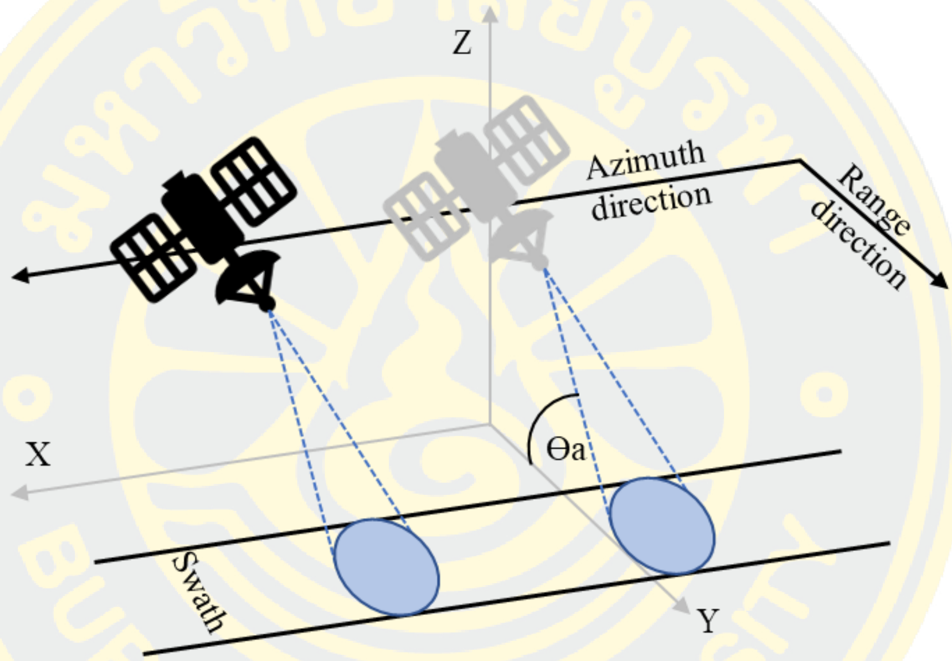

Figure 9 The synthetic aperture radar geometry.

A 2D grayscale reflectance map represents the detected SAR image. Targets with an effective backscattered signal, like exposed land and residence areas, seem bright in comparison to flat surfaces, which appear dark because the radiation is primarily reflected away from the radar. Range and azimuth, the two dimensions of the image, correspond to cross-track and along-track directions in satellite geometry.

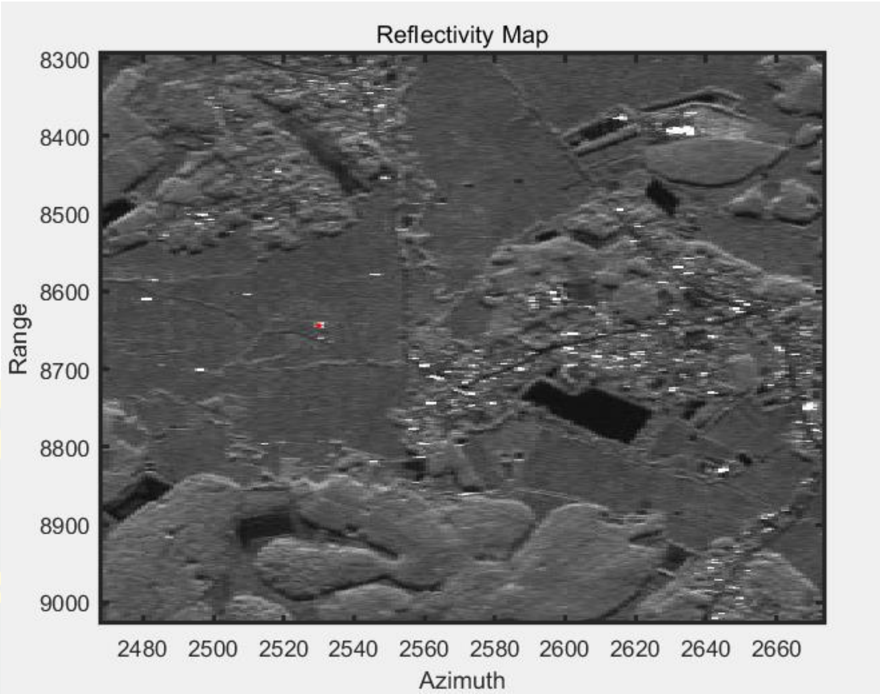

Figure 10 A SAR Image shows residence areas appear bright, the lake appears dark, and vegetated areas appear medium tone.

Each pixel's phase corresponds to the difference in phase between the transmitted and received signals. Since the phase of the outgoing wave is known, the phase of the returning wave can be compared. The phase of the received signal is related to the distance between the sensor and the target because the length of the path between the sensor and the target is composed of whole wavelengths plus certain portions of wavelengths. Accurate measurements are made of this additional wavelength component. It is possible to generate the topography and track changes in the terrain by taking advantage of the difference in phase between a pair of SAR images obtained from slightly different perspectives.

For SAR satellite operation, the L-band, X-band, C-band, S-band, and P-band are domain frequencies. The usage of various frequencies is based on their various advantages; for example, lower frequencies correspond to longer wavelengths that may penetrate thick vegetation. The L-band satellites such as ALOS, ALOS-2. The X-band satellites such as TerraSAR-X, Cosmo-SkyMed. The C-band satellites such as ERS-1/2, Sentinel-1. The S-band satellite is HJ-1C and the P-band satellite is BIOMASS. The SAR missions from 1980 to 2025 are shown in Figure 12.

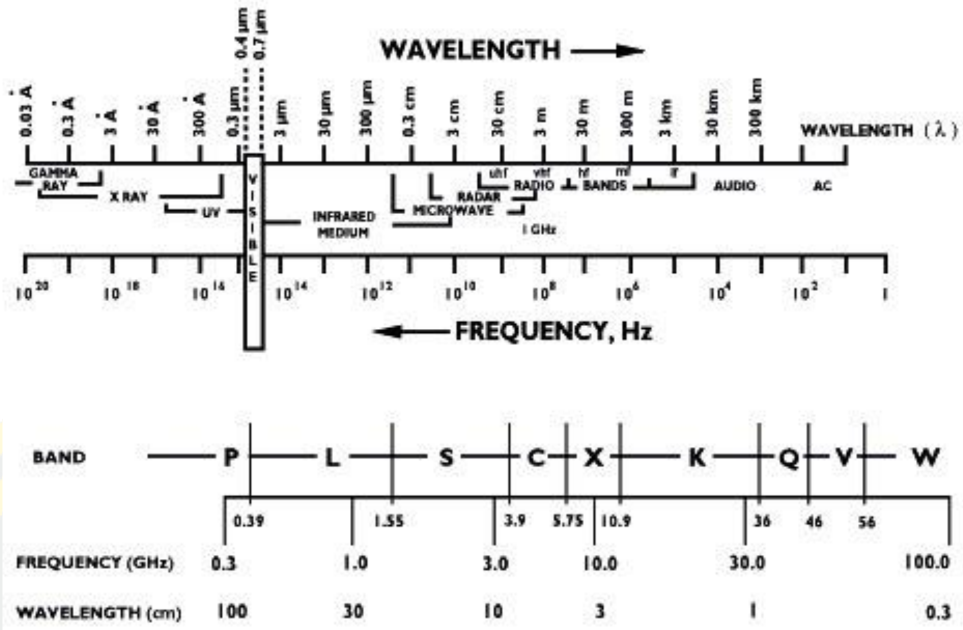

Figure 11 The spectrum of electromagnetic radiation and the bands of radar (created by ESA, 2023).

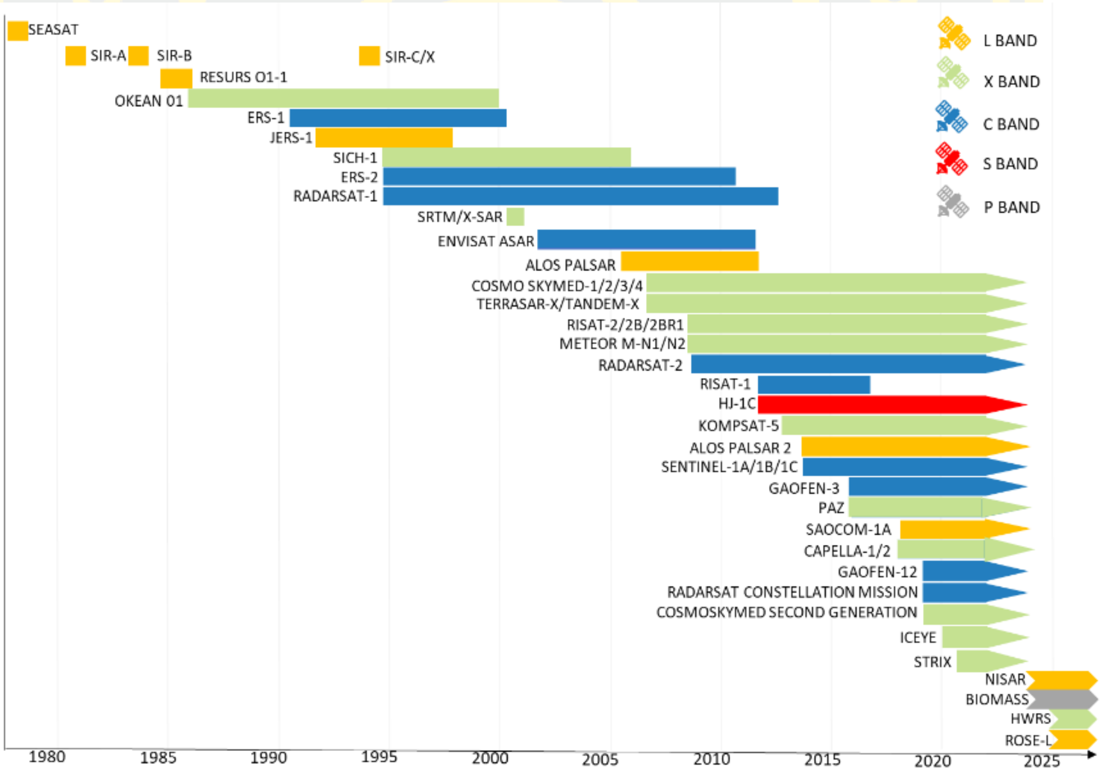

Figure 12 History of SAR missions, including its primary characteristics from 1980 to 2025 (created by Detektia, 2023).

2.4 Synthetic Aperture Radar Interferometry (InSAR)

InSAR uses the phase difference between two image acquisitions, which can be interpreted as surface displacement or as changes in the Line of Sight (LoS). This method has a high level of precision and dependability for identifying even the smallest changes on the surface using distinct phase measurements from transmitted-received system satellite SAR data (Beladam et al., 2019). Furthermore, SAR interferometry is an important technology that uses two components on each pixel (amplitude and phase), which describe the distance between the sensor and the object and the intensity of backscattering (Figure 13).

SAR interferometry has been successfully used to measure deformation with reliable source parameters and high resolution for monitoring and mapping land subsidence, landslides, land displacement caused by earthquakes or volcanoes, and measuring flow rates of large ice sheets. If the phase difference is a result of ground surface deformation, the InSAR system can capture the phase difference of a SAR picture many times on the same object. After processing a pair of images, the image with colored fringes, known as the "flattened interferogram", illustrates the difference in phase values between the first and second acquisitions. The colors range from -π to π.

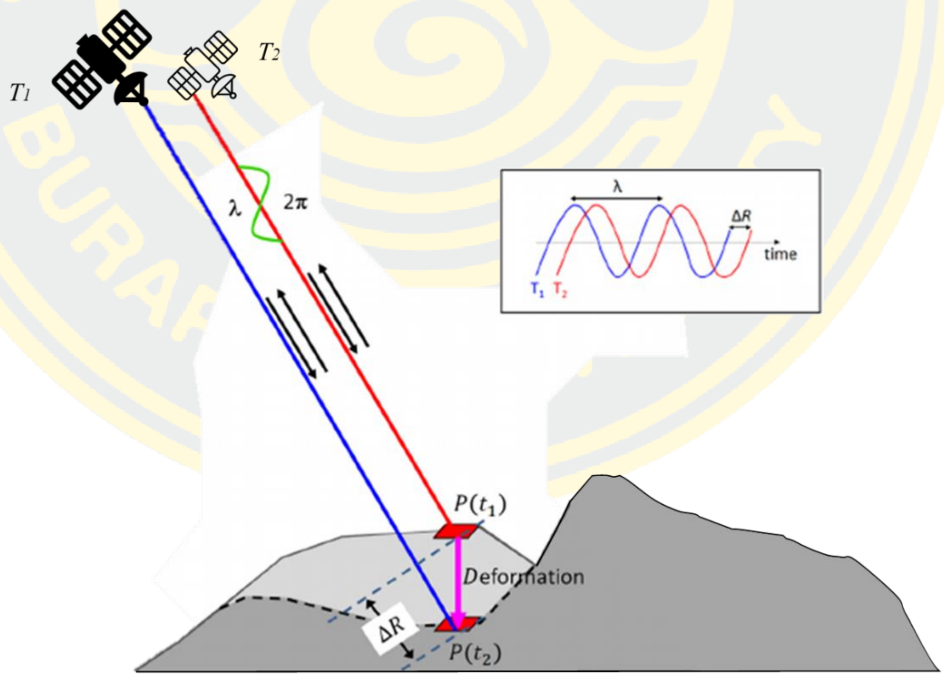

Figure 13 The Interferometric Synthetic Aperture Radar basic concept (modified from Sousa & Bastos, 2013).

The phase and amplitude of the pulse are transmitted by the SAR system, and after that, the phase difference between two SAR images can describe the movement of the land. The phase difference ($\Delta\phi$) represents the Earth's surface movement, as shown in Equation 1. But to measure the movement of land in a satellite's line of sight, the interferometric phase must first be unwrapped to calculate the deformation. The fundamental InSAR principle is applied to identify the ground deformation by using two images for processing the phase difference, known as differential SAR interferometry (DInSAR). The phase difference ($\Delta\phi$) is the result of several factors, including mistakes in satellite positioning and topography, which affect deformation readings (Ferretti et al., 2001; Kampes et al., 2001). Furthermore, the deformation signal is degraded by atmospheric delay, as shown in Equation 2.

$$\Delta\phi = \phi 1 - \phi 2 = \frac{4\pi}{\lambda}\,\Delta r \qquad \text{Equation 1}$$

where
$\phi 1$, $\phi 2$: the phase of each acquisition
Δr: the difference in range (LOS) between two SAR acquisitions
λ: wavelength of the radar

$$\Delta\phi = \phi def + \phi orbit + \phi topo + \phi noise + \phi atm \qquad \text{Equation 2}$$

where
$\Delta\phi$: interferometric phase (or phase difference)
ϕdef: phase contribution related to ground deformation
ϕorbit: Orbit Error
ϕtopo: Topographic Effect
ϕnoise: Noise
ϕatm: Atmospheric Delay

2.5 Persistent Scatterer (PS)-InSAR for land displacement estimation

Persistent Scatterer Interferometric Synthetic Aperture Radar (PS-InSAR), an advancement over DInSAR, was pioneered in Milan by Ferretti et al. in 2001. This innovative technique leverages coherent radar targets with stable characteristics that remain identifiable across multiple radar images, facilitating their utility in analytical applications (Ferretti et al., 2001). These radar targets, often referred to as "persistent scatterers," derive their name from their enduring properties. Notably, PS-InSAR effectively mitigates atmospheric interference by harnessing the stability of these persistent scatterers in its measurements.

The primary processing steps in the PS-InSAR technique encompass several key stages. First, it involves the creation of a single master stack interferogram. This master stack serves as a reference for subsequent analyses. The process continues with the removal of the topographic phase, followed by the selection of Persistent Scatterer Candidates (PSC) based on an amplitude dispersion index. This index selects PSCs by considering the standard deviation ratio, which is determined by the amplitude values of the scatterers. Notably, this selection process accounts for the fact that strong scatterers with high amplitudes yield significantly lower phase change induced by noise at the same level as compared to weak scatterers with low amplitudes.

Once the master image is estimated, the next step involves calculating the Atmospheric Phase Screen (APS). This APS is pivotal in subsequent computations, as it allows for the generation of all interferograms by averaging out the residual atmospheric effects. The PSCs form a spatial network, and velocities can be calculated for each PSC by removing any extraneous signals from the observations, assessing the Digital Elevation Model (DEM) error, and estimating the APS, as outlined by Ferretti et al., (2001).

Land displacement in the Line of sight (LoS) component distinguishes between stable and unstable areas. The temporal coherence and reflectivity properties of items on the ground surface affect PS dispersion. Nevertheless, the one drawback of the spatial density of stable points is that it can only supply a few points in vegetated regions and hundreds of stable points per square kilometer in urban areas (Perissin & Wang, 2011). More steady scatterers can be generated by efficient PS in urban regions with man-made structures than in non-urban settings. In rural areas, stable points like man-made structures are less evident, and in the event of land displacement, the deformation velocity rate alternative may not be enough. When natural terrain is insufficient, high backscatter in man-made buildings with enough coherence reflects backscatter from the target (Chang et al., 2010).

The temporal evolution of ground movement is further analyzed through time series data at Persistent Scatterer locations, providing valuable insights into deformation patterns (Hooper et al., 2007). This technology has found wide-ranging applications, including the monitoring of urban subsidence, landslides, and volcanic activity (Crosetto & Monserrat, 2016). In the context of urban subsidence, PS-InSAR allows for the detection and measurement of ground deformations with millimeter-level precision over large areas. This capability is crucial for urban planners and authorities to assess the stability of infrastructure and mitigate potential risks to buildings and transportation networks. Studies such as those by Ferretti et al. (2011) and Li et al. (2015) showcase the effectiveness of PS-InSAR in monitoring urban subsidence, providing valuable insights into the causes and rates of ground movement.

Landslide monitoring is another area where PS-InSAR excels. The technique enables the identification of deformation patterns on slopes, allowing for early detection of potential landslide-prone areas. Cascini et al. (2011) and Tofani et al. (2019) have demonstrated the applicability of PS-InSAR for landslide monitoring, emphasizing its role in hazard assessment and risk management. The high spatial and temporal resolution of PS-InSAR provides a comprehensive understanding of landslide dynamics and helps in developing effective mitigation strategies.

In the realm of volcanic activity, PS-InSAR has become an indispensable tool for monitoring ground deformation associated with volcanic processes. The technique allows for the identification of precursory signals and the quantification of volcanic subsidence or uplift. Studies such as those by Hooper et al. (2007) and Biggs et al. (2014) highlight the significance of PS-InSAR in tracking volcanic deformation, contributing to the assessment of volcanic hazards and aiding in early warning systems.

PS-InSAR principles and applications reveal a nuanced comprehension of its strengths and limitations. This technique can significantly investigate land displacement monitoring, offering invaluable insights for environmental management, infrastructure planning, and hazard mitigation. PS-InSAR has demonstrated its effectiveness in monitoring urban subsidence, landslides, and volcanic activity, as evidenced by numerous studies. These applications underscore the versatility of PS-InSAR and its role in providing crucial information for assessing hazards, managing risks, and informing decision-making in the context of various geohazards.

CHAPTER 3
MATERIAL AND METHODOLOGY

3.1 Study area

The capability of land displacement and monitoring is increased by identifying the various sites of the depositional environment. Bangkok is the case study in the deltaic plain environment, and Chiang Mai is the case study in the basin plain environment.

3.1.1 Bangkok

Bangkok, Thailand's capital, has a central location and covers around 1,569 square kilometers. Bangkok City is a floodplain and deltaic plain that connects to the Gulf of Thailand in the south. The altitude of the Chao Phraya River delta averages 1.5 meters above sea level.

The research areas cover Bangkok City's area of around 1,385 square kilometers, which intersects an area of 3,000 square kilometers of descending track and 2,700 square kilometers of ascending track. These areas are bounded by latitudes 13.634–13.916°N and longitudes 100.374–100.787°E. Most of the study area is in the Bangkok Plain, which has a geological environment where active neotectonic activity is important in regulating the evolution of basins.

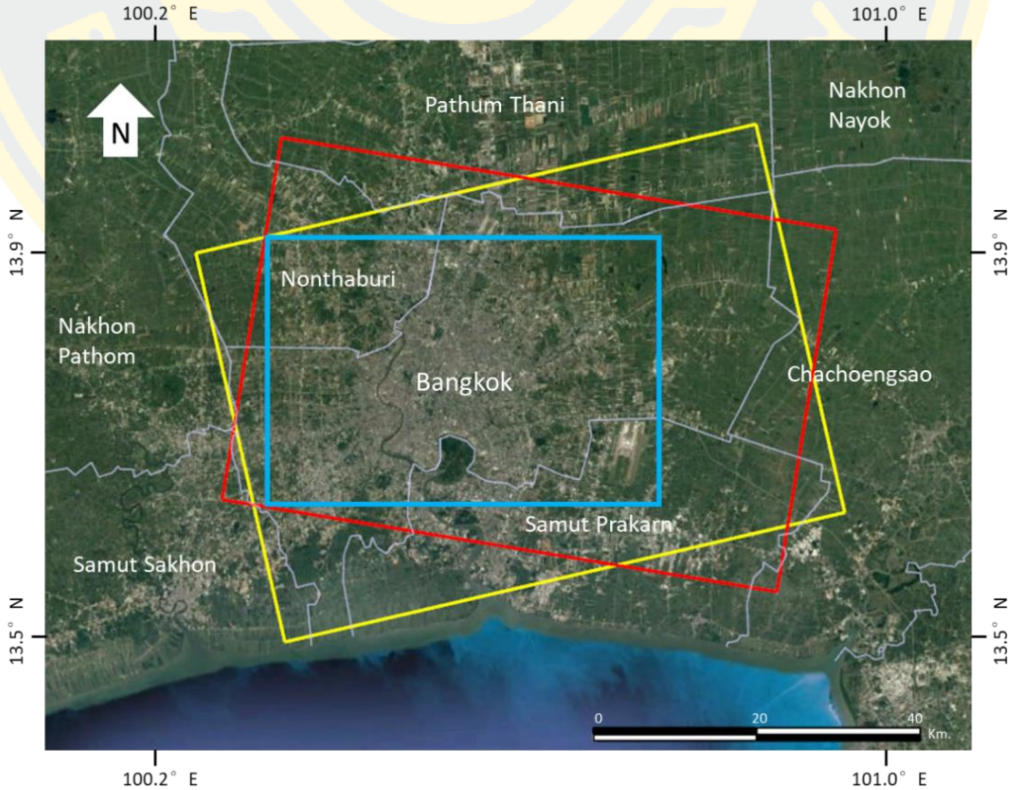

Figure 14 Bangkok study area (blue box) with Sentinel-1A footprint of descending track (red box) and ascending track (yellow box).

3.1.2 Chiang Mai

Chiang Mai province has an area of 20,107 square kilometers and is located in northern Thailand. The topography is a high mountain range with sporadic plateau sections. The mountains are approximately 1,500–2,000 meters above sea level. Mueang Chiang Mai District, Hang Dong District, San Patong District, San Kamphaeng District, San Sai District, and Saraphi District are the plains along the river basin in the center of the region. It stands 310 meters above sea level.

The research areas cover Chiang Mai City's area of around 1,405 square kilometers. All the area is in Chiang Mai and some parts of Lamphun province. The area of interest intersects between the descending track, with 2,410 square kilometers, and 1,985 square kilometers of the ascending track. These areas are bounded by latitudes 18.824806–18.511480°N and longitudes 98.800152–99.181851°E. Based on a satellite image, the NNE-SSW trending fault line is clearly visible in the steep and mountainous terrain and is the most important tectonic feature in the research region. It is a normal fault at the basin edge that is currently active. This fault is connected to tertiary extensional basins made up of the Chiang Mai basins and extends from west to east.

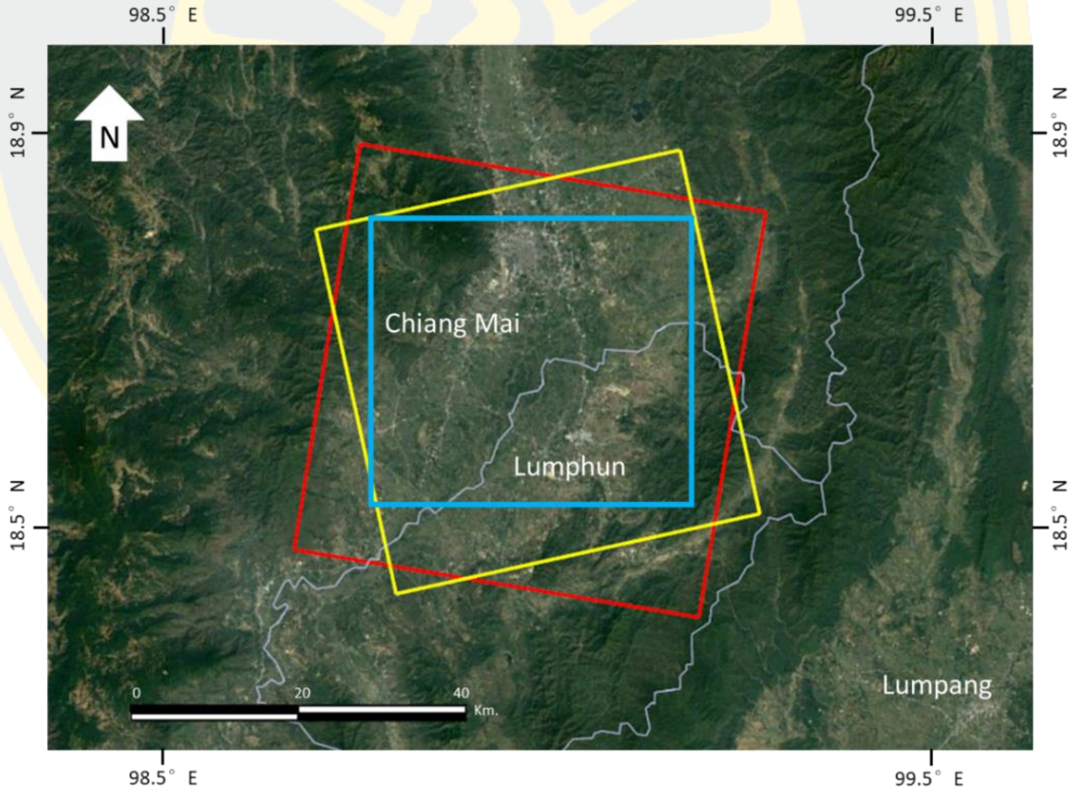

Figure 15 Chiang Mai study area (blue box) with Sentinel-1A footprint of descending track (red box) and ascending track (yellow box).

3.2 Data set

Sentinel-1 SAR images

Sentinel-1A SAR images for the study area were obtained from the Copernicus website, which is the European Union's Earth observation programme. The C band with Single Look Complex (SLC) data has a wavelength of 5.547 centimeters. An interferometric wide swath length of 250 kilometers with a resolution of 5x20 meters. All the images were selected: 61 images from 2020 to 2023 in the Bangkok City area, as well as 62 images from 2020 to 2023 in the Chiang Mai City area, as shown in Table 3.

Table 3 Property of the SAR images in the Bangkok area and the Chiang Mai area.

Area	Bangkok	Chiang Mai
Acquisition period	11/01/2020 - 19/05/2023	16/01/2020 - 24/05/2023
Number of scenes	61	62
Normal baseline	<200	<200
Orbit	Descending and Ascending	
Mode	Interferometric Wide swath (IW)	
Type	Single Look Complex (SLC)	
Level	1	
Polarization	Vertical-Vertical (VV)	

Bangkok city area was captured by a descending orbit with 30 SAR images and an ascending orbit with 31 SAR images from January 2020 to May 2023. Chiang Mai City and rural areas were captured by a descending orbit with 32 SAR images and an ascending orbit with 30 SAR images from January 2020 to May 2023. Both areas show the details of the dataset in the PS-InSAR method in Figures 16 and 17.

In the standard and temporal baseline of the PS-InSAR pre-processing of Bangkok and Chiang Mai Cities, the interferometric was shown as a star graph, with each point displaying the image and each link an interferogram. The dataset's time correlation can be entirely guaranteed with a minimum time interval of 12 days. The normal baseline of the Bangkok dataset and the Chiang Mai dataset is less than 200 meters. In order to eliminate errors and atmospheric influences, the short baseline can enable accurate registration and good coherence. The maximum Doppler centroid parameter of the Bangkok dataset is less than 0.15 Hz/PRF and less than 0.1 Hz/PRF in the Chiang Mai dataset.

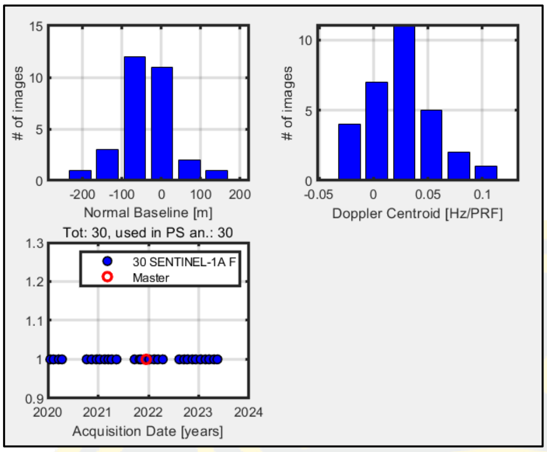

(a)

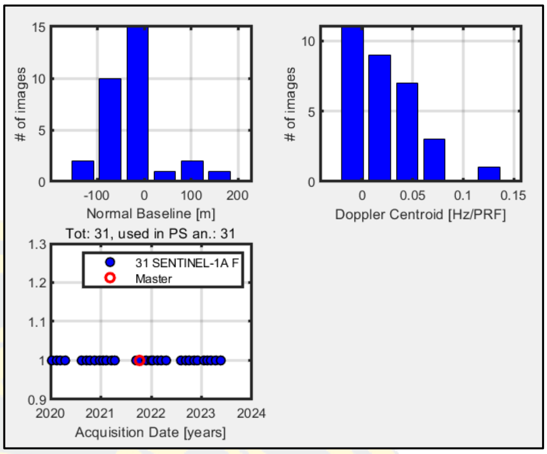

(b)

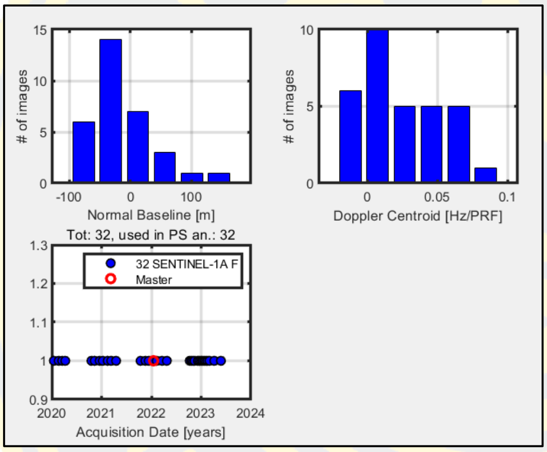

(b)

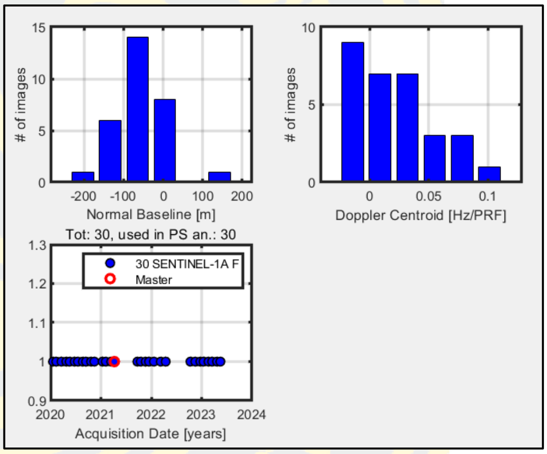

(d)

Figure 16 The detail of the dataset in the PS-InSAR method (a) Descending orbit of Bangkok (b) Ascending orbit of Bangkok, (c) Descending orbit of Chiang Mai, and (d) Ascending orbit of Chiang Mai.

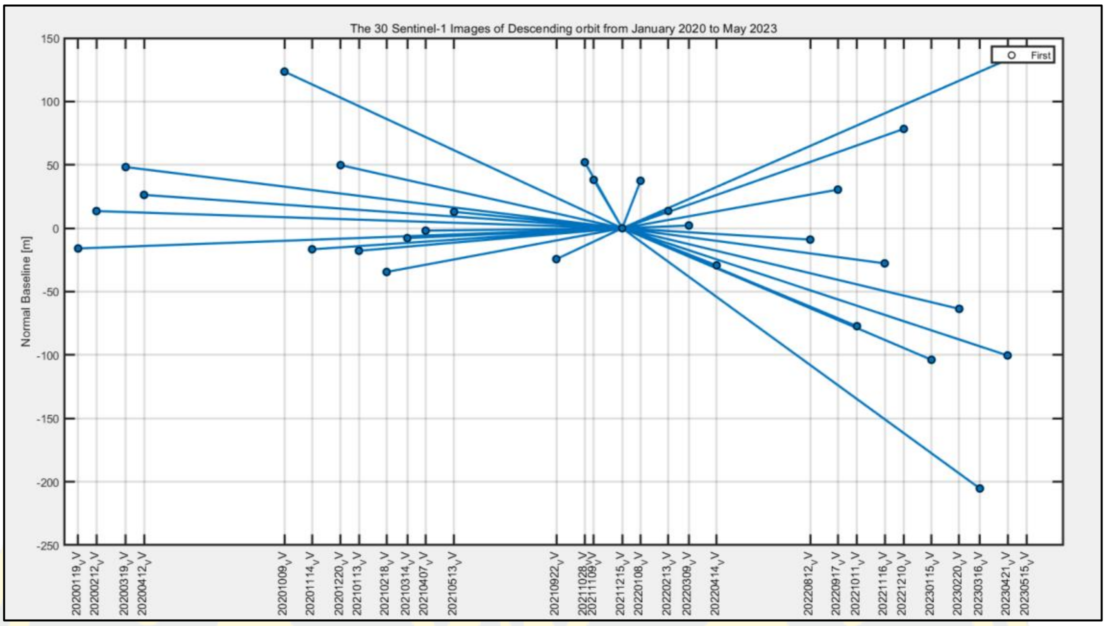

The 30 Sentinel-1 Images of Descending orbit from January 2020 to May 2023
Normal Baseline [m]
First
150
100
50
0
-50
-100
-150
-200
-250
20200119_V
20200212_V
20200319_V
20200412_V
20201009_V
20201114_V
20201220_V
20210113_V
20210218_V
20210314_V
20210407_V
20210513_V
20210922_V
20211028_V
20211109_V
20211215_V
20220108_V
20220213_V
20220309_V
20220414_V
20220812_V
20220917_V
20221011_V
20221116_V
20221210_V
20230115_V
20230220_V
20230316_V
20230421_V
20230515_V

(a)

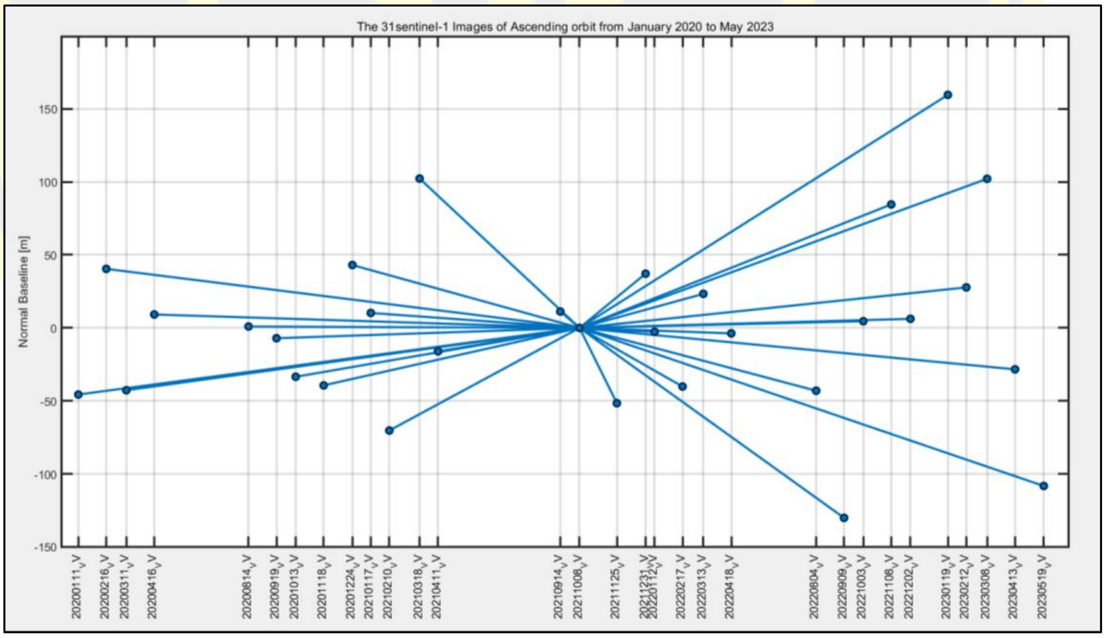

The 31sentinel-1 Images of Ascending orbit from January 2020 to May 2023
Normal Baseline [m]
150
100
50
0
-50
-100
-150
20200111_V
20200216_V
20200311_V
20200416_V
20200814_V
20200919_V
20201013_V
20201118_V
20201224_V
20210117_V
20210210_V
20210318_V
20210411_V
20210914_V
20211008_V
20211125_V
20211231_V
20220217_V
20220313_V
20220418_V
20220804_V
20220909_V
20221003_V
20221108_V
20221202_V
20230119_V
20230212_V
20230308_V
20230413_V
20230519_V

(b)

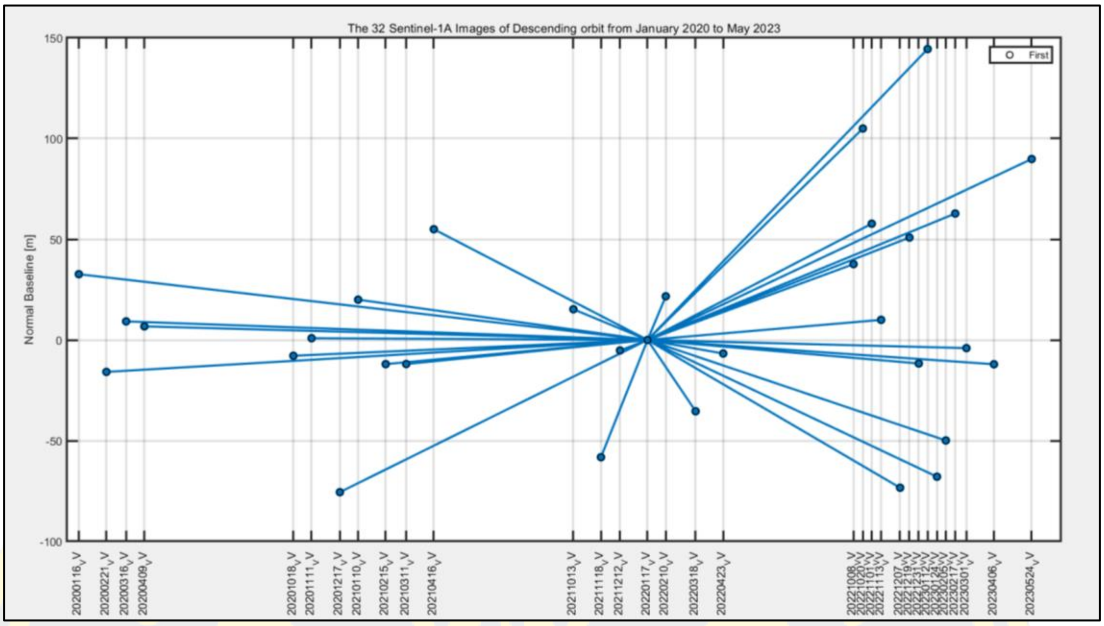

(c)

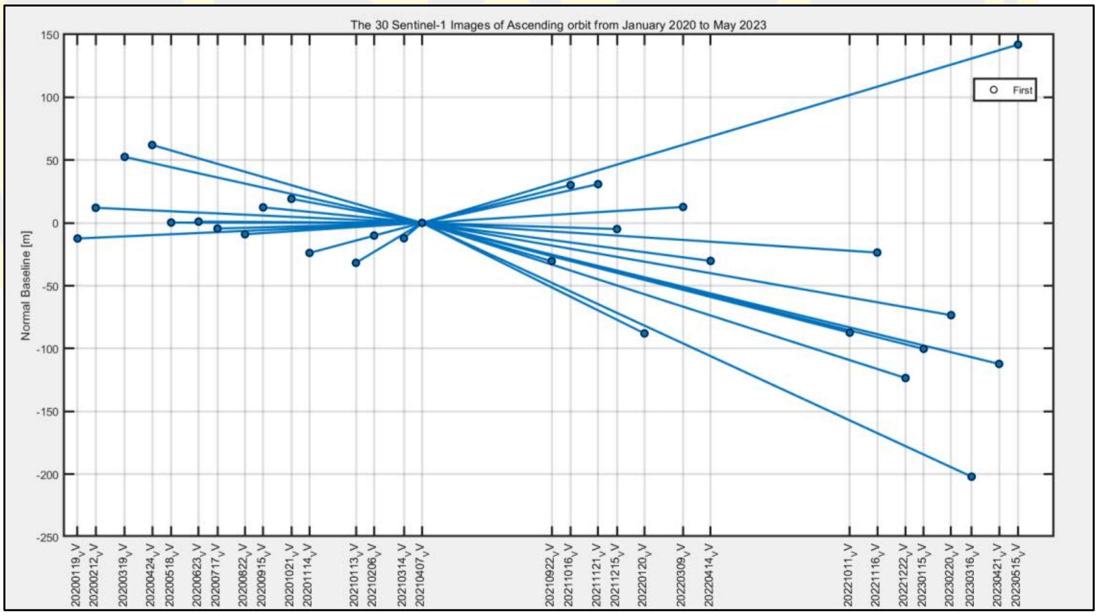

(d)

Figure 17 The detail of the dataset in the PS-InSAR method (a) The total number of Sentinel-1A descending from Bangkok with 30 images, (b) The total number of Sentinel-1A ascending from Bangkok with 31 images, (c) The total number of Sentinel-1A descending from Chiang Mai with 32 images, and (d) The total number of Sentinel-1A ascending from Chiang Mai with 30 images.

The time component was the focus of this investigation by collecting images simultaneously in both the Chiang Mai and Bangkok regions. However, it is important to note that due to variations in satellite footprints across different time periods, there are instances where data for analysis is missing. Nevertheless, the overall quality of the collected images remains adequate to effectively illustrate land deformation occurring in both the Bangkok and Chiang Mai areas.

3.3 Methodology

PS-InSAR time-series technique

The PS-InSAR method uses the strong stable point to minimize the impact of the atmosphere and geometric correlation. This technique can detect land displacement with comparatively high precision in the line-of-sight velocity (Perissin, 2008). The approach entails pre-processing, processing (geocoding), and InSAR processing, as shown in Figure 18. Moreover, SARPROZ software typically follows a well-defined methodology to monitor land displacement over time. Below, the outline a general methodology for PS-InSAR analysis using SARPROZ.

After successfully acquiring all the Sentinel-1 data, the initial phase of the PS-InSAR methodology is the pre-processing stage. This critical step involves the meticulous selection of an appropriate master image from the images captured in SLC-IW mode, obtained from both descending and ascending orbits. The selection process is driven by a rigorous assessment of geometric and temporal alignment, adhering to the specified normal baseline criteria. A meticulous orbit correction process is executed to enhance precision. Subsequently, the area of interest is defined, and the co-registration process is carried out. This involves detailed pixel-to-pixel comparisons between the master and slave images to ensure not only accurate noise reduction but also the precise calculation of phase differences.

In the second phase of the process, preliminary and geocoding processing steps are undertaken to generate InSAR data. This involves creating a reflectivity map and an amplitude stability index, utilizing the local maxima option to identify potential Persistent Scatterer Candidates (PSC) within a sparse point mask. Subsequently, ground control points (GCPs) are carefully chosen to extract topographic influences and integrate an external Digital Elevation Model (DEM), like the Shuttle Radar Topography Mission (SRTM) 1 arcsec data. Notably, GCP selection is restricted to areas unaffected by ground movements to ensure accurate identification of Persistent Scatterers, and the external DEM aids in projecting SAR data into geographic coordinates while correcting for geometric errors.

The third stage in SARPROZ encompasses critical InSAR processing steps: interferogram processing, Atmospheric Phase Screen (APS) estimation, and sparse point processing. Interferogram processing initiates with coherence calculation, followed by generating interferograms that capture phase differences between SAR images captured at different times. APS estimation is pivotal for correcting atmospheric disturbances, and phase unwrapping is subsequently applied to transform wrapped phase values into continuous displacement measurements, considering temporal baselines for deformation rate sensitivity. Sparse point processing then focuses on identifying and analyzing radar targets, particularly PSC, by applying selection criteria, calculating the Amplitude Stability Index (ASI), establishing point connections, and implementing thresholding.

The displacement time series module was further developed by meticulously selecting a subset of the filtered coherent interferogram, allowing precise calculation of the deformation velocity rate at each point along the Line of Sight (LoS) in millimeters per year. This comprehensive result comprises velocity, displacement time series, cumulative displacement, height, height above the ground, and temporal coherence. The evaluation of phase residual dispersion through temporal coherence proves crucial in result identification. The velocity of stable points and the assessment of susceptibility zones are effectively visualized using Google Earth software. Collectively, these InSAR processing steps enhance the accuracy and reliability of ground deformation, making SARPROZ a valuable tool for applications in geology, environmental monitoring, infrastructure assessment, and more.

Following the processing of Sentinel-1 data, areas of land deformation that piqued interest were identified through statistical analysis, accompanied by visual representations such as images and graphics. Subsequently, the comparison of displacement data from Sentinel-1 images captured in both descending and ascending orbits was necessary to validate the observed trends in land displacement. This displacement data is meticulously presented by latitude, longitude, and elevation, providing a high-precision assessment of land deformation rates. To gain deeper insights and evaluate the regions of deformation, this study integrated the PS-InSAR data with geological and morphological information through GIS analysis. This holistic approach enables us to refine and update existing land motion maps based on this enriched dataset. Furthermore, these outcome layers serve as a foundation for conducting geological and morphological interpretations, allowing us to corroborate or refine the PS-InSAR estimates.

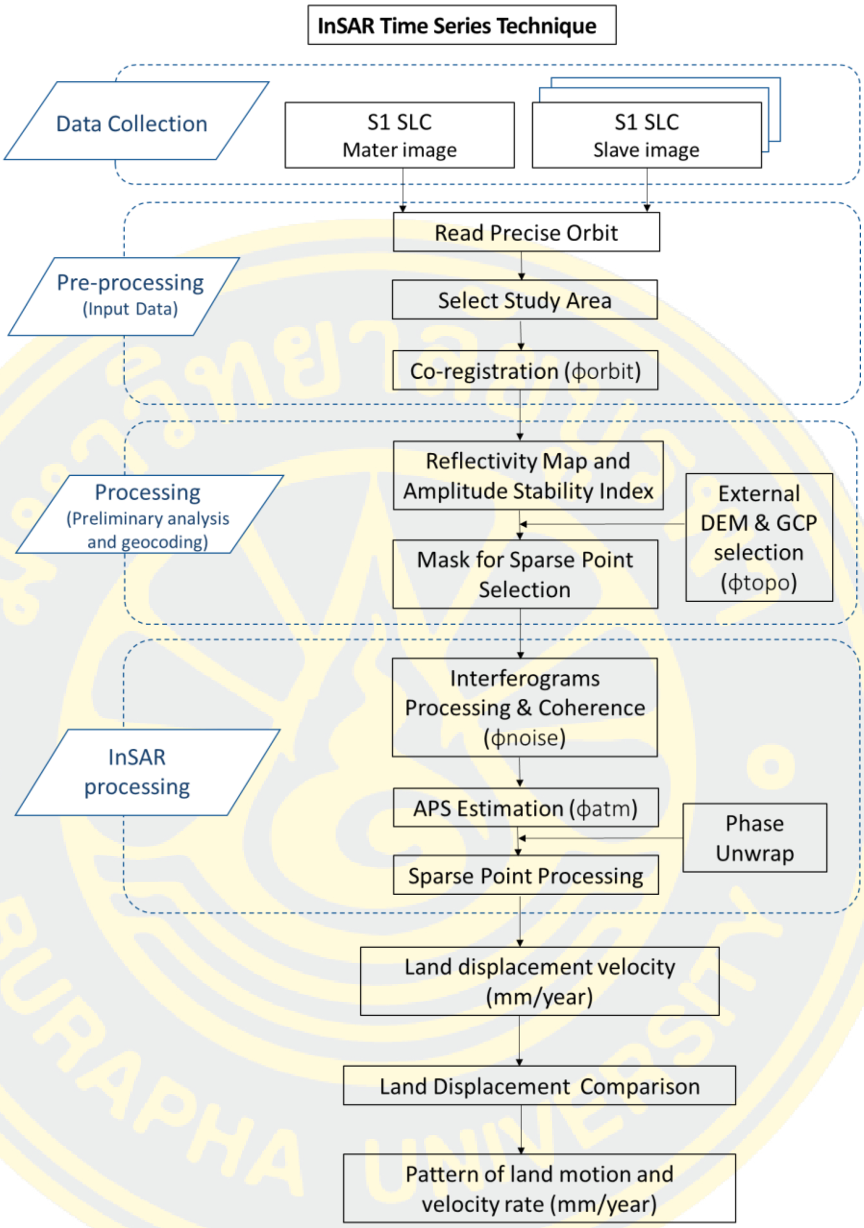

Figure 18 Research method workflow.

CHAPTER 4
LITERATURE REVIEW

The Sentinel-1 SAR image processing by SARPROZ software was used to provide a result and show the velocity map of stable points. The descending and ascending Sentinel-1 datasets at the SLC level can be obtained from platforms run by the European Space Agency (ESA). The land motion in descending and ascending orbits was processed by the PS-InSAR time series approach. The estimated movement of the land along the direction of the satellite or line-of-sight (LOS) is based on the measured persistent scatterer (PS) points. PS-InSAR analyzes the relative movement to the reference point, which was located in a study area that had strong coherence and was continuously constant throughout the time series. The velocity maps demonstrate positive movements toward the sensor, which can be seen in blue, and negative movements away from the sensor, which can be seen in red. Although the PS-InSAR time series techniques can identify various land deformations on the Earth's surface along the LOS direction, it is vital to remove the error or other effects such as orbit error, noise, atmospheric delay, and topographic effect. In order to measure the velocity of the land motion in the research region, a number of stages are included in the PS-InSAR time series processing.

After that, the relative displacement of points between descending and ascending PS-InSAR results was compared. Using the collected time series, the deformation velocity is estimated to create the deformation map. Several PS points are used to create the time-series deformation maps that were acquired. Each PS is connected to the estimated annual velocity (millimeters per year) across the studied period and the accumulation of displacement at each sensor collection date.

4.1 Bangkok Result from the PS-InSAR time series

The PS-InSAR was implemented to locate the main deformations in Bangkok City. The velocity map from the descending orbit was obtained from January 19, 2020, to May 15, 2023, and the ascending orbit covers the period from January 11, 2020, to May 19, 2023. The areas of interest on the descending and ascending tracks cover Bangkok City, some parts of Nonthaburi province in the northwest, and some parts of Samut Prakarn province in the southeast (see Figure 19). The estimated result indicates that the area of interest has great PS point coverage. The descending track found 376,697 PS points, and the ascending track found 350,912 PS points.

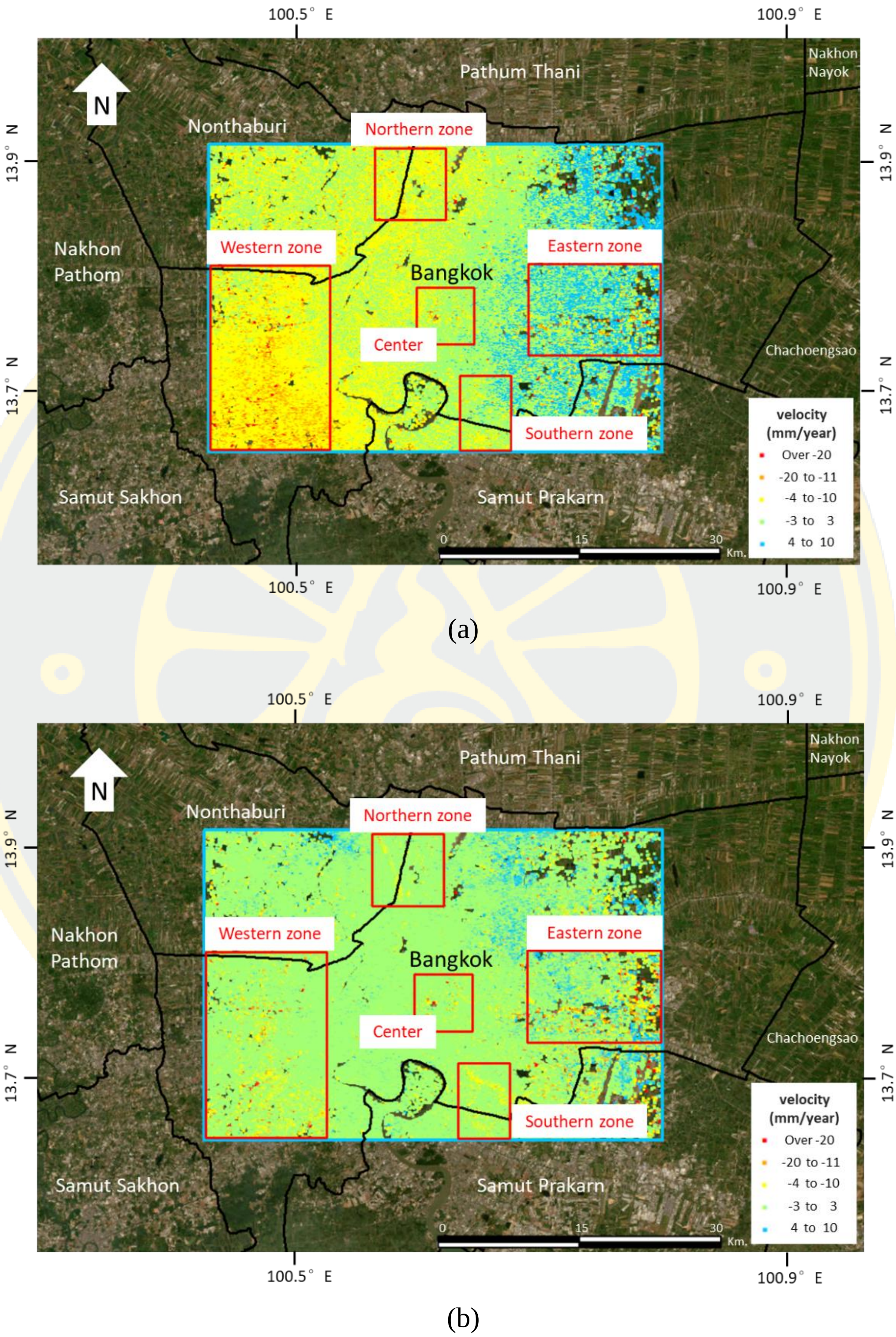

Figure 19 The deformation map of the area of interest from the descending orbit (a) and ascending orbit (b) in Bangkok.

The two stacks' results show that the area is steady (in green), and it can be observed that the deformation pattern is clearly defined with zones of ground deformation found in several locations in Bangkok and the surrounding area. The overview of Figure 19 reveals movement in the western part, the northern part near the Don Mueang International Airport, the center part, the southern part near the Chao Phraya River, and the east part near the Suvarnabhumi International Airport.

The data from the descending orbit and the ascending orbit both reveal negative velocity or motion away from the sensor, which is a sign of vertical motion known as subsidence. The most significant deformations, with values ranging from -12 to -24 mm/year of descending orbit and -11 to -22 mm/year from ascending orbit are observed in Western Bangkok in places like Phasi Charoen, Chom Thong, Bang Khae, Bang Bon, and Bang Khun Thain, as shown in Figure 20. It is evident that the motion exhibits great linearity, which makes it a suitable fit for the fundamental presumption of a linear deformation pattern.

Subsidence is also observed in the middle of the deformation map at three locations: the center zone of Bangkok, the northern zone near the Don Mueang International Airport, and the southern zone near the Chao Phraya River. Land motion in the northern zone (Lak Si and some parts of Nonthaburi province) is between -4 and -16 mm/year from the descending orbit and -5 to -12 mm/year from the ascending orbit, as shown in Figure 21. In the center zone, the subsidence found in the Huai Khwang and Wang Thong Lang areas ranges between -3 and -14 mm/year from the descending and ascending orbits, as displayed in Figure 22. Moreover, subsidence can be found in the southern zone of Bangkok. Especially at the boundary between Bangkok (Phra Khanong, Bang Na, and Pra Wet areas) and Samut Prakarn province, the negative velocities from the descending orbit are between -4 and -12 mm/year, and the negative velocities from the ascending orbit range between -3 and -11 mm/year, as can be seen in Figure 23.

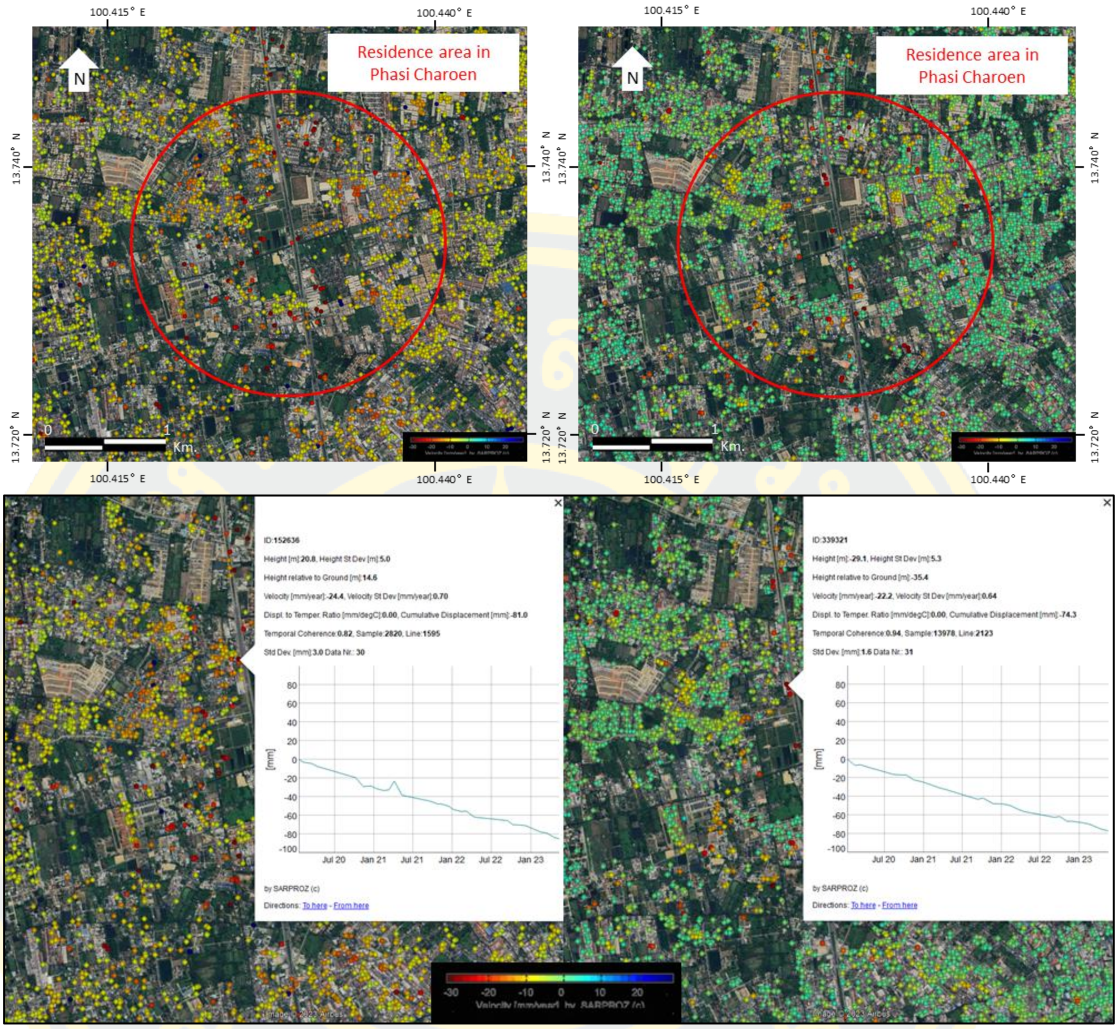

Figure 20 The time series of land displacement at two points in the western zone of Bangkok (Khet Phasi Charoen) from the descending track (left) and ascending track (right) shows the motion exhibits great linearity; the most significant deformations are in the residence areas, with maximum values of -24.4 mm/year from the descending track and -22.2 mm/year from the ascending track. The two stacks' results show the same subsidence trend, but the descending track has a 2.2 mm higher subsidence rate than the ascending track.

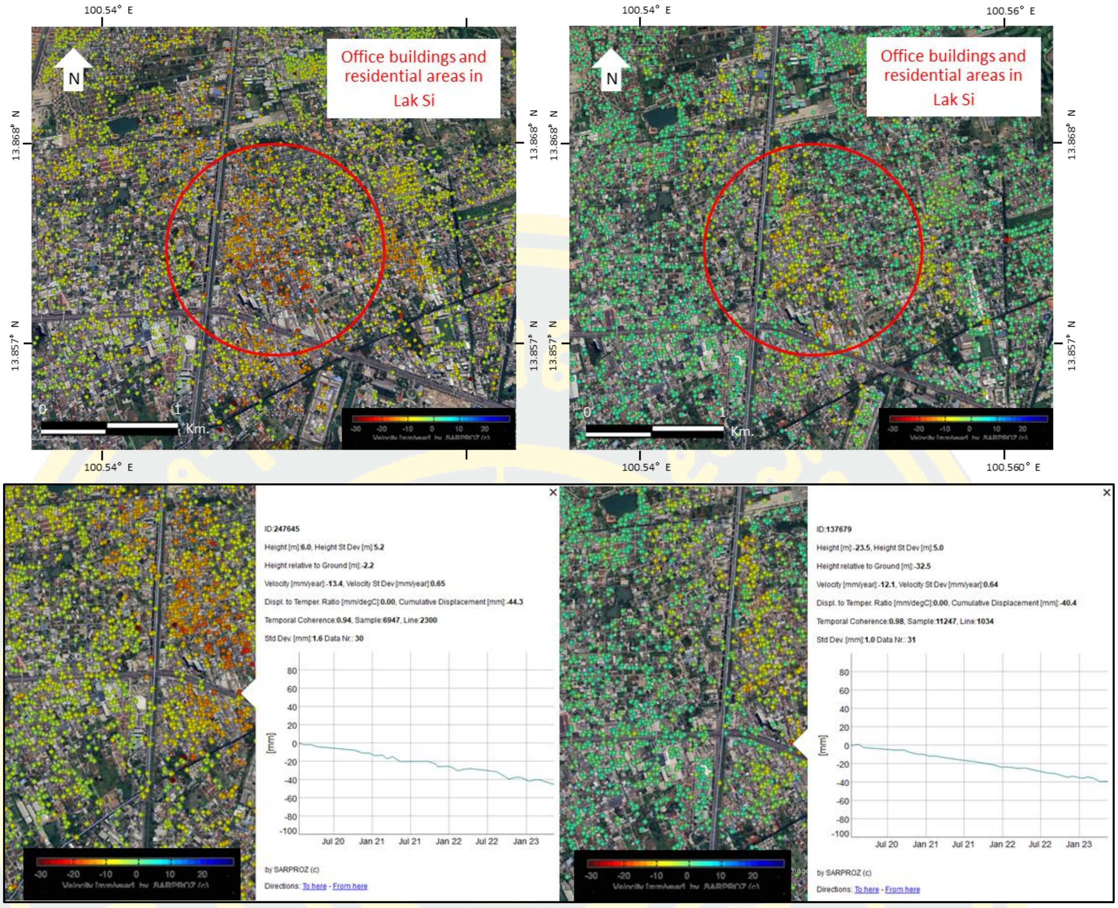

Figure 21 The time series of land displacement at two points in the northern zone of Bangkok (Khet Lak Si) from the descending track (left) and ascending track (right) shows the motion exhibits great linearity; the most significant deformations are in the office buildings and residence areas, with maximum values of -13.4 mm/year from the descending track and -12.1 mm/year from the ascending track. The two stacks' results show the same subsidence trend, but the descending track has a 1.3 mm higher subsidence rate than the ascending track.

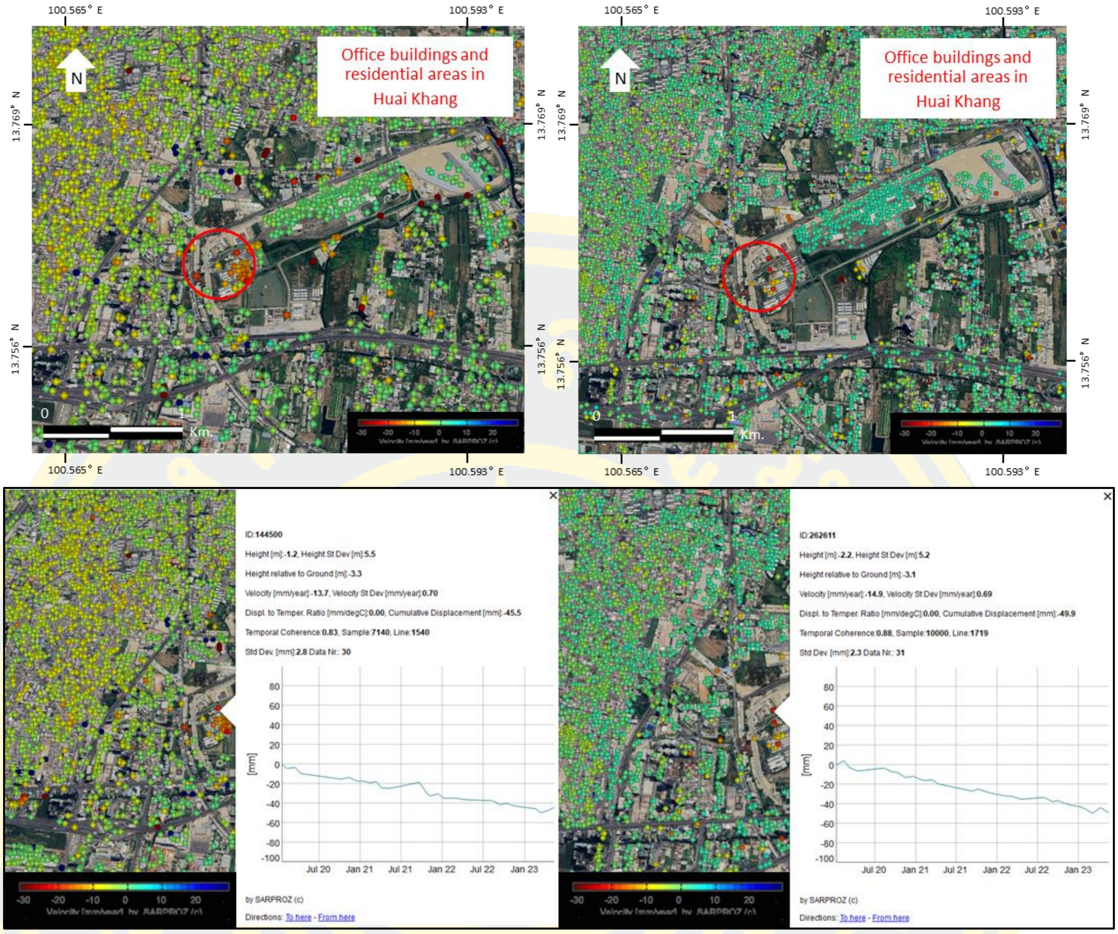

Figure 22 The time series of land displacement at two points in the center of Bangkok (Khet Huai Khang) from the descending track (left) and ascending track (right) shows the motion exhibits great linearity; the most significant deformations are in the office buildings and residence areas, with maximum values of -13.7 mm/year from the descending track and -14.9 mm/year from the ascending track. The two stacks' results show the same subsidence trend, but the ascending track has a 1.2 mm higher subsidence rate than the descending track.

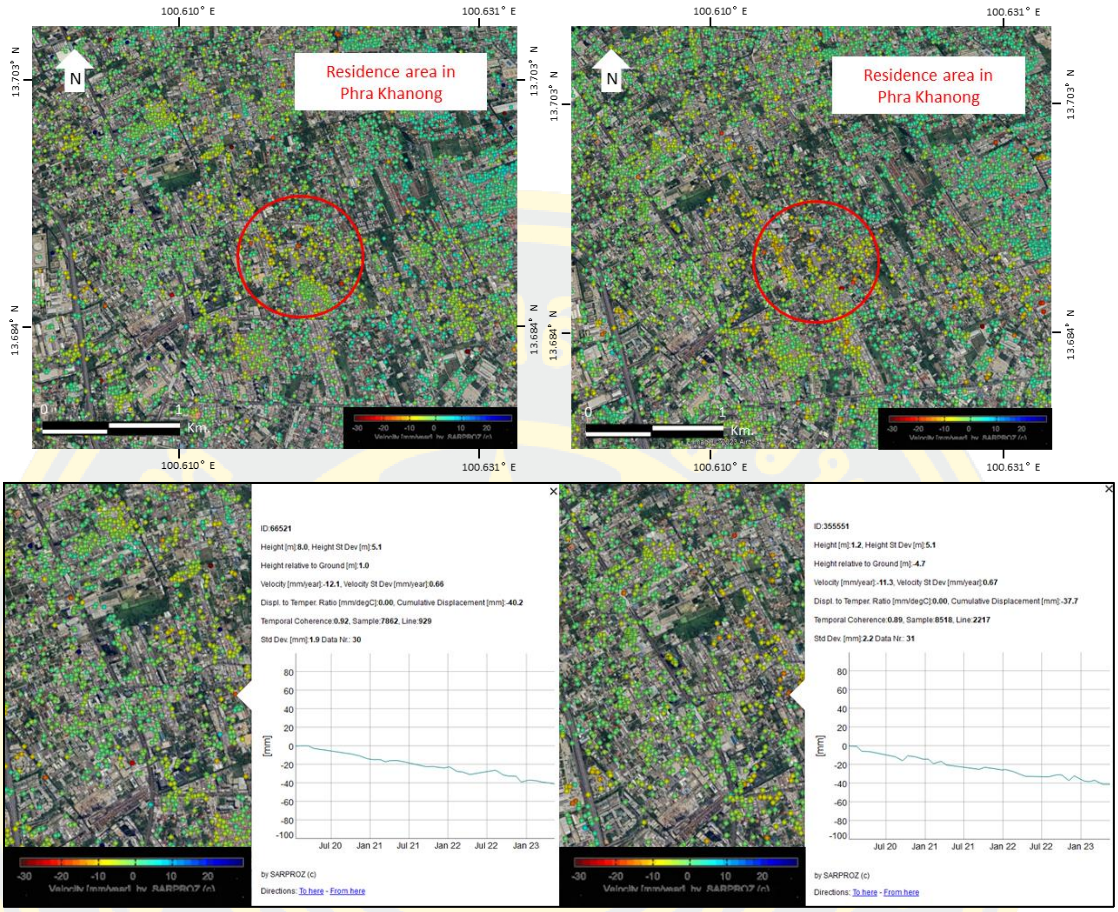

Figure 23 The time series of land displacement at two points in the southern zone of Bangkok (Khet Phra Khanong) from the descending track (left) and ascending track (right) shows the motion exhibits great linearity; the most significant deformations are in the residence areas, with maximum values of -12.1 mm/year from the descending track and -11.3 mm/year from the ascending track. The two stacks' results show the same subsidence trend, but the descending track has a 0.8 mm higher subsidence rate than the ascending track.

The land motion in the eastern zone of Bangkok is less clear in suburban and rural areas because of temporal decorrelation. The deformation is visible in Saphan Sung, Lat Krabang, and Min Buri (see Figure 24). The motion direction varies depending on the land use from descending and ascending orbits, with -14 to 7 mm/year motion from the descending orbit and -13 to 3 mm/year motion from the ascending orbit.

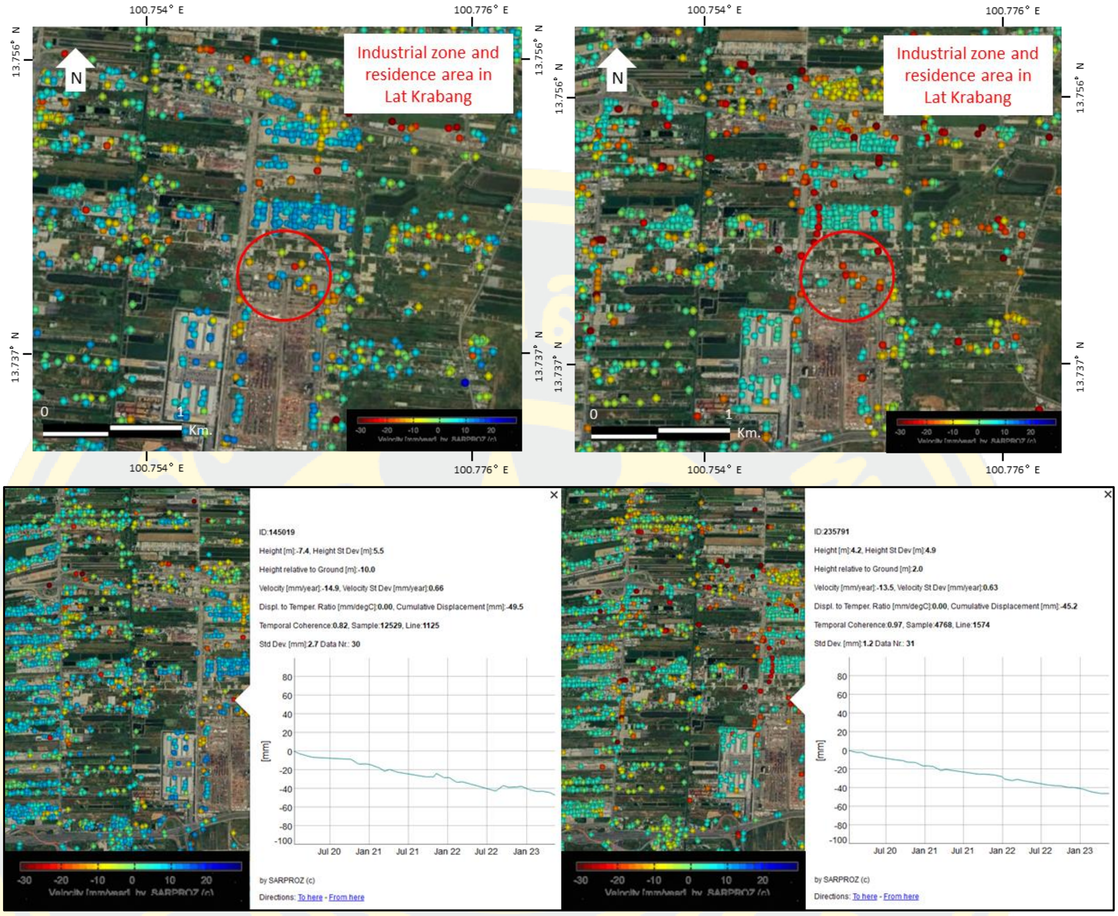

Figure 24 The time series of land displacement at two points in the eastern zone of Bangkok (Khet Lat Krabang) from the descending track (left) and ascending track (right) shows the motion exhibits great linearity; the most significant deformations are in the industrial zone and residence areas, with maximum values of -14.9 mm/year from the descending track and -13.5 mm/year from the ascending track. The two stacks' results show the same subsidence trend, but the descending track has a 1.4 mm higher subsidence rate than the ascending track.

4.2 Chiang Mai Result from the PS-InSAR time series

The PS-InSAR was implemented to locate the main deformations in Chiang Mai City. The velocity map from the descending orbit was obtained from January 16, 2020, to May 24, 2023, and the ascending orbit covers the period from January 19, 2020, to May 15, 2023. The areas of interest on the descending and ascending tracks cover Chiang Mai City and some parts of Lumphun province in the southeast (Figure 25). The estimated result indicates that the area of interest has great PS point coverage. The descending track found 114,459 PS points, and the ascending track found 80,038 PS points.

The results from the two stacks indicate that the area is stable (in green), and it can be seen that the deformation pattern is clearly visible, with zones of ground deformation discovered in three locations in Chiang Mai and one location in Lamphun. Figure 25's overall perspective displays movement in the western region next to Doi Suthep-Pui and the eastern region close to Doi Khun Tan.

The data from the descending orbit and the ascending orbit both reveal negative velocity or motion away from the sensor, which is a sign of vertical motion known as subsidence. The most significant deformations, with values ranging from -4.4 to -12.4 mm/year of descending orbit and -4.2 to -14.7 mm/year from ascending orbit are observed in the western part of Chiang Mai (Amphoe San Patong), as shown in Figure 26. It is evident that the motion exhibits great linearity, which makes it a suitable fit for the fundamental presumption of a linear deformation pattern.

Subsidence is also observed in the east of Chiang Mai at two locations, which are around the northern and southern zones of the deformation map. Land motion in the northern zone (Amphoe San Kamphang) is between -4.1 and -11.8 mm/year from the descending orbit and -4.4 and -11.7 mm/year from the ascending orbit, as shown in Figure 27. In the southern zone, the subsidence found in Amphoe Muang Lamphun ranges between -3.5 and -13 mm/year from the descending orbit and -4.5 and -10 mm/year from the ascending orbit, as displayed in Figure 28.

Moreover, the motion direction is different from the descending and ascending orbits in Amphoe Hang Dong, which is a mountain area located in the western part of Chiang Mai. The positive velocities from the descending orbit are between 2.7 and 4.7 mm/year, and the negative velocities from the ascending orbit range between -25.3 and -28.3 mm/year, as can be seen in Figure 29. The data from the descending orbit shows positive motion, or motion toward the sensor, while the data from the ascending orbit shows negative motion, or motion away from the sensor, both of which indicate horizontal motion primarily toward the east.

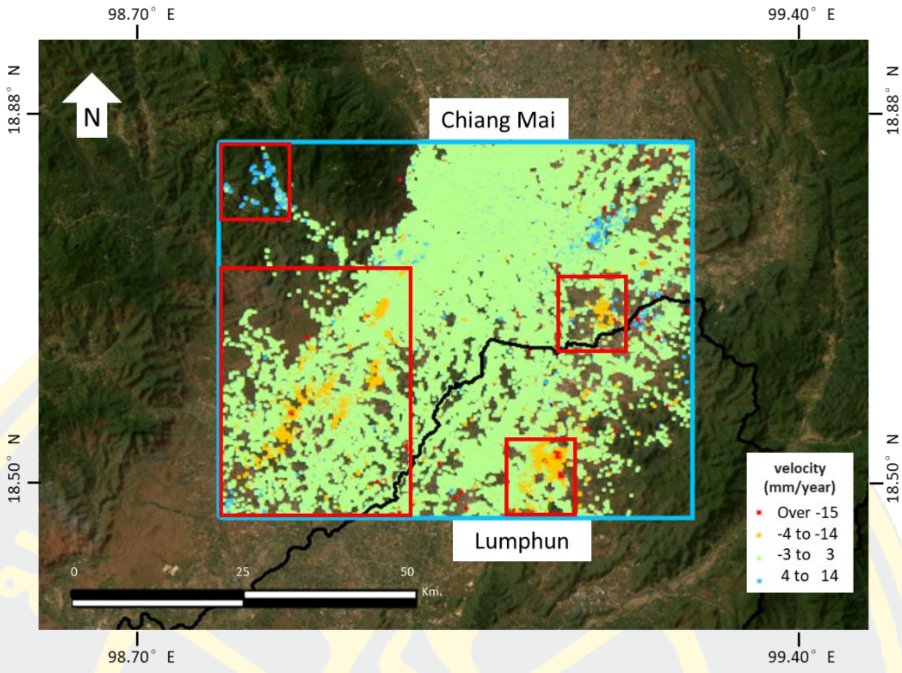

(a)

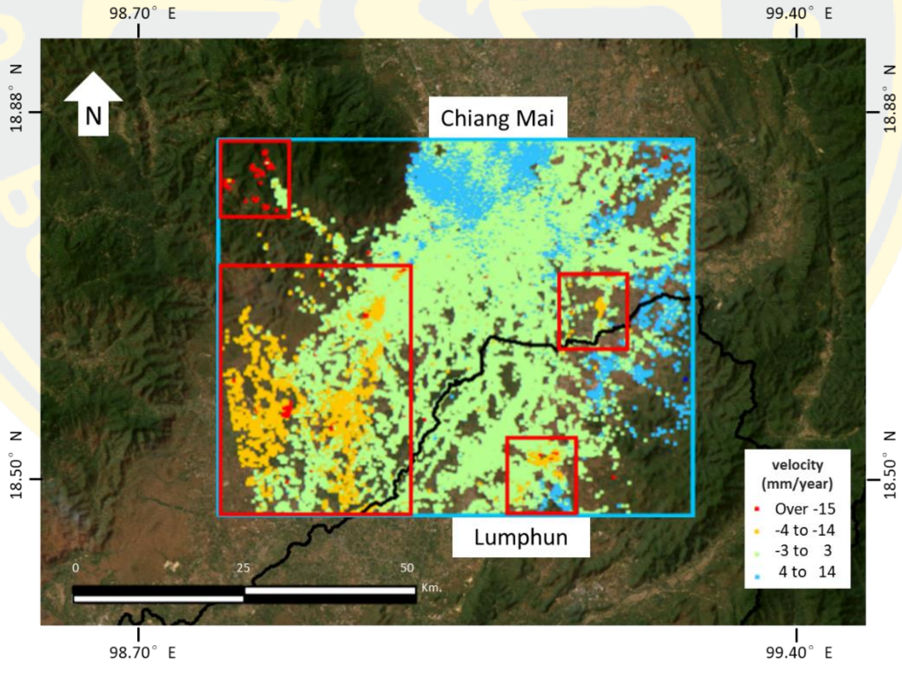

(b)

Figure 25 The deformation map of the area of interest from the descending orbit (a) and ascending orbit (b) in Chiang Mai.

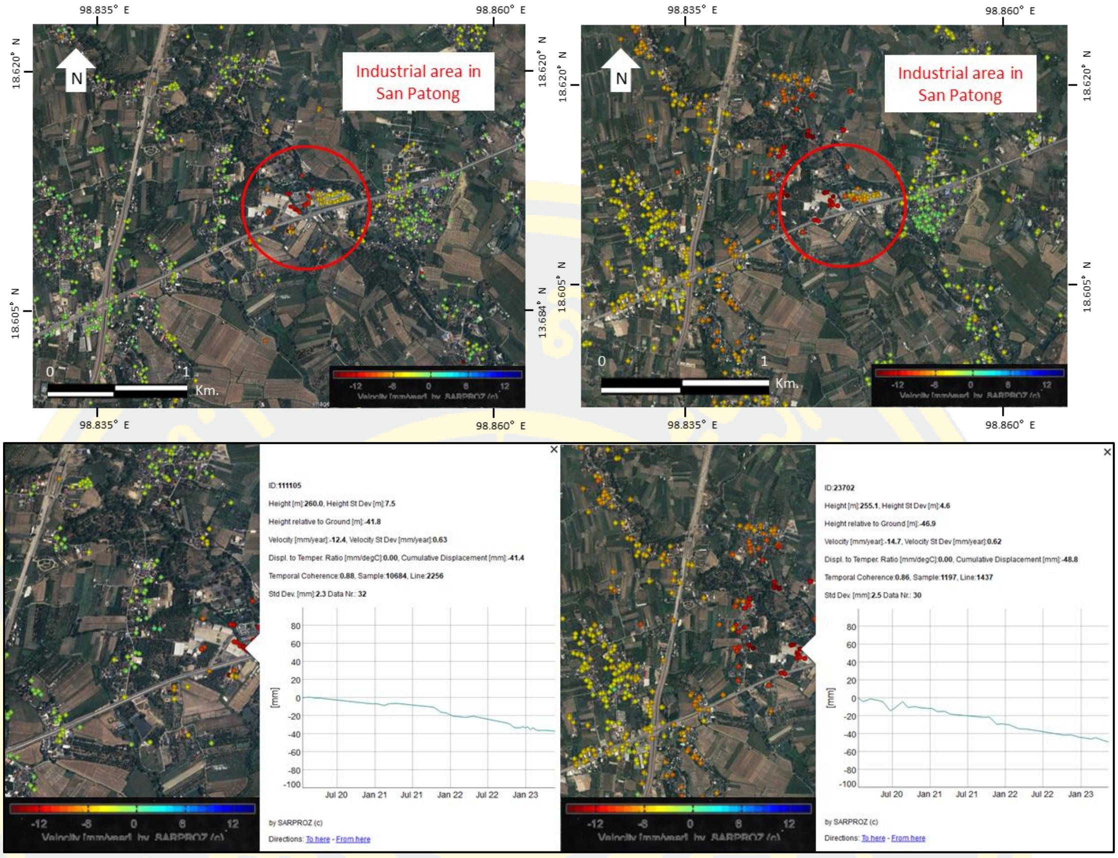

Figure 26 The time series of land displacement at two points in the west of Chiang Mai (Amphoe San Patong) from the descending track (left) and ascending track (right) shows the motion exhibits great linearity; the most significant deformations are in the industrial areas, with maximum values of -12.4 mm/year from the descending track and -14.7 mm/year from the ascending track. The two stacks' results show the same subsidence trend, but the ascending track has a 2.3 mm higher subsidence rate than the descending track.

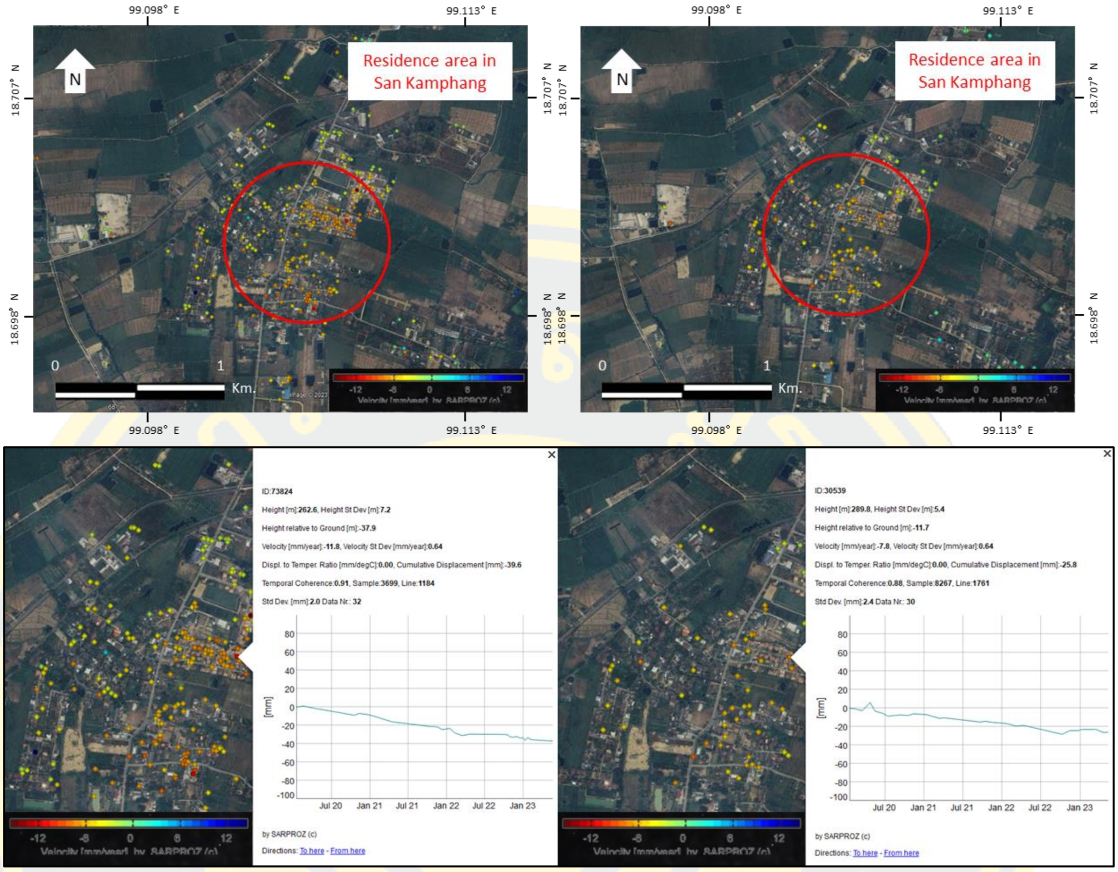

Figure 27 The time series of land displacement at two points in the east of Chiang Mai (Amphoe San Kamphang) from the descending track (left) and ascending track (right) shows the motion exhibits great linearity; the most significant deformations are in the residence areas, with maximum values of -11.8 mm/year from the descending track and -7.8 mm/year from the ascending track. The two stacks' results show the same subsidence trend, but the descending track has a 4 mm higher subsidence rate than the ascending track.

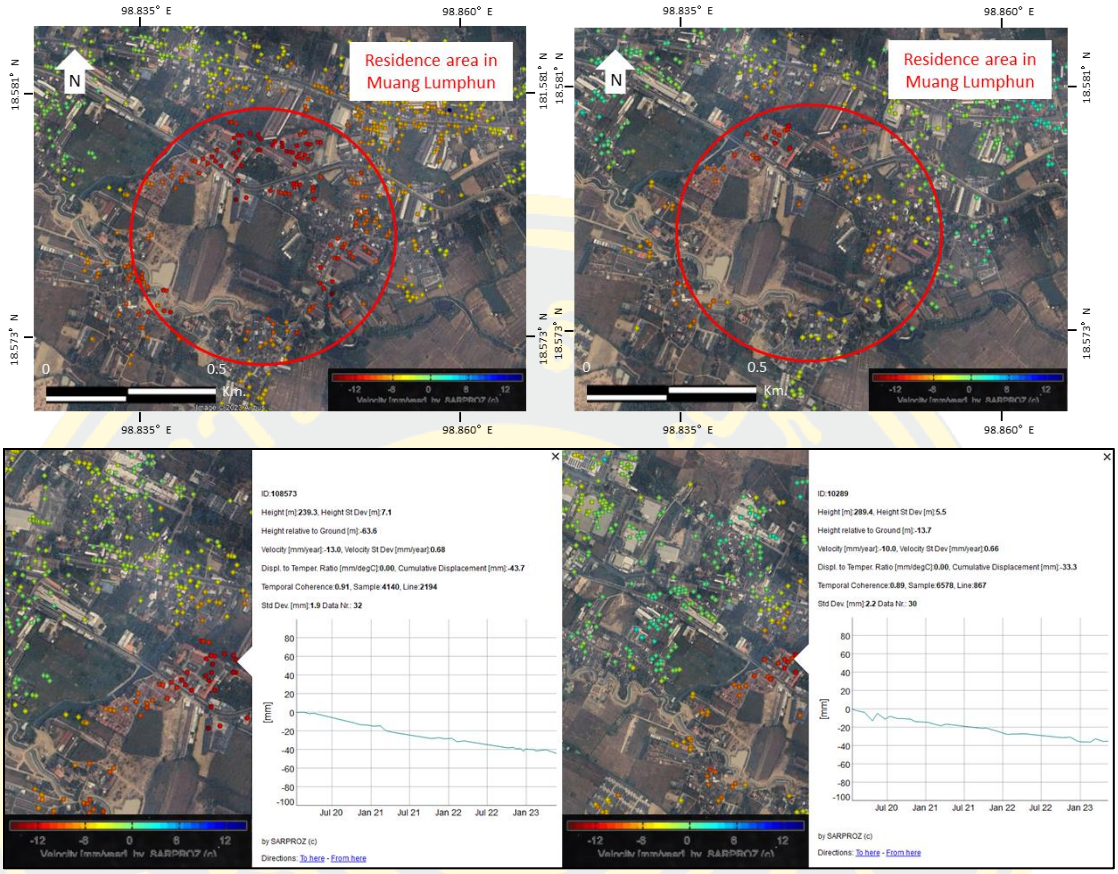

Figure 28 The time series of land displacement at two points in the east of Chiang Mai (Amphoe Muang Lamphun) from the descending track (left) and ascending track (right) shows the motion exhibits great linearity; the most significant deformations are in the residence areas, with maximum values of -13 mm/year from the descending track and -10 mm/year from the ascending track. The two stacks' results show the same subsidence trend, but the descending track has a 3 mm higher subsidence rate than the ascending track.

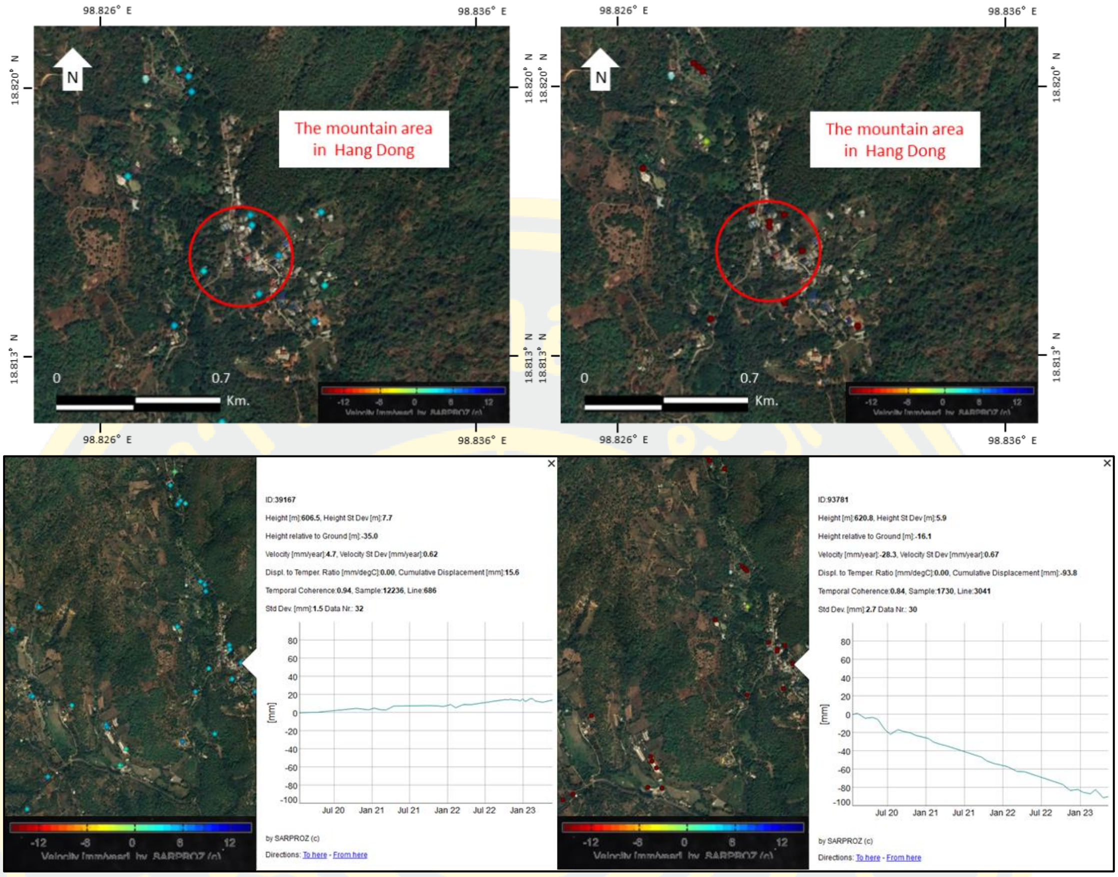

Figure 29 The time series of land displacement at two points in the western zone of Chiang Mai (Amphoe Hang Dong) from the descending track (left) and ascending track (right) shows the motion exhibits great linearity; the most significant deformations are in the mountain areas, with maximum values of 4.7 mm/year from the descending track and -28.3 mm/year from the ascending track. The two stacks' results show a different trend with a deficit value of 33 mm; the descending track shows positive motion, or motion toward the sensor, while the ascending track shows negative motion, or motion away from the sensor, both of which indicate horizontal motion primarily toward the east.

The SARPROZ software plays a crucial role in this analysis, as it provides the raw data results and estimates the linear velocity trendline within the PS-InSAR time series. Furthermore, the software generates a graphical representation that highlights deformation variations relative to the estimated overall velocity. This approach is predicated on the assumption that these deviations are attributable to non-linear motion elements.

This study leverages PS-InSAR time-series data, obtained through SARPROZ software, to analyze the land motion in the Bangkok area. Specifically, the study focuses on the fifth comparison pair between descending and ascending tracks, covering the period from January 2020 to May 2023. The findings reveal that the comparison pairs within the PS-InSAR point data along the descending and ascending tracks exhibit a deficit value range spanning from 0.8 to 2.2 mm. Standard deviations within this dataset range from 1 to 3. Notably, the significant standard deviations observed in the ascending time series are lower than those in the descending time series. Additionally, the analysis includes an examination of the relative velocity of land surface movement along both the descending and ascending tracks of the PS-InSAR in Bangkok. Through linear regression analysis, the result observes a declining trend, indicative of subsidence. According to Table 4, the difference in surface displacement rates, as derived from the PS-InSAR, ranges between -11.3 mm/year and -24.4 mm/year. These findings provide valuable insights into the vertical motion in the Bangkok area.

Table 4 An association between the velocity of RSQ, which is equal to or higher than 0.8, and significant statistics of descending (DES) and ascending (AS) orbits in the Bangkok study area.

Bangkok study area	PS point	Velocity (mm/year)	Standard deviations	Motion pattern
Western (Phasi Charoen)	DES152636 AS339321	-24.4 -22.2	3.0 1.6	Vertical motion
Northern (Lak Si)	DES247645 AS137679	-13.4 -12.1	1.6 1.0	Vertical motion
Center (Huai Khang)	DES144500 AS262611	-13.7 -14.9	2.8 2.3	Vertical motion
Southern (Phra Khanong)	DES66521 AS355551	-12.1 -11.3	1.9 2.2	Vertical motion
Eastern (Lat Krabang)	DES145019 AS235791	-14.9 -13.5	2.7 1.2	Vertical motion

In this comprehensive analysis, the study also delves into the land motion of the Chiang Mai area, focusing on the fourth comparison pair between descending and ascending tracks, spanning from January 2020 to May 2023. The investigation centers on the PS point within the descending and ascending tracks, where they observe a deficit value range of 2.3 to 33 mm. Notably, the examination reveals standard deviations ranging from 1.5 to 2.7, with the descending time series exhibiting lower significant standard deviations compared to the ascending time series. Furthermore, this study extends its scope to assess the relative velocity of land surface movement along both the descending and ascending tracks of the PS-InSAR in Chiang Mai. Through rigorous linear regression analysis, this finding uncovered a declining trend that characterizes vertical motion in several areas, namely San Patong, San Kamphang, and Muang Lamphun. Intriguingly, the Hang Dong area demonstrates a distinct pattern in the descending and ascending tracks. While the descending track showcases an inclining trend indicative of uplift, the ascending track displays a declining trend, signaling subsidence. This area exhibits horizontal motion. As illustrated in Table 5, the findings pinpoint the differences in PS-InSAR pairs for vertical displacement rates, ranging between -7.8 mm/year and -14.7 mm/year. This meticulous analysis sheds light on the intricate vertical motion patterns within the Chiang Mai region, providing valuable insights into its geological factors.

Table 5 An association between the velocity of RSQ, which is equal to or higher than 0.8, and significant statistics of descending (DES) and ascending (AS) orbits in the Chiang Mai study area.

Chiang Mai study area	PS point	Velocity (mm/year)	Standard deviations	Motion pattern
Western (Hang Dong)	DES39167 AS93781	4.7 -28.3	1.5 2.7	Horizontal motion
Western (San Patong)	DES111105 AS23702	-12.4 -14.7	2.3 2.5	Vertical motion
Eastern (San Kamphang)	DES73824 AS30539	-11.8 -7.8	2.0 2.4	Vertical motion
Eastern (Muang Lamphun)	DES108573 AS10289	-13.0 -10.0	1.9 2.2	Vertical motion

In the realm of PS-InSAR time-series analysis, the relative velocities derived from the descending and ascending orbits exhibit congruence in Bangkok. However, the situation is more nuanced in Chiang Mai, where there is both agreement and disagreement between these velocities. It is noteworthy that both ascending and descending orbits can yield distinct estimates of relative velocity, as delineated in Tables 4 and 5. This discrepancy arises due to the inherent differences in satellite geometric orbits and the Earth's surface motion, which comprises both horizontal and vertical components.

The key comparison between the two areas is that both experience vertical land motion, albeit with different characteristics. Bangkok demonstrates consistent subsidence, with surface displacement rates ranging from -11.3 mm/year to -24.4 mm/year. In contrast, Chiang Mai exhibits a lower vertical motion rate than Bangkok, including subsidence in some areas and horizontal motion in others. This variation may be attributed to diverse geological factors and local conditions within the Chiang Mai region. In summary, while both Bangkok and Chiang Mai experience vertical land motion, Chiang Mai exhibits more diverse patterns, likely influenced by its geological heterogeneity. Understanding these patterns is crucial for assessing the potential impact on infrastructure and the environment in both regions.

The analysis and comparison of land motion patterns between Chiang Mai and Bangkok, utilizing PS-InSAR time-series data obtained through SARPROZ software, reveals distinct characteristics in each area. In the forthcoming discussion section of this research, we will delve into the underlying factors contributing to the divergent results observed in Bangkok and Chiang Mai. By doing so, we aim to provide a comprehensive understanding of the intricacies surrounding relative velocity estimation in these two regions.

CHAPTER 5
DISCUSSION AND CONCLUSION

5.1 Discussion

This study addresses the key results and implications of utilizing Sentinel-1 InSAR data to track land motion in Bangkok and Chiang Mai and emphasizes the significance of our findings with regard to geological characteristics and local factors. The utilization of PS-InSAR over Bangkok showed a number of previously known sites demonstrating deformation, such as Phasi Charoen in the west, Lak Si in the north, Huai Khwang in the center, Phra Khanong in the south, and Lat Krabang in the east. All these results are based on the density of the residence area and industrial zone. When this result is compared with the previous research and the field survey, there is a good overlap. On the other hand, Chiang Mai demonstrates motion that was not previously documented by detecting both vertical and horizontal motion with the PS-InSAR technique.

5.1.1 Land Motion Pattern from PS-InSAR Detection

Various patterns of land motion in Bangkok and Chiang Mai over a number of years were effectively identified and measured by this study. Both vertical displacements known as subsidence and horizontal displacements were present in these patterns, which are essential signs of underlying instability. For instance, the city area and surroundings of Bangkok were shown to be localized regions with considerable vertical displacement through the analysis of the PS-InSAR (Figure 30). On the other hand, the mountain area of Chiang Mai shows horizontal movement, and the low plain area shows vertical movement through the analysis of the PS-InSAR (Figure 31).

The differences in geological structure and sediment deposition have led to distinct land motion patterns between Bangkok and Chiang Mai. Bangkok is situated in the southern part of the Thon Buri Basin, which constitutes a deltaic plain environment within the Lower Central Plain. This region's geological history reveals a significant influence of sedimentary deposition, particularly during the Quaternary period. The Bangkok Deltaic Plain is characterized by the predominant presence of soft clay interbedded with a tidal-shallow marine environment. Notably, the Bangkok clay stratigraphic sequence in the Thon Buri Basin emerges as a critical unit in understanding land subsidence dynamics. Comprising soft marine clay with a thickness range of 15 to 30 meters, this Quaternary Basin clay is notably prone to inducing land subsidence, making it a key contributor to the observed patterns of land motion in Bangkok (Sinsakul, 2000).

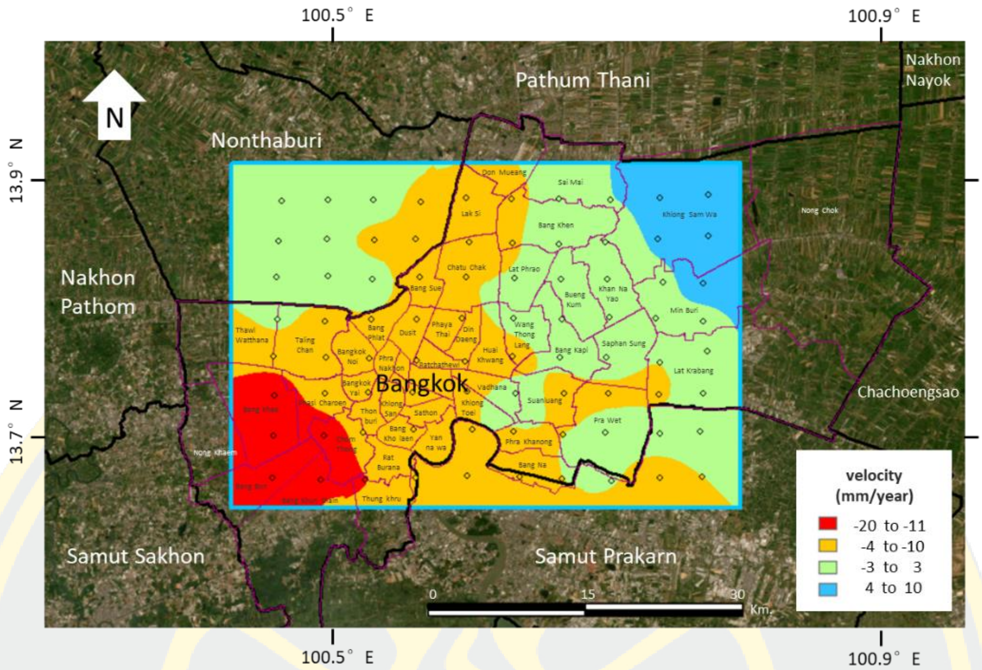

Figure 30 The vertical motion can be seen most clearly in the western part of Bangkok by the intersection of stable points between descending and ascending tracks in 2020–2023.

On the other hand, Chiang Mai experiences tectonic forces due to the presence of low-angle normal faults (LANF) dating back to the late Oligocene–Miocene, creating an intermontane basin with an east-west extension. These basins are primarily filled with fluvial and lacustrine sediments, which are prone to compaction under excessive load, resulting in vertical land motion (blue box in Figure 31). Furthermore, Chiang Mai's geological structure is influenced by its location as a basin nestled between two mountain ranges: Doi Khun Tan Mountain to the east and Doi Suthep-Pui Mountain to the west. The steep slopes of these mountains increase susceptibility to landslides, as the stronger gravitational forces make material movement downhill easier. Inherent weaknesses in the rock or soil, such as cracks or fractures, play a pivotal role in landslide occurrences, while heavy rainfall saturating the soil can trigger landslides, leading to horizontal land motion (red box in Figure 31).

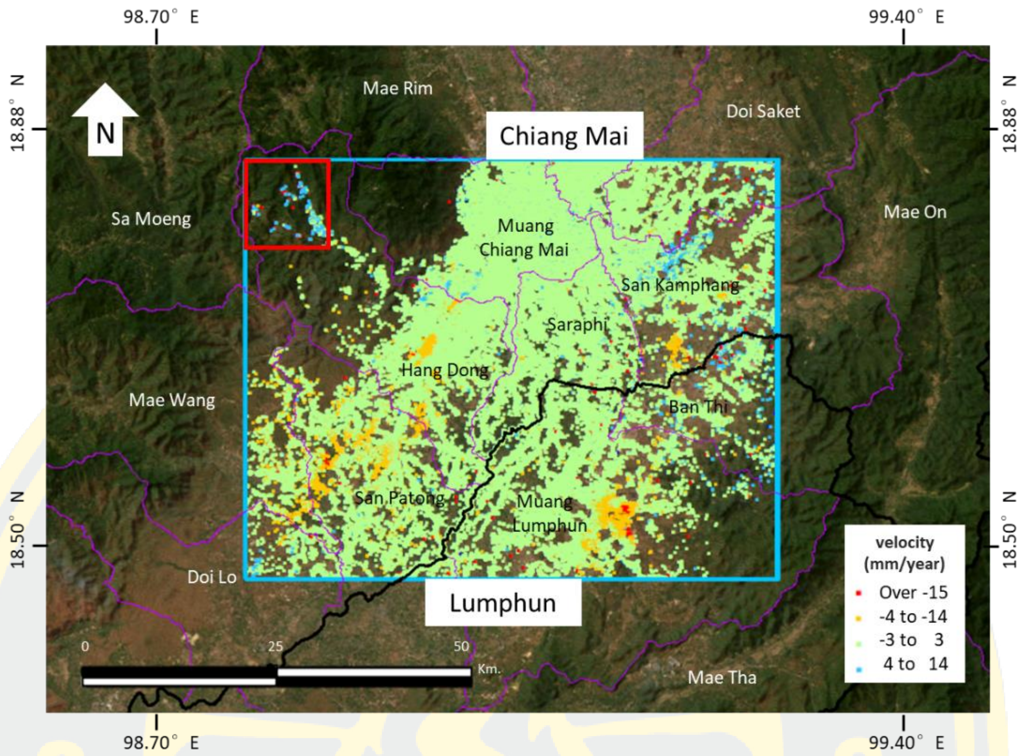

Figure 31 The intersection of stable points between descending and ascending tracks in 2020–2023 shows the horizontal motion can be seen clearly in the mountain areas of the western parts (red box), while the vertical motion can be seen in both the low plain areas, which is the edge of Chiang Mai Basin (blue box).

Bangkok and Chiang Mai exhibit distinct land motion patterns due to their unique geological characteristics and local factors. Bangkok experiences primarily vertical subsidence driven by soft clay deposits and exacerbated by human activities, while Chiang Mai experiences a combination of vertical and horizontal motion influenced by geological structure, sediment deposition, mountainous terrain, rock type, and heavy rainfall that also trigger the land motion. Both cities face challenges related to land motion, but the scale and specific factors involved differ significantly between the two regions.

5.1.2 The Geological characteristics and Land Motion

The impact of geology on deformation holds substantial importance and can be elucidated through a multitude of geological factors and mechanisms. The distinct patterns of motion observed in both Bangkok and Chiang Mai owe their origins to the geological attributes unique to their respective regions. These disparities stem from variations in factors such as tectonic setting, the presence of fault zones, the type and strength of rocks, as well as sedimentary deposition and compaction. This delves deeper into how geology influences deformation.

Tectonic Setting

The geographical location of an area, particularly concerning its proximity to tectonic plate boundaries, wields a significant influence on deformation patterns. Regions situated near plate boundaries are predisposed to undergo notable deformation due to the dynamic interplay between these massive tectonic plates. Within the crucible of plate boundaries, formidable tectonic forces manifest as compression, extension, and lateral shearing, subjecting the Earth's crust to immense pressures that catalyze various deformation processes. For instance, in the crucible of convergent plate boundaries, the relentless forces of compression coerce rocks into bending and folding, sculpting majestic mountain ranges. Conversely, at divergent plate boundaries, where extensional forces dominate, rift valleys are born, and the Earth's crust undergoes stretching.

Chiang Mai resides within an area shaped by active tectonic forces, particularly characterized by the presence of a low-angle normal fault (LANF) on which the Chiang Mai Basin is situated. LANF is indicative of continuous crustal extension in this region, generating stress within the Earth's crust and leading to distinctive geological features. The primary tectonic influence in Chiang Mai is related to crustal extension, resulting from the gradual movement of tectonic plates away from each other. This dynamic has given rise to the formation of the intermontane Chiang Mai Basin. Additionally, Chiang Mai's location between towering mountains, intricately affected by its geological structure, contributes to a gradual land deformation over geological periods. On the contrary, Bangkok is situated in a deltaic plain setting intricately associated with the Chao Phraya River, far from active tectonic zones and relatively stable. Hence, the impact of tectonic forces on the landscape is more pronounced in Chiang Mai than in Bangkok, significantly influencing deformation patterns. This geological contrast plays a pivotal role in defining the distinct topography and depositional environments of Chiang Mai and Bangkok, ultimately manifesting in varying land motion dynamics experienced by these two locales.

Fault Zones

Chiang Mai, situated in northern Thailand, boasts a geologically complex landscape. Within the Chiang Mai Basin, the terrain rests upon the hanging wall of a low-angle normal fault (LANF). The foundational rock in this basin consists of metamorphic varieties like orthogneiss and paragneiss, primarily found in the footwall of the fault. This geological context sets Chiang Mai apart from Bangkok, which lies in a relatively stable continental region, far from active plate boundaries, resulting in less pronounced tectonic forces. The presence of normal faults, including the LANF, in Chiang Mai serves as a clear indicator of ongoing crustal extension and tectonic deformation. This region experiences dynamic geological processes due to the interactions among Earth's lithospheric plates.

Faults, as zones of weakness within the Earth's crust, play a pivotal role in shaping deformation patterns in a given area. Deformation along fault lines occurs as stress accumulates and gradually releases through fault movement. This movement

can manifest as both vertical and horizontal displacement, contingent on the specific type of fault, whether it's normal, reverse, or strike-slip. Moreover, when stress builds up within the Earth's crust, it seeks release along fault lines, giving rise to a range of deformation forms, including faulting, folding, and fracturing.
The specific character and orientation of deformation depend on the type and alignment of the fault systems.

This geological contrast between Chiang Mai and Bangkok explains why Chiang Mai displays a blend of both vertical and horizontal land motion. In contrast, Bangkok predominantly undergoes vertical motion. The tectonic and fault-related activity in Chiang Mai results in a more intricate pattern of deformation. The utilization of PS-InSAR technology aids in discerning these deformation patterns in Chiang Mai. In terms of vertical motion, it appears relatively modest compared to Bangkok and is primarily localized near the edge of the Chiang Mai basin. Conversely, horizontal motion is chiefly observed in mountainous regions. The PS-InSAR data identifies land motion within the Chiang Mai basin, albeit within a relatively limited area. This suggests that the geological structure gradually influences land motion over extended periods, possibly not significantly impacting the timeframe of this research. However, it's noteworthy that the vertical motion, as revealed by PS-InSAR, exhibits a discernible southwest trend, presenting an intriguing challenge for future investigations aimed at exploring more pronounced land motion patterns.

Rock Type and Strength

Rock type and strength are pivotal factors in land deformation processes. Different rock types possess varying degrees of resistance to deformation, largely influenced by their inherent physical properties. Metamorphic rocks like gneiss tend to be strong and less deformable due to their tightly interlocked mineral structures, while sedimentary rocks such as shale or clay are often more susceptible to deformation due to their loosely packed particles and lower cohesion. The strength properties of rocks, encompassing compressive, tensile, and shear strength, dictate their ability to withstand stress without fracturing or deforming. Consequently, regions with strong, resistant rocks typically experience less pronounced land deformation, whereas areas characterized by weaker, deformable rock types are more likely to exhibit various forms of deformation, including compaction, faulting, and subsidence, when subjected to geological forces and stress.

In the Bangkok area, soft clay predominates, whereas Chiang Mai exhibits a diverse lithology such as sandstone, siltstone, conglomerate, limestone, granite, orthogneiss, and phyllite. The nature of the rocks in a region plays a pivotal role in shaping deformation processes. Different rocks exhibit varying degrees of resistance to deformation, resulting in distinct responses to stress and pressure. For instance, metamorphic rocks like orthogneiss in Chiang Mai are characterized by their strength and high compressive resistance, making them less prone to significant deformation because the presence of robust rocks like gneiss and granite, with its high compressive strength, contributes to its relatively lower susceptibility to deformation. In contrast, sedimentary rocks such as shale or clay in Bangkok tend to be more susceptible to deformation when subjected to stress. This discrepancy in rock types and their inherent strength properties determines their reaction to external forces. The weaker rocks lack the cohesion and internal strength needed to withstand the forces exerted upon them. As a result of these geological distinctions, Bangkok experiences a higher rate of subsidence compared to Chiang Mai. The combination of weaker rocks and the tendency to deform more readily under pressure leads to more pronounced land subsidence in Bangkok.

Sedimentary Deposition and Compaction

Sedimentary deposition and compaction are pivotal geological processes that contribute significantly to land deformation, particularly in areas dominated by sedimentary rock formations. Consider a coastal region where layers of fine-grained sediments, such as clay and silt, accumulate over millennia. Initially, these sediments are loose and unconsolidated, but as subsequent layers are added, the weight of the overlying sediments compresses the lower layers. This compaction gradually transforms the sediments into solid sedimentary rocks. However, the accumulated stress and pressure within these rocks can lead to deformation. For instance, the coastal sediments, when subjected to tectonic forces or changes in sea level, may undergo subsidence, causing the land surface to sink. In urban areas, excessive groundwater extraction can further exacerbate subsidence as it reduces support pressure on the sediments, allowing them to compact further. This dynamic is vividly illustrated in regions like Bangkok, where extensive sedimentary deposition and subsequent compaction have resulted in significant land subsidence, impacting the city's infrastructure and susceptibility to flooding.

In the context of Chiang Mai, the geological composition of its basin differs significantly from that of Bangkok. The Chiang Mai Basin is characterized by coarser-grained sediment, resulting from floodplain-alluvial deposition, which stands in stark contrast to Bangkok's Thon Buri Basin situated within the Chao Phraya floodplain. Bangkok's landscape is primarily defined by its low-lying deltaic plain environment, where soft clay formations have gradually accumulated over extended geological periods. These sediments, particularly fine-grained ones like Bangkok clay, exhibit relatively high elastic properties and are susceptible to compaction when subjected to the weight of overlying layers. This compaction process leads to land subsidence, a gradual sinking of the land surface as sediments progressively compress under the pressure of newer deposits. While Figures 32 and 33 indicate a wide subsidence area (yellow area) in Bangkok, it is relatively small in Chiang Mai, even though the floodplain area and the rate of land subsidence are comparable. This difference is attributed to the type of sedimentary deposition, with fine-grained sediment being more responsive to deformation than coarser-grained sediment. These distinct geological conditions underlie the phenomenon of land subsidence, which is the primary driver of the extensive vertical motion observed in Bangkok and its notably higher subsidence rate compared to Chiang Mai.

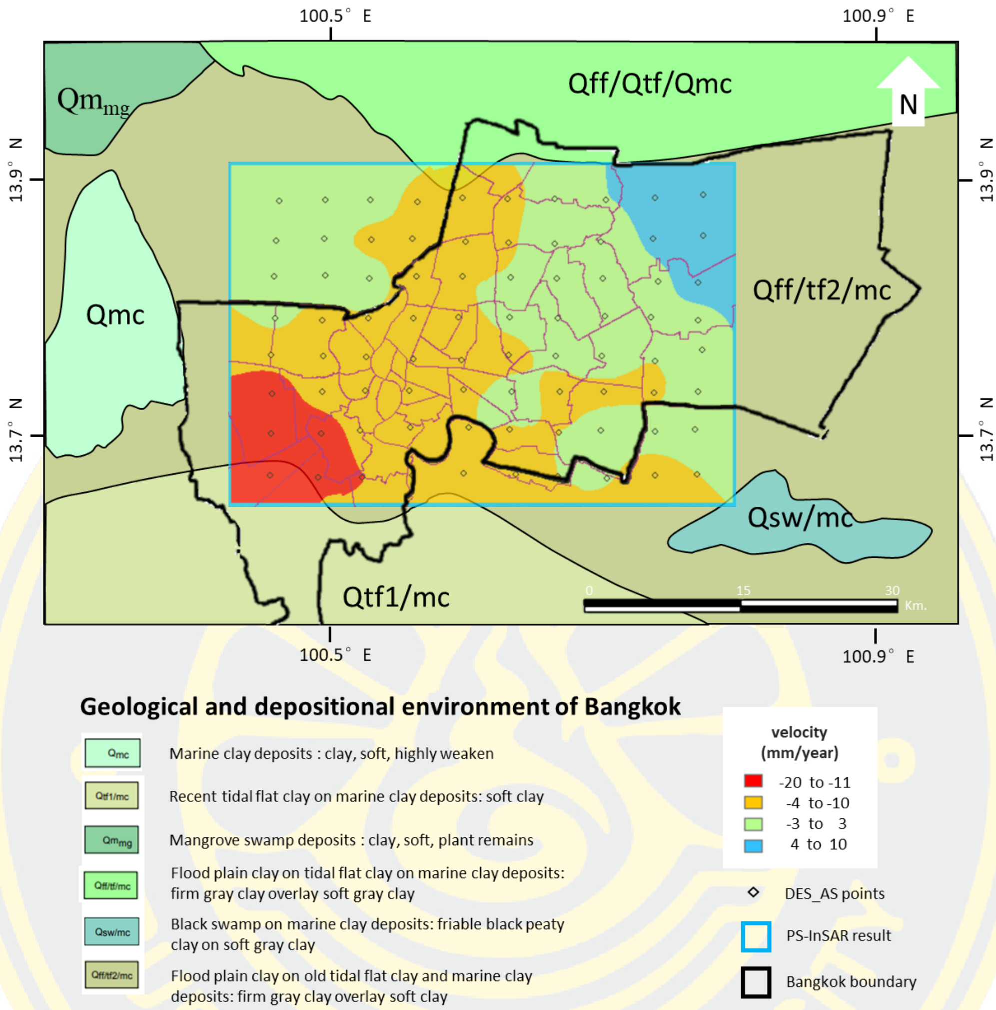

Figure 32 The vertical motion of Bangkok relates to a geological and depositional environment where the red area shows the high rate of subsidence and is flood plain clay and recent tidal flat clay on marine clay deposits; the yellow area shows the moderate rate of subsidence and is flood plain clay on old tidal flat clay and marine clay deposits; the green area shows the low to stable rate; and the blue area shows the uplift area where there is higher terrain and near the mountain on the east of Bangkok.

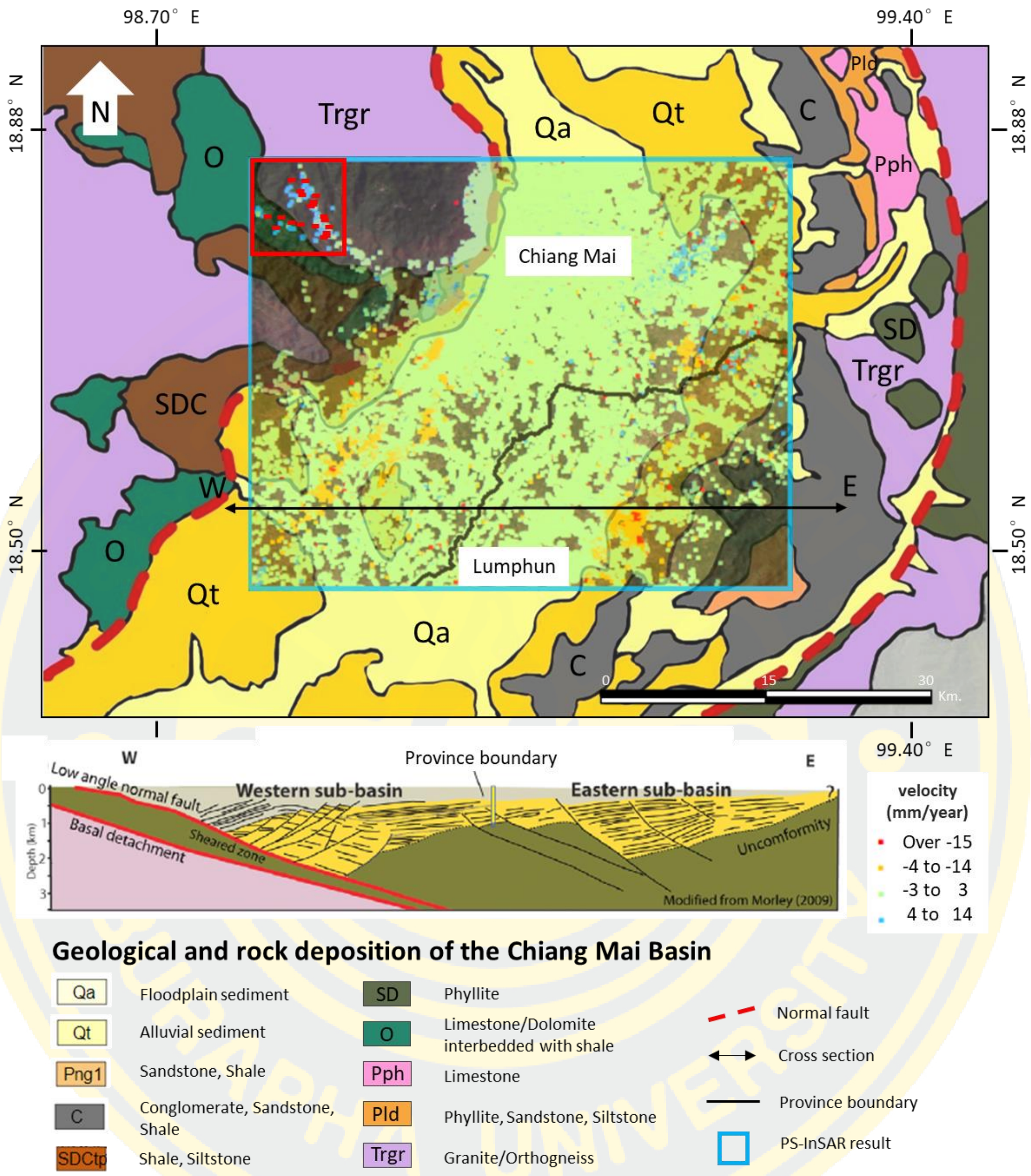

Figure 33 The land motion of Chiang Mai relates to a geological map and deposition environment where the small yellow area shows the subsidence is near the edge of the Chiang Mai basin and it's a floodplain-alluvial deposition, while a mountain area on the west of Chiang Mai is represented by the red (indicating subsidence from an ascending track) and blue (indicating uplift from a descending track), and the different directions of motion indicate horizontal motion.

In summary, geology influences deformation through the tectonic setting of an area, the presence of geological structures like faults, the inherent properties of rocks, and sedimentary processes. Understanding these geological factors is crucial for predicting and mitigating deformation-related risks and impacts in different regions. The type and intensity of deformation in a specific area are a result of the complex interplay between geological conditions and external forces. These observed trends from PS-InSAR align with the unique geological characteristics of each region.

5.1.3 Local factors and Land Motion

Human activities, encompassing practices like groundwater extraction, mining, and construction, wield significant influence over deformation patterns in specific regions. Excessive groundwater extraction, for instance, can trigger land subsidence as it depletes underground aquifers. The withdrawal of water diminishes the supporting pressure on surrounding rocks or sediments, compelling them to compress, ultimately causing the land surface to sink. Similarly, activities such as mining and the construction of substantial infrastructure can perturb the stress distribution within the Earth's crust, resulting in localized deformation.

Bangkok, Thailand's vibrant capital city, is a testament to the nation's economic advancement, with its innovative technology and modern architectural marvels showcased in the central business district. This urban dynamism positions Bangkok as a thriving hub for job opportunities and residential living, leading to overuse of groundwater in the city. In contrast, Chiang Mai, nestled amidst its breathtaking natural landscapes, has a lower population density compared to Bangkok. The population density and construction activity in these cities are closely linked to the respective subsidence rates observed in Chiang Mai and Bangkok. In essence, human activities play a pivotal role in shaping the deformation dynamics of these regions, with the distinctive characteristics and development trajectories of Bangkok and Chiang Mai contributing to variations in subsidence rates.

The fast urbanization and infrastructure development in the studied region were highly linked with the observed land motion patterns. Subsidence can occur in highly populated urban areas because of increasing groundwater extraction, building weight, and construction activity. Critical infrastructure, such as utility systems and transportation networks, is significantly in danger from this. However, some of the improperly located building construction on the land may have been prevented by deploying surface motion surveillance based on PS-InSAR in advance.

The western region of Bangkok City is one of the places where such phenomena can be seen most clearly, as shown in Figures 20. In May 2023, Khet Nong Khaem received a complaint of land subsidence (see in Figure 34). Since more and more infrastructure is being built in western Bangkok, the surrounding area has begun to subside. Moreover, this location is in a deltaic plain environment and covered with Bangkok clay (Figure 32), which leads to compaction when this area has a lot of loads from construction. The land-use zoning plan for the Bangkok Comprehensive Plan from 2020 by the Department of City Planning in Figure 35 shows the relationship between the density of the residence area and the PS-InSAR result, the high density of the residence zone (brown and orange color) responds to a high subsidence rate in the western, northern, center, and southern areas of Bangkok.

Figure 34 The damage from land subsidence in Khet Nong Khaem, the western region of Bangkok City by the news report in May 2023 (CH7HD News, 2023).

According to the fieldwork data shown in Figure 34, land subsidence was to blame for the recorded damage. Due to surface motion, the walls and primary structure of many homes sustained the most notable damage. In addition, the PS point was found here between -11 and -23 mm/year. This may be a result of the building work that was done during the data collection period. Moreover, the PS-InSAR analysis reveals the time series of subsidence in the northern, central, and southern zones of Bangkok, which coincide with densely populated residential areas, as depicted in Figures 21, 22, and 23. The areas experiencing pronounced subsidence align with the high-density residential zones, indicating a direct correlation between the rate of subsidence and the concentration of residential development in these regions. The findings have immediate ramifications for Bangkok authorities and urban planners. In order to assess the risk and develop mitigation methods, it is crucial to identify locations that are subject to land motion. Authorities may make educated decisions about land use, zoning, and the creation of resilient infrastructure by incorporating our findings into urban planning.

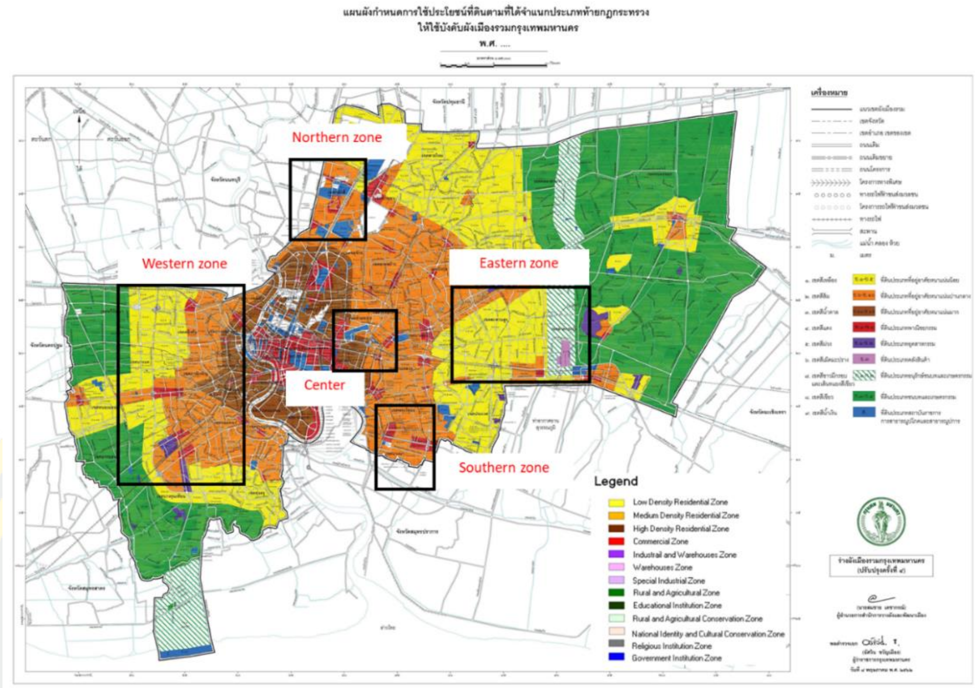

Figure 35 Bangkok Metropolitan Administrator's draft land-use zoning plan for the Bangkok Comprehensive Plan from 2020 by The Department of City Planning.

Furthermore, the number of buildings and residences increased, resulting in an excessive reliance on groundwater because humans still need water to survive. However, the overuse of groundwater has caused the pore water pressure in the rock formation to drop, the level of groundwater to drop, and the effective stresses in the aquifers to rise. Additionally, it is more difficult for deep groundwater sources to recharge and recover. Because of this, groundwater levels in the region, especially the deep groundwater, have remained low. As a result of the deep groundwater's slow rate of recharge and ongoing extraction, the aquifer's skeleton is crushed, and surface displacement occurs.

As per the Groundwater Level Fluctuations report from the Department of Groundwater Resources, the Bangkok metropolitan area and its adjacent regions, encompassing Phra Nakhon Si Ayutthaya, Nakhon Pathom, Pathum Thani, Nonthaburi, Samut Sakhon, and Samut Prakan provinces, are currently facing a severe groundwater crisis characterized by a complex multi-layered aquifer system. Between 2017 and 2021 (see Table 6), the groundwater levels in these regions ranged from 20 to 25 meters below the ground surface but exhibited an average annual decline of approximately 0.34 meters. Notably, the most significant declines occurred in Pathum Thani Province, with substantial decreases also observed in Phra Nakhon Si Ayutthaya, Samut Prakan, and Nakhon Pathom Provinces, where the average annual decline exceeded 2 meters. In contrast, Chiang Mai's groundwater system comprises three distinct primary levels, with current groundwater depths ranging from 5 to 10 meters. However, specific areas such as Chom Thong Subdistrict in Chom Thong District, Ban Klang Subdistrict in San Pa Tong District, and Santisuk Subdistrict in Doi Lor District feature significantly deeper groundwater levels, ranging from 29 to

84 meters, and experience an average annual decrease of 3.76 meters (see Table 6). This groundwater level change data highlights a clear correlation between the overuse of groundwater and declining groundwater levels in both Bangkok and Chiang Mai, aligning with the observed subsidence patterns in these regions as indicated by PS-InSAR results.

Table 6 Groundwater Level Fluctuations in the Sand-Gravel Sediment Aquifer from 2017 to 2021.

Area	Groundwater Level (m)	Groundwater level change (m)	Remark
Bangkok	0-50	13-14	declining trend of approximately 0.34 meters per year.
	50-100	13-17	
	100-150	16-22	
	150-200	17-23	
	200-300	20-24	
	350-450	29	
Chiang Mai		5-10	Chom Thong, San Pa Tong, and Doi Lor District experiencing an average annual decrease of 3.76 meters.

Additionally, natural factors like precipitation and slope angles play pivotal roles in driving horizontal motion in Chiang Mai. Heavy rainfall, particularly on steep slopes, is a primary trigger for landslides, which are relatively common occurrences in mountainous regions like Chiang Mai. In May 2022, the local authorities reported that the lower plain areas experienced flooding and the high terrain experienced landslides in many districts of Chiang Mai and the surrounding area. These phenomena are affected by surface motion, leading to damage in a wide area.

Figure 36 The damage from flooding and landslides in Amphoe Hang Dong, Chiang Mai by the news report in May 2022 (Khaosod, 2023; Bangkokbiznews, 2023).

The horizontal motion from the PS-InSAR approach were corroborated by a report and the Chiang Mai landslide susceptibility map, as shown in Figures 36 and 37, respectively. The site is suffering from disaster, which endangers the survival of the population. The high terrain is damaged by landslides and observed on the roads, while the lower plain is often seriously damaged by floods.

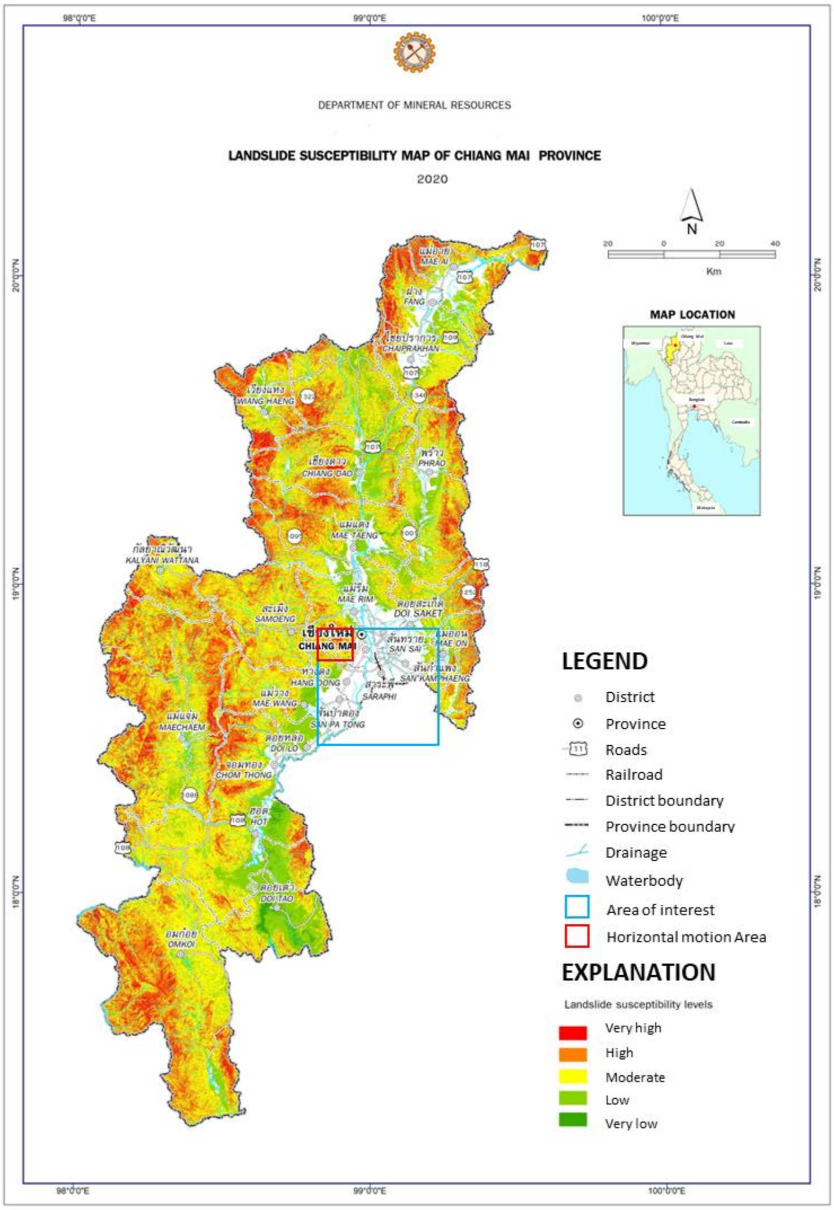

Figure 37 Chiang Mai landslide susceptibility map (update 2020) by the Department of Mineral Resources.

Analysis of Sentinel-1's temporal data has unveiled long-term trends in land motion, revealing the gradual occurrence of landslides in specific regions. The utilization of Sentinel-1 or other radar satellite surveillance proves indispensable for monitoring the evolution of these patterns and assessing their potential environmental ramifications.

In summation, both Bangkok and Chiang Mai undergo land motion, albeit shaped by distinctive geological influences and localized factors. Bangkok's subsidence primarily stems from the natural consolidation of soft clay deposits, exacerbated by human activities. Conversely, Chiang Mai experiences a composite of vertical and horizontal movement due to a medley of natural elements, including sediment deposition, the presence of mountainous terrain, lithological attributes, and precipitation. Furthermore, human activities play a pivotal role in steering land motion dynamics in both locales. These discernible trends align with the distinctive geological traits characterizing each region.

Ultimately, this study underscores the paramount importance of community engagement and informed policymaking. Collaborative efforts involving local governments, researchers, and community stakeholders are essential in devising strategies to mitigate the impacts of land motion on urban areas. Initiatives aimed at raising public awareness and imparting knowledge to the populace can further support the judicious management of water resources and appropriate land utilization.

5.2 Conclusion

This research uses the InSAR time series technique with Sentinel-1 images for detecting land motion in Chiang Mai and Bangkok, Thailand, to compare the results between the different geology and depositional environments from this technique and to analyze the direction of land motion for allocating the surveillance area. All the images, both descending and ascending orbits, were selected, including 61 images in Bangkok and 62 images in Chiang Mai, from January 2020 to May 2023.

The findings of this study demonstrate instances of morphological and geological hazards posing threats to urban areas in Chiang Mai and Bangkok, with a focus on natural factors such as geology, morphology, and depositional environment. Utilizing the PS-InSAR technique, which enables a high-density sampling of observations, yielding several hundred measurements of the PS point per square kilometer, we were able to identify deformation zones within these regions.

Chiang Mai and Bangkok exhibit distinct geological and morphological environments, leading to disparate geological hazard profiles. Nevertheless, both urban areas share the common challenge of land subsidence attributed to the rapid expansion of urbanization and overuse of groundwater, resulting in substantial structural damage. Additionally, these regions are susceptible to flood risks, particularly in close proximity to rivers and low areas.

In Bangkok, the natural causes are linked to the evolution of the Thon Buri Basin in the early Miocene and making the deltaic plain environment covered with Bangkok clay, which led to compaction when this area had a lot of loads from the construction and overuse of groundwater. Thus, the deformation appears in the density of residence zones such as Phasi Charoen in the west, Lak Si in the north, Huai Khwang in the center, Phra Khanong in the south, and Lat Krabang in the east, with an extreme subsidence rate of 24 mm/year. On the contrary, Chiang Mai experiences a blend of vertical subsidence and horizontal movement due to a range of natural factors. The depositional environment, the proximity of mountainous terrain (morphology), and lithological factors can act as potential vertical motion with an extreme subsidence rate of 14 mm/year. However, natural factors such as precipitation and slope angle are also causes of horizontal motion in the mountain area.

Finally, several potentially dangerous geological hazards have been identified in Chiang Mai and Bangkok. Building damage is the result of land displacement from natural and man-made factors over many years. Therefore, monitoring the impacted areas requires ongoing control. PS-InSAR is an effective and reasonably priced technique for estimating surface motion, especially now that Sentinel-1 data is widely available globally. Risk management and its application have been a major focus of the current work on hazard monitoring as well as the inventory of previous studies on land motion. Up-to-date results from PS-InSAR can be used to estimate natural disasters such as land subsidence and landslides more accurately.

REFERENCES

Beladam, O., Balz, T., Mohamadi, B., & Abdalhak, M. (2019). Using ps-insar with sentinel-1 images for deformation monitoring in northeast Algeria. *Geosciences*, *9*(7), 315.

Biggs, J., Wadge, G., & Mothes, P. (2014). Stratovolcano growth by co-eruptive intrusion: The 2008 eruption of Tungurahua Ecuador. Geophysical Research Letters, 41(12), 4233–4240.

Bontebal,M. 2001. "Land Subsidence in Bangkok." Accessed August 25, 2010. http://www.unescap.org//esd/energy-security-and-water-resources/water/urbangeology/land/index.asp

Brand, E.W., and T. Paveenchana. 1971. "Deep-well Pumping and Subsidence in the Bangkok Area." In 4th Asian Regional Conference on Soil Mechanics and Foundation Engineering, Vol. 1, 1–7. Bangkok, Thailand: Asian Institute of Technology, July 1971.

Cascini, L., Peduto, D., Ferlisi, S., et al. (2011). Persistent scatterer interferometry analysis of Cosoleto, southern Italy: An approach to investigate landslides affecting transportation infrastructures. Landslides, 8(3), 281–293.

CH7HD News. (2023). land subsidence in Khet Nong Khaem. CH7 News. https://www.youtube.com/watch?v=VuRHA2vBGdU

Chang, C. P., Yen, J. Y., Hooper, A., Chou, F. M., Chen, Y. A., Hou, C. S., Hung, W. C., & Lin, M. S. (2010). Monitoring of surface deformation in Northern Taiwan using DInSAR and PSInSAR techniques. Terrestrial, Atmospheric and Oceanic Sciences, 21(3), 447–461. https://doi.org/10.3319/TAO.2009.11.20.01(TH)

Charusiri, P., Pum Im, S., 2009. Cenozoic tectonic evolution of major sedimentary basins in Central, Northern, and the Gulf of Thailand. Bull. Earth Sci. Thailand 2, 40–62.

Charusiri, P., Pailoplee, S., Kosuwan, S., Takashima, I., & Rhodes, B. (2022). Bulletin of Earth Sciences of Thailand Active fault and seismic zonation in Thailand: An empirical compilation (Vol. 14, Issue 1).

Chaithavee, S. (2015). InSAR time-series analysis for land subsidence monitoring in eastern greater Bangkok. Master dissertation, Department of Survey Engineering, Faculty of Engineering, Chulalongkorn University.

Chinbunchorn, N., Prapidtan, S. & Sattayarak, N. 1989. Petroleum potential of Tertiary intermontane basins in Thailand. International Symposium on Intermontane Basins: Geology and Resources. Chiang Mai University, Thailand, 29–41.

City Planning Department. (2023). land-use zoning plan for the Bangkok Comprehensive Plan from 2020. City Planning Department. https://webportal.bangkok.go.th/cpud

Crosetto, M., & Monserrat, O. (2016). Persistent Scatterer Interferometry: A review. ISPRS Journal of Photogrammetry and Remote Sensing, 115, 78–89.

Dechkamfoo, C., Sitthikankun, S., Kridakorn Na Ayutthaya, T., Manokeaw, S., Timprae, W., Tepweerakun, S., ... & Rinchumphu, D. (2022). Impact of rainfall-induced landslide susceptibility risk on mountain roadside in northern Thailand. Infrastructures, 7(2), 17.

Department of Mineral Resources. (2023). Chiang Mai landslide susceptibility map_updated March 2020. Department Of Mineral Resources.

https://www.dmr.go.th/
Detektia. (2023). Synthetic-aperture radar missions. Detektia. https://detektia.com/en/sar-synthetic-aperture-radar/
Dunning, G.R., MacDonald, A.S., Barr, S.M., 1995. Zircon and monazite U-Pb dating of the Doi Inthanon core complex, northern Thailand: implications for extension within the Indosinian Orogen. Tectonophysics 251, 197±213.
Fenton, C.H., Charusiri, P., Wood, S.H., 2003. Recent paleoseismic investigations in Northern and Western Thailand. Anal. Geophys. 46, 957–981.
Edward,W., 1976. “Soil Compressibility and Land Subsidence in Bangkok.” In Publication No. 121 of the International Association of Hydrological Sciences, Proceedings of the Anaheim Symposium, Anaheim, CA, December 13–17.
ESA. (2023). eoPortal Directory - Satellite Missions Database. European Space Agency. https://directory.eoportal.org/web/eoportal/satellite-missions/
Ferretti, A., Prati, C., & Rocca, F. (2001). Permanent scatterers in SAR interferometry. IEEE Transactions on Geoscience and Remote Sensing, 39(1), 8–20.
Ferretti, A., Prati, C., & Rocca, F. (2011). Nonlinear Subsidence Rate Estimation Using Permanent Scatterers InSAR. Geoscience and Remote Sensing Letters, IEEE, 8(1), 158–162.
Haley&Aldrich Inc. (1970). Effect of Deep Well Pumping on Land Subsidence in Bangkok, part of “Master Plan, Water Supply and Distribution, Metropolitan Bangkok, Thailand”. 4, Report by Camp, Dresser & Mckee Inc., submitted to Metropolitan Water Works Association, Bangkok.
Hooper, A., Zebker, H., & Segall, P. (2007). Persistent scatterer interferometric synthetic aperture radar for crustal deformation analysis, with application to Volcán Alcedo, Galápagos. Journal of Geophysical Research: Solid Earth, 112(B7).
Japan International Cooperation Agency (JICA). (1995). The study on management of groundwater and land subsidence in the Bangkok Metropolitan Area and its vicinity. Report submitted to the Department of Mineral Resources. Bangkok: JICA. Bangkok.
Kampes, B. M., Hanssen, R. F., & Swart, L. M. T. (2001). Strategies for non-linear deformation estimation from interferometric stacks. IGARSS 2001. Scanning the Present and Resolving the Future. Proceedings. IEEE 2001 International Geoscience and Remote Sensing Symposium (Cat. No. 01CH37217), 6, 2828–2831.
Khaosod, (2023). flooding and landslides in Amphoe Hang Dong, Chiang Mai. Khaosod. https://www.khaosod.co.th/around-thailand/news_565316
Li, Z., Ding, X., & Li, Z. (2015). Monitoring land subsidence in Beijing, China, with Sentinel-1A radar data and PS-InSAR. Remote Sensing, 7(12), 15467–15485.
Luachapichatikul, S., & BALZ, T. (2020). Measuring Land Subsidence with PS-InSAR in Bangkok using Sentinel-1 Time-Series Techniques (Doctoral dissertation, Burapha University).
Macdonald, A.S., Barr, S.M., Miller, B.V., Reynolds, P.H., Rhodes, B.P., Yokart, B., 2010. P–T–t constraints on the development of the Doi Inthanon metamorphic core complex domain and implications for the evolution of the western gneiss belt, northern Thailand. Journal of Asian Earth Science, 37, 82–104, doi: 10.1016/j.jseaes.2009.07.010.

Malod, J. A., & Kemal, B. M. (1996). The Sumatra margin: oblique subduction and lateral displacement of the accretionary prism. Geological Society, London, Special Publications, 106(1), 19–28.

Mankhemthong, N., Morley, C. K., Takaew, P., & Rhodes, B. P. (2019). Structure and evolution of the Ban Pong Basin, Chiang Mai Province, Thailand. Journal of Asian Earth Sciences, 172, 208–220. https://doi.org/10.1016/j.jseaes.2018.09.010

Metcalfe, I. (1996). Pre-Cretaceous evolution of SE Asian terranes. Geological Society, London, Special Publications, 106(1), 97–122.

Metcalfe, I. (2011). Tectonic framework and Phanerozoic evolution of Sundaland. Gondwana Research, 19(1), 3–21. https://doi.org/10.1016/j.gr.2010.02.016

Mitrearth. (2023). Chiang Mai Topography. https://www.facebook.com/mitrearth/photos/a.517871335446372/1007517883148379/?type=3&theater

Morley, C. K. 2007. Variations in Late Cenozoic-Recent strike-slip and oblique-extensional geometries, within Indochina: the influence of pre-existing fabrics. Journal of Structural Geology, 29, 36-58.

Morley, C.K., 2009, Geometry and evolution of low-angle normal faults (LANF) within a Cenozoic high-angle rift system, Thailand: implications for sedimentology and the mechanisms of LANF development. Tectonics, 28, 1–30.

Morley, C.K., Charusiri, P., and Watkinson, I.M., 2011, Structural geology of Thailand during the Cenozoic. In: Ridd, M.F., Barber, A.J., and Crow, M.J. (eds.), The Geology of Thailand. Geological Society, London, Geology of Series, p. 273–334.

Morley, C. K. (2015). Five anomalous structural aspects of rift basins in Thailand and their impact on petroleum systems. Geological Society Special Publication, 421(1), 143–168. https://doi.org/10.1144/SP421.2

Nutalaya, P. 1981. Investigation of Land Subsidence Caused by Deep Well Pumping in the Bangkok Area. Comprehensive Report 1978–1981, Submitted to National Environmental Board, Asian Institute of Technology, Bangkok.

Nutalaya, P., Chandra, S., & Balasubramaniam, A. S. (1984). Subsidence of Bangkok clay due to deep well pumping and its control through artificial recharge. Land Subsidence. Proc. 3rd Symposium, Venice, 1984, 727–744. https://doi.org/10.1016/0148-9062(88)92699-x

O’Leary, J. (1989). Tertiary basin development in the southern plains Thailand. Proceedings of the International Symposium on Intermountain Basins: Geology and Resources, Chiangmai University, 1989, 254–264.

Packham, G. H., 1990. Plate motions in Southeast Asia: some tectonic consequences for basin development. In Proceedings of the 8th Offshore South East Asia Conference, 119-132.

Packham, G. H. (1993). Plate tectonics and the development of sedimentary basins of the dextral regime in western Southeast Asia. Journal of Southeast Asian Earth Sciences, 8(1–4), 497–511.

Panchuk, K. (2019). Physical Geology. University of Saskatchewan.

Perissin, D. (2008). Validation of the submetric accuracy of vertical positioning of PSs in C-band. IEEE Geoscience and Remote Sensing Letters, 5(3), 502–506.

Perissin, D., & Wang, T. (2011). Repeat-pass SAR interferometry with partially

coherent targets. IEEE Transactions on Geoscience and Remote Sensing, 50(1), 271–280.
Phien-wej, N., Giao, P. H., & Nutalaya, P. (2006). Land subsidence in Bangkok, Thailand. Engineering Geology, 82(4), 187–201. https://doi.org/10.1016/j.enggeo.2005.10.004
Piromthong, P. (2015). Detection of 1996-2000 rates and trend of land subsidence in Greater Bangkok by InSAR time-series analysis (Master dissertation, Department of Survey Engineering, Faculty of Engineering, Chulalongkorn University). Retrieved from www.nature.com.
Polachan, S., Pradidtan, S., Tongtaow, C., Janmaha, S., Intarawijitr, K., & Sangsuwan, C. (1991). Development of Cenozoic basins in Thailand. Marine and Petroleum Geology, 8(1), 84–97.
Pumpuang, A., & Aobpaet, A. (2020). The comparison of land subsidence between east and west side of Bangkok, Thailand. Built Environment Journal (BEJ), 17(3), 1-9.
Ramnarong, V. 1983. “Groundwater Depletion and Land Subsidence in Bangkok.” In Proceedings of Conference on Geology and Mineral Resources of Thailand. Department of Mineral Resources, Bangkok, Thailand, November 19–28.
Ramnarong, V., S. Buapeng, S. Chootnatut, and A. Loupensri. 1998. Groundwater and Land Subsidence Crisis in Bangkok Metropolitan and Vicinity, Vol. 3. Technical Report of Department of Mineral Resources, Bangkok, Thailand.
Replumaz, A., Tapponnier, P., 2003. Reconstruction of the deformed collision zone between India and Asia by backward motion of lithospheric blocks. J. Geophys. Res. 108. https://doi.org/10.1029/2001JB000661.
Rhodes, B. P., Blum, J., and Devine, T., 2000, Structural development of the mid-Cenozoic Doi Suthep metamorphic core complex and western Chaing Mai basin, northern Thailand. Journal of Asian Earth Sciences, 18, 97 – 108, doi:10.1016/S1367-9120(99)00019-X.
Rhodes, B.P., Conejo, R., Benchawan, T., Titus, S., and Lawson, R., 2005, Paleocurrents and provenance of the Mae Rim Formation, Northern Thailand: implications for tectonic evolution of the Chiang Mai Basin. Journal of the Geological Society of London, 162, 51–63.
RTSD. (2010). Subsidence in Bangkok from leveling result. Royal Thai Survey Department. https://www.rtsd.mi.th/main/language/en/
Sinsakul, S. (2000). Late Quaternary geology of the Lower Central Plain, Thailand. Journal of Asian Earth Sciences, 18(4), 415–426. https://doi.org/10.1016/S1367-9120(99)00075-9
Sousa, J. J., & Bastos, L. (2013). Multi-temporal SAR interferometry reveals acceleration of bridge sinking before collapse. Natural Hazards and Earth System Sciences, 13(3), 659–667.
Tofani, V., Gigli, G., & Morelli, S. (2019). A review of the application of persistent scatterer interferometry (PSI) in landslide studies. Remote Sensing, 11(18), 2168.
Uttamo, W., Nichols, G.J., Elders, C.F., 2000. The Tertiary sedimentary basins of northern Thailand. In: Symposium on Mineral, Energy and Water Resources of Thailand: Towards the Year, pp. 71–93.
Wattananikorn, K., Beshir, J.A., and Nochaiwong, A., 1995, Gravity interpretation of

Chiang Mai Basin, northern Thailand: concentrating on Ban Thung Sieo area. Journal of Southeast Asian Earth Science, 12, 53–64.

Yamanaka, T., Mikita, M., Lorphensri, O., Shimada, J., Kagabu, M., Ikawa, R., ... & Tsujimura, M. (2011). Anthropogenic changes in a confined groundwater flow system in the Bangkok Basin, Thailand, part II: how much water has been renewed?. Hydrological Processes, 25(17), 2734-2741.

Yong, R. N., H.Maathuis, and E. Turcott. 1995. "Groundwater Abstraction-Induced Land Subsidence Prediction: Bangkok and Jakarta Case Studies." In The Fifth International Symposium on Land Subsidence, FISOLS-95, The Hague, The Netherlands, October 16–20.

BIOGRAPHY

NAME	Kunlacha Inpai
DATE OF BIRTH	25 March 1993
PLACE OF BIRTH	Lampang, Thailand
PRESENT ADDRESS	50/3 Villa No.3 Soem Sai Subdistrict, Soem Ngam District, Lampang, Thailand 52210
POSITION HELD	2015 – 2017 Geologist (Employee); Department of Fuel 2017 – 2019 Geologist (Practitioner Level); Department of Fuel 2019 – present Geologist (Practitioner Level); Department of Mineral Resources
EDUCATION	2011 - 2015 Graduated with Bachelor's degree in Science (Geology), Chiang Mai University